博士論文

Changes in precipitation and temperature extremes over South Asia using dynamical downscaling of climate change prediction results

(気候変動予測結果の力学的ダウンスケーリングを用いた 南アジア域における降水と気温の極値変化)

ラムザン メーウィッシユ

MEHWISH RAMZAN

March 2015

“Changes in precipitation and temperature extremes over South Asia using dynamical downscaling of climate change prediction results”

(気候変動予測結果の力学的ダウンスケーリングを用いた南アジア域における降水と気温の極値変化)

MEHWISH RAMZAN

Student ID: 37-127013

A dissertation submitted to The University of Tokyo in partial fulfillment of the requirements for the degree of Doctor of Philosophy

PhD Dissertation

Department of Civil Engineering

Graduate School of Engineering

The University of Tokyo

March 2015

Doctoral Committee

Prof. Kei YOSHIMURA (Chair)

Prof. Taikan OKI

Prof. Toshio KOIKE

Prof. Satoshi TAKIZAWA

Prof. Koji DAIRAKU

Acknowledgements

I would like to thank my Supervisor Dr. Kei Yoshimura for his tremendous efforts to guide me for my research throughout the study period. Many thanks to my co-supervisors Dr. Taikan Oki, Dr. Toshio Koike, Dr. Satoshi Takizawa and Dr. Koji Dairaku for their constructive comments and kind guidance for obtaining my research goals. I would like to extend my thanks to Oki Laboratory members; Dr. Kazuo Oki, Dr. Hyunjun Kim, Dr. Noda, Dr.Suryun Ham, Dr.Eun-Chul Chang, Dr. Murakami, Dr. Mouri, Dr. Nakamura, Mr. Utsumi, and my colleagues Mr. Atsushi Okazaki, Dr. Rajan Bhattarchariya, Dr. Satoh, Dr. Nitta, Miss Cherry Mateo, Mr.Mukaida, Miss Saya, Miss Hatono, Mr Wei and Mr. Amjad (from Pakistan) for their wonderful support and fruitful discussions. I am grateful to Ministry of Education, Culture, Sports, Science and Technology, Japan (MEXT) who provided me this opportunity to study in Japan for my higher education with sufficient funding. I am really grateful to the secretaries Miss Motani, Ms. Kurosawa, Miss Noguchi for their kind help in managing my travel for the conferences and workshops very well. Thanks are extended to The University of Tokyo for the provision of best possible sources for computation purposes. Special regards for the SOUSEI project (Program for Risk Information on Climate Change) for covering the travel and other expenses of conferences and workshops attended during the research. I am extremely grateful to Korea Meteorological Administration for providing HadGEM2-AO data produced by the support of Grant Number NIMR-2012-B-2 to drive the regional climate model. Last but not least, lots of regards to my parents, siblings, my husband and his family to support me in every possible way. Thank you all

This thesis is dedicated to my parents

Major (Retd.) Mahar Muhammad Ramzan

and

Mrs. Rubina Ramzan

Abstract

Climate change is very diverse in nature with large spatial coverage. The impacts of climate change can be seen via its fingerprint in term of extreme unpredictable weather. These weather extremes are associated with both natural and anthropogenic activities. Understanding these extremes requires an ample amount of available observations to determine the cause of the change. Unfortunately, the quality of observation datasets varies from region to region which lessens the confidence in studying regional details. Example of one such region is South Asia where the observation coverage is sparse in last few decades with almost no digital long-term record of the past climate in most of the regions.

In order to compensate such data lacks, climate models are very useful tools in studying the historical climate and can also be used for future projection studies. The use of climate models provides homogenous data record over large time scale. One cannot classify the model as good or bad. Therefore, it raises a question as which model to be used. One answer to this question will be that; it depends on the purpose of your study. For example, General Circulation Models (or GCMs) usually have coarse horizontal resolution (>100km). They can provide us with the large-scale picture of the phenomena such as El-Nino Southern Oscillations (ENSO), Inter-tropical Convergence Zone (ITCZ) Positions and Maiden Julian Oscillation (MJO) etc. On the other hand, if we need to study only some particular region of the earth then the GCMs shows constraint in providing finer details for that region of interest. Therefore, to study one specific region

we need Regional Climate Models (RCM) of relatively high resolution than GCM, which can compensate our demand for regional study.

In current study, the Regional Spectral Model (RSM) originally developed at the National Center for Environmental Predictions (NCEP) by Juang and Kanamitsu in 1994 is applied to downscale the South Asian region using high resolution. The outcome of this research will contribute to the World Climate Research program (WCRP), which initiated an effort to generate high-resolution regional information for all land parts of the world. The project under which these efforts are being conducted is known as Coordinated Regional Climate Downscaling Experiment (CORDEX). The domain size of this study ranges from 7^oE to 128^oE and 10^oS to 50^oN with 256x169 grid size and 50km resolution. CORDEX-South Asian experiment (CORDEX-SA) using RSM is initiated with an aim to choose the optimum Convective Parameterization schemes (CPs), by determining their skill in reproducing the precipitation over South Asia. Downscaling of South Asia poses great challenges to the modelers. A few of them is mentioned below.

First is the heterogeneous nature of South Asian monsoon identified by previous researches, so that it is indeed a challenge for the model's performance that how realistically it can capture this climatic phenomenon. The second well known problem faced by models in simulating South Asian precipitation is the wet bias of Atmospheric GCMs over the Equatorial Indian Ocean (EIO), which according to some researchers is associated with insufficient resolution and inappropriate model physics selected. The third challenge faced by coarser resolution models is to capture the South Asian complex topography composed of highest Himalayan and Karakorum ranges towards north, Hindu Kush ranges towards northwest, Suleiman ranges towards west of Pakistan and small hills such as eastern and western Ghats of India, Aravalli and Vidhyan ranges, Myanmar prominent peak, Nat Ma Taung (also known as Mount Victoria). All these topographic barriers play an important role in shaping the monsoon mechanism in South Asia. Multiple AGCMs or Atmosphere-Ocean coupled models are also being used in South Asia, which usually features large-scale phenomenon.

My research uses RSM to first capture the disastrous event of 26 July 2005 when Maharashtra, Mumbai received 944 mm of rain in 18 hours which claims hundreds of lives, impacted large infra-structure and badly hit the agricultural sector of the metropolis state of India. Such short-term extreme event becomes the motivation to determine the skill of four CPs that includes; new Kain Fritsch (KF2) scheme, Relaxed Arakawa Schubert (RAS) scheme, Simplified Arakawa Schubert (SAS) scheme and Community Climate Model version 3 (CCM) scheme. The time period selected for CPs evaluation is from 25 July till 28 July 2005, with 24 July 2005 as a spin-up day. The comparison of four selected CPs and their ensemble showed SAS scheme has relatively better reproducibility of precipitation than other convective schemes for the whole CORDEX-SA domain and for sub-domains such as South Asia, Pakistan and Myanmar. The wet bias over the EIO is also minimized more significantly by the SAS scheme than others. The physical ensemble experiment of four CPs does not minimizes the wet bias over equatorial Indian ocean as it combines the over estimations of KF2, RAS and CCM schemes making it less reliable as compared to SAS convective scheme.

The dynamic downscaling approach which nests the RCM over GCM in the domain of interest sometimes create systematic biases in newly formed regional model domain. In order to remove or minimize those biases multiple approaches are adopted. One such method is Scale Selective Bias Correction (SSBC) method. The systematic biases are minimized by using the combination of spectral tendency damping correction and areal averaging of temperature, humidity and pressure, or by replacing the spectral tendency nudging with field nudging, which removes the errors of large-scale inter-annual variability of seasonal mean. It applies nudging only to the rotational components of wind that is present as a default option (SSBC_def) in RSM. The third method is the application of full wind nudging along with vertically weighting damping coefficient method (SSBC_new) instead of height independent damping coefficient. The later two SSBC methods are applied for 10 years sensitivity experiments for CORDEX-SA. The result of analysis shows that due to the greater relaxation time at the ground level provided by SSBC_new, the RSM shows somewhat realistic results for precipitation as compared to SSBC_def. The high spatial correlations and low root mean square error shown by SSBC_new further confirm its capability in simulating South Asian monsoon precipitation for the selected time period.

After the aforementioned sensitivity experiments, the optimized model options are selected to run the historical and future simulations driven by Hadley Center Global Environmental Model version2 (HadGEM-AO) of National Institute of Meteorological Research of Korea Meteorological Administration. The atmospheric part has 1.875^o x 1.25^o horizontal resolution and 38 vertical levels with top altitude of 38km while the ocean part has 1^o horizontal resolution with 40 vertical levels. The selected model options includes SAS convective scheme with SSBC_new.

RSM simulation for 20^{th} century analysis are conducted for the time period of 1980-2005 and their results are validated using multiple datasets of varying resolutions in order to determine the performance of RSM in all aspects (land only, land and ocean, high resolution etc.) for surface precipitation as it is known as the difficult variable to validate. The results of surface precipitation validation shows RSM performance greatly depends upon the type of observation dataset used as it shows higher spatial correlation and more realistic intra-seasonal variability if both land and ocean parts are included in the validation process. The inter-annual variation of precipitation further confirms the RSM skills in capturing observation trend fairly well as compared to HadGEM. The results of 20th century analysis for surface air temperature showed improved performance of both driving parent model (HadGEM) and RSM, which can be attributed to the fact that temperature has large spatial homogeneity therefore global and regional models showed nice reproducibility with slightly warm bias in summer (JJA) and cold bias in winter (DJF).

To determine the future climate change, 21st century analysis is conducted from 2020 till 2100 using two Representative Concentration Pathways scenarios (RCP4.5 and RCP8.5). The result of surface air temperature shows an increasing trend for both RCP4.5 and RCP8.5 scenarios as compared to current climate of South Asia. However, steeper increase is observed for RCP8.5 scenario than RCP4.5. The spatial analysis shows increased temperature in winter of both RCP scenarios, which starts increasing from higher latitudes and progressing towards the tropics. For surface precipitation, the first half of 21st century (2020-2050) showed decreased precipitation in most parts of South Asia while the later half (2051-2100) showed increasing trend especially in mountainous regions of South Asia. The wind vector and precipitation analysis showed that due to the presence of huge mountain chain all around the South Asian region (starting from west of Pakistan to its north than extending towards east making a roof top over Nepal, India and Bangladesh) hinders the precipitation and wind to transcend the topographic borders between South and Central Asia. Due to the windward directions of these mountains for South Asia, precipitation becomes more localized phenomenon as compared to temperature. The leeward sides such as Afghanistan, and parts of Tibet remains drier as compared to monsoon hit South Asia.

To assess the climate extremes in South Asia various indices are analyzed to understand their causes and occurrences. The first index in this context is Hydro-climate Intensity (HY-INT) index with reference to global warming. This index is defined as the multiple of “wet days intensity” and “dry spell length” over a certain period of time. The HY-INT will increase if either one or both of its components will increase. The results of HY-INT for future projections of South Asia show an increasing trend, which is mainly contributed by the increasing wet days intensity over Pakistan, India, Nepal and Bhutan regions. The HY-INT spread over South China and Indonesia (Kalimantan region) is due to the increase in dry spell length during the mid and far future.

Extreme Indices for temperature and precipitation are calculated using the Expert Team on Climate Change Detection and Indices (ETCCDI) definitions. These extreme indices include; One-day maximum precipitation (Rx1day), summer days (SU) when maximum surface air temperature (Tmax) is greater than 25^{o}C and tropical nights (TR) when minimum surface air temperature (Tmin) is greater than 20^{o}C. The RSM simulated indices are validated against the observed global gridded land based temperature and precipitation climate extreme indices (HadEX2). Two reanalysis datasets available on ETCCDI Extreme Indices archive are also included in this study. The result of 20th century evaluation for Rx1day shows more realistic results for RSM simulations as compared to the two selected reanalysis datasets. For extreme temperature indices (SU and TR), RSM shows almost similar spatial pattern when compared to observation and both reanalysis indices. The future projections for Rx1day shows decreasing one day precipitation in near future (2020-2039) which shifts to increasing trend in mid future (2050-2069) and far future (2080-2099) over almost all parts of South and South East Asia. The number of summer days shows steady increase in all the three time slices mentioned above. The spread of increasing SU in future spans 20^{o}N to 40^{o}N and slight increase along the Western Ghats of India. TR will increase in future starting from three points of origins; one will start from South-East Asia, the second will starts from Western Ghats of India and the third will start from Middle East progressing to the western Baluchistan province of Pakistan.

The quantitative analysis of daily precipitation and temperature shows an increase in mean and 99 percentile in future. The results indicate that the regions will suffer from not only the average shift, but also even larger shift in extreme events. Therefore the adaptation measures by the local society need to take these into account.

The entire research is present in dissertation from Chapter 1 to Chapter 6. Chapter 1 is based upon introduction. Chapter 2 describes the setup of sensitivity experiment. Chapter 3 is based upon the 20C analysis of RSM simulations and the validation of its simulations. Chapter 4 describes the future projection studies for South Asia. Chapter 5 describes the extreme indices results for 20C and 21C RSM simulations. The final section is based upon Chapter 6 which includes the conclusions and recommendations.

Table of Content

CHAPTER 1

Introduction

CHAPTER 2

Twentieth Century analysis for CORDEX-South Asia

CHAPTER 3

Twentieth Century Analysis of Temperature and Precipitation Climatology

CHAPTER 4

Assessment of Future climate Projections of South Asia using Representative Concentration Pathways Scenarios

CHAPTER 5

Hydro-temperature Intensities for South Asia and Extreme Indices

CHAPTER 6

Concluding Remarks and Recommendations

Reference

List of figures

List of Tables

CHAPTER 1

Introduction

1.1 General Background

Climate change is often predicted in terms of Temperature or precipitation change. This in tern leads to the broad field of analysis, which includes floods, droughts, heat waves, and their return periods, etc. The correct estimation of their changes can give us useful information that how climate change be like in future. In fact we can say that the whole water cycle depends upon the interactive behavior of these two variables. Therefore, understanding their trends in future is really important.

This global warming is not only identified by an increase in the mean temperature, but is also associated with an increase in interannual climate variability that promotes the occurrence of certain extreme meteorological events, such as heavy precipitation events, droughts, and hot spells (Giorgi and Bi., 2005). Daily mean temperature is generally used as a universal metric for climate change study (Qu et al., 2014).

The United Nations Intergovernmental Panel on Climate Change (IPCC) has been supporting the model-based narrative for two decades which supports the fact that carbon dioxide (CO_2) generated global warming is responsible for extreme weather events such increased heat waves frequency and intensity, precipitation extremes suc as droughts, floods, storms, tropical cyclones, and numerous extreme weather-related events which will continue to increase in future (*Climate Change Reconsidered II: Physical* Science, 2013.For details; http://climatechangereconsidered.org)

The extreme events tendency will increase in South Asia with increased frequency of heat waves, enormous precipitation and more variability in daily precipitation of summer monsoon (Lal et al., 2011).

The extreme weather events related to precipitation (including droughts and floods) are of great interest to many researchers and efforts are being made to comprehend their spatial and temporal variations (Yao et al., 2008). The study of South-east Asia and South Pacific in 1961 to 1998 showed less spatial coherence of extreme rainfall than extreme rainfall for these regions (M.J. Manton et al., 2001). Regions such as US, China, Australia, Canada, Norway, Mexico, Poland and the Former Soviet Union are experiencing more increased precipitation than before (Groisman *et al*., 1999).

The availability of water in terms of its temporal and spatial spread is greatly depended upon rainfall (De Luis et al., 2000). The most recent events (June 2013) are the heavy rainfall observed in Maharashtra (approximately 300% more than the average during 1st to 16th June, 2013 in Mumbai and adjoining areas) and Uttarakhand (approximately 800% more than the average during 13th–19th June, 2013 in Kedarnath and adjoining areas) within states of India (Dube et al., 2014).

In order to project the change in extreme precipitation, climate model data are analyzed and compared to observations (Roth et al., 2014). Future climate shows not only possible changes in the mean climate of the Earth system but also changes in extreme weather and climate events.

There are several studies done on regional scale to study the fate of region in perspective of global warming in future. For example, the regional studies of climate variability under global warming conditions found an increase of summer temperature and precipitation variability over Europe (Schar et al. 2004 and Giorgi et al. 2004). In another regional study which analyzed interannual variability of regional analysis of surface air temperature and precipitation interannual variability in an ensemble of 18 different AOGCM climate change experiments for the 21st century using the IPCC A2 forcing scenario (Giorgi and Bi., 2005). The future projection study of Europe shows in-consistency between three climate variables (precipitation, temperature and wind). There is more confidence for changes in temperature extremes than precipitation while less confidence in extreme wind (Nikulin et al., 2009).

The daily temperature and precipitation observations data of 116 meteorological stations in central and south Asia (for the time period of 1901–2000) suggests that minimum temperature extremes are more consistent with long-term trends than maximum temperature extremes in terms of multidecadal climate variability (Tank et al., 2006).

The observations collected from 1950 onwards shows changes in few extremes. A change in observed extremes depends upon the availability of qualitative and quantitative data and the studies analyzing them which differs from region to region regions and it is different for each regional extreme. Less confidence in observed changes in a specific extreme on regional or global scales does not exclude the probability of changes in extreme (Field et al., 2012). The bigger picture at global scale shows changes in extremes over large areas with dispersed data coverage or none at all. Example of such areas includes parts of central and south Asia. The digital long-term daily data (required for the analysis of extremes) is not available internationally. An increase in mean temperature values cannot be related to the extreme. If both mean and extremes were interrelated than a shift in distribution would have great impact on society and ecosystems (such as less frost days and increased heatwave duration)

(Frich et al., 2002).

South Asia is blessed with diversity of climate, highest mountains in the world, and well-developed Monsoon system. Unfortunately, very few researches in terms of application of modern techniques are applied on this region at large scale. Along with other parts of the world, South Asia is also experiencing the abnormal climate extremes ever before. The report launched by World Bank (2013) namely 'Turn Down the Heat' warned that, although all nations will suffer from the impact of Climate change but the most vulnerable among them will be the sub-Saharan Africa, South Asia, and South East Asia. These climate extremes include heavy precipitation events, heat waves, tropical cyclones, droughts etc. According to another report, 'stories of Impact' by International Finance Corporation (IFC) of World Bank Group for South Asia (2014), brought attention to the melting glaciers of Himalayas which pose great risk of flood outbursts with the increase in sea-level rise specially for coastline countries such as Bangladesh and Maldives along with abnormal monsoon rainfall in South Asia (http://www.ifc.org/).

The past and present climate trends in South Asia can be classified as rising air temperature and an increasing intensity and frequency of extreme events over last century in South Asia. There are number of factors which became the cause of being hit hard by climate change effects and increased green house gases concentration. It can be split into social and environmental practices prevailing in society. The social factors include increasing population growth, urbanization, poverty, food insecurity while the environmental factors include the natural resources degradation, land use, land degradation, biomass burning etc. Therefore, it's a two-way process between humans and environment. The existing socio-economic conditions are fragile and if the disaster of even normal intensity hits the region its impacts goes to a worst scale because of the regional instability. Now if added the current emissions activity in the region than there is no sustainable practice going on large scale. The biomass burning for example can emit considerable amount of particulate matter and related pollutants in the atmosphere. The study conducted in Punjab, India accounts the agricultural crop residues from wheat and rice crops in May and October 2005 have been analyzed for estimating the extent of burnt areas and thereby greenhouse gas (GHG) emissions from crop residue burning.

Another important contributor in causing climate change is the dusts existing in the region mostly contributed from the deserts of western China, Afghanistan/Pakistan, and the Middle East gets transported and accumulates against northern and southern slopes of Tibetan Plateau.

This dust has capability of absorbing solar radiations and heats up the surface air over the elevated slopes. The local emissions emit black carbon and further add to atmospheric heating. This heated air mass rises through dry convection creating a positive temperature anomaly in middle to upper troposphere of Tibetan plateau as compared to the southern parts. This phenomenon also knows as “elevated heat pump” draws the moist air causing south Asian monsoon. Due to the increased dust and black carbon loading in early summer seasons, the rainy period is advancing further in northern India, which leads to intensified rainfall in future. As it is well know saying that climate change respects no borders so the enhanced rainfall over India is associated with the development of an aerosol induced large scale sea level pressure anomaly pattern, which causes the East Asia (*Mei-yu*) rain belt to shift northwestward, suppressing rainfall over East Asia and the adjacent oceanic regions (Lau and Kim, 2006).

These recent reports emphasize the impact of extreme events, which are increasing in the region, therefore it is necessary to study South Asian region in more detail. Climate models, which are designed to give us projections of the future climate, can only compensate this need. It raises a question as which model to be used for this purpose? General Circulation Models; (or GCMs) usually have coarse horizontal resolution (>100km). They can provide us with the large-scale picture of the phenomena such as El-Nino Southern Oscillations (ENSO), Inter-tropical Convergence Zone (ITCZ) Positions and Maiden Julian Oscillation (MJO) etc. On the other hand, if we need to study only some particular region of the earth then the GCMs shows constraint in providing finer details for that region of interest. Therefore, to study one specific region we need Regional Climate Models (RCM) of high resolution, which can compensate our demand for regional study.

In current study, the Regional Spectral Model (RSM) originally developed at the National Center for Environmental Predictions (hereafter referred as NCEP) by Juang and Kanamitsu (1994) is applied to see the South Asian region in high resolution. The outcome of this research will contribute to the World Climate Research program (WCRP), which initiated an effort to generate high-resolution regional information for all land parts of the world. The project under which these efforts are being conducted is known as COordinated Regional climate Downscaling Experiment (CORDEX). In the first phase of the CORDEX, 50km resolution is selected to involve large community to participate in this effort of generating future climate projections for multiple regions of the world (http://wcrp-cordex.ipsl.jussieu.fr). CORDEX-South Asian experiment (hereafter referred as CORDEX-SA) using RSM is initiated with an aim to choose the optimum convective parameterization schemes (hereafter referred as CPs), by determining their skill in reproducing the precipitation over South Asia. Evaluation and selection of best convective scheme can greatly influence the precipitation pattern for future projection studies, which are intended to carry out after the successful completion of sensitivity test experiments.

According to Sabin et al. (2013), South Asian Monsoon (hereafter referred as SAM) is heterogeneous in nature in both time and space. It greatly depends upon the model, that how realistically they can capture such variations. The findings of Gadgil and Sajani (1998) showed the limited performance of coarse resolution Atmospheric GCMs in capturing SAM in the sub-continents. Their findings highlighted the wet precipitation bias over the equatorial Indian Ocean (hereafter referred as EIO), which they attribute to coarse resolution of AGCMs as well as to the physical processes that show inefficiency. Topographic complexity of the region including Western Ghats of India, Myanmar Mountains and northern Pakistan plays an important role in shaping the monsoon mechanism. Although, previous researches have been carried out to use multiple model options for example selecting multiple CPs in order to get reasonable precipitation trends, but they used mostly AGCMs or Atmosphere-Ocean coupled models featuring large-scale phenomenon (e.g., Chao and Deng., 1998; Lee et al., 2003; Park et al., 2010, Ham and Hong., 2013) . Our research is different from other CPs studies in a way that it is applied on more regional level using RSM to first capture the event of 26 July 2005 when Maharashtra, Mumbai received 944 mm of rain in 18 hours. 1100 people died in the metropolis state of India. Other damages included the crop losses of approximately 5.5 lakh hectares with 20,000 hectares of top fertile soil washed away by floodwater. In terms of property damage, 357,917 houses were partially damaged while 14,142 houses were completely damaged. This event is considered to be the worst disaster in 100 years according to the official reports by the Government of Maharashtra (http://mdmu.maharashtra.gov.in, Retrieved on 11 November 2014). To analyze the skill of four convective schemes for this heavy precipitation event become the motivation for CPs evaluation of RSM. The time period selected for CPs evaluation is from 25 July till 28 July 2005, with 24 July 2005 as a spin-up day. Four days average of all selected schemes will be discussed in more detail in section 2.1 Along with the selection of convective schemes, which plays an important role in reproducing precipitation closer to global driving field, the dynamic downscaling approach which nests the RCM over GCM in the domain of interest sometimes create systematic biases in newly formed regional model domain. In order to remove or minimize those biases multiple approaches are adopted. According to Xu and Yang. (2012), reanalysis driven RCMs are supposed to carry less biases than GCM driven RCMs, and vice versa. In both cases, facing bias is an indispensable part of downscaling. In case of obtaining future projection for a particular region, relying on GCMs as source of Lateral boundary conditions for RCMs is the only choice left, therefore we adopted a method by creating a combination of reasonably performing CPs with bias correction methods used in RSM.

In the history of RSM, the systematic biases are minimized by Kanamaru and Kanamitsu (2007) using the combination of spectral tendency damping correction and areal averaging of temperature, humidity and pressure. This correction method left the lateral boundary relaxation very fragile. Their correction method becomes popular as Scale Selective Bias Correction Method (SSBC) in RSM community. (For more details please see; Kanamaru and Kanamitsu., 2007). Kanamitsu et al. (2010), refined the SSBC method by replacing the spectral tendency nudging with field nudging, which removed the errors of large-scale inter-annual variability of seasonal mean. This field nudging is applied only to the rotational components of wind. The modified method reduces synoptic to planetary scale errors of the model. Their results showed the improvements in analysis field variables such as geo-potential height, temperature and wind at 500hPa agreeable with global analysis. However, the model-diagnosed variables (such as surface precipitation and near surface temperature) do not showed as great improvements in this category. This method by Kanamitsu et al. (2010), used by default in RSM, will be referred as SSBC_Def hereafter.

Chang et al. (2012), revised the RSM SSBC_Def method (hereafter referred as SSBC_New). SSBC_New method applied full wind nudging along with vertically weighting damping coefficient method instead of height independent damping coefficient of SSBC_Def. The results of SSBC_New showed wind fields closer to the driving global analysis over East Asia, even though at the same time it causes distortion of temperature and geo-potential height. SSBC_New gradually reduces the vorticity nudging from model top to the ground, which showed better results in terms of precipitation capturing behavior of the model. The vertically weighting damping coefficient applied in SSBC_new gave relaxing time of less than 2 hours at 800 hPa and above, while the relaxing time is greater than 6 hours below 850hPa (See Chang et al.

(2012), for details). 10 years of June-July-August (hereafter referred as JJA) simulations for their CORDEX-EA experiment further confirmed the superiority of SSBC_New over SSBC_Def in terms of capturing Monsoonal rainfall over East Asia quite well. The following chapters are categorized in the following order; Chapter 2 will describe the setup of sensitivity experiment in more details. Chapter 3 will base upon the 20C analysis of RSM simulations and the validation of its simulations observation and reanalysis datasets. Chapter 4 describes the future projection studies for South Asia. Chapter 5 describes the extreme indices results for 20C and 21C RSM simulations. Conclusions and recommendations are described in Chapter 6.

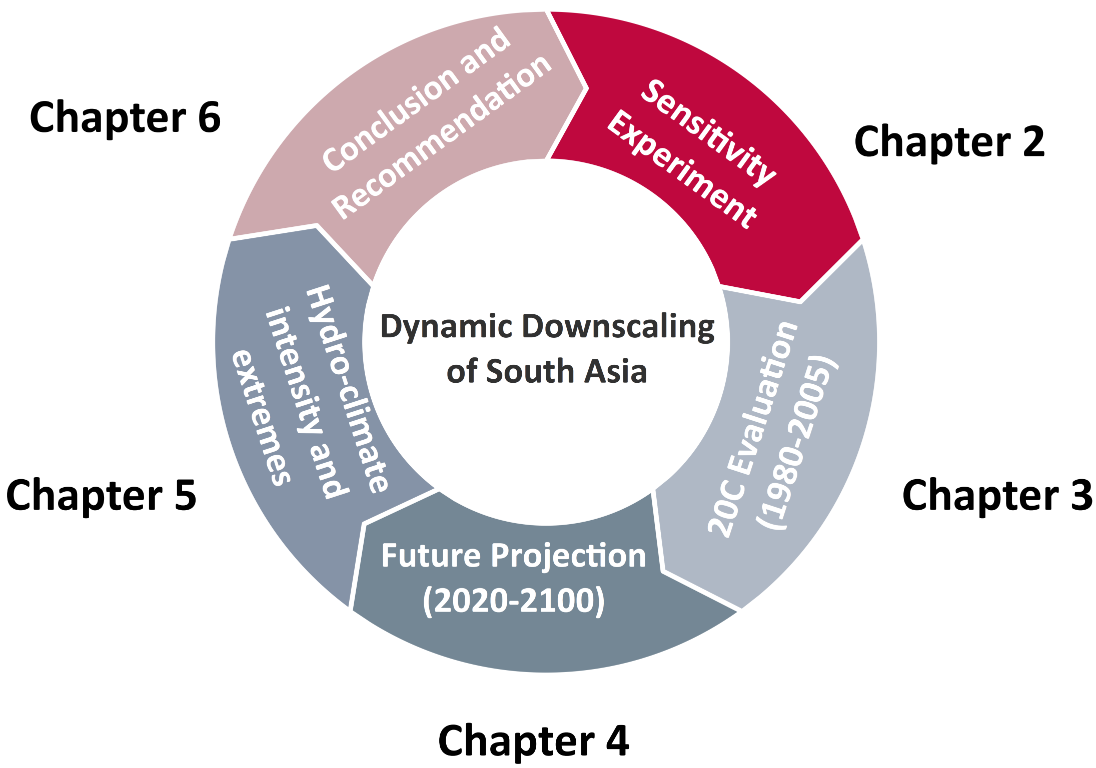

Figure 1. Schematic description of Thesis chapter's summary

CHAPTER 2

Twentieth Century analysis for CORDEX-South Asia

2.1 Sensitivity Experiments

2.1.1. Introduction

The current study is an extension of the SSBC schemes analysis over the domain of CORDEX-SA. This research will be more focused on South Asian Monsoon, which is popular in the field of hydro-climate science. Intergovernmental Panel of Climate Change (IPCC) describes monsoon as 'the seasonal reversal of wind due to the differential heating of land and ocean in tropical and sub-tropical regions causing precipitation mostly over the land' (http://www.ipcc.ch/publications_and_data/ar4/, Retrieved on 1 November, 2014). The clear mechanism of these southwesterly winds is still not yet understood but it clearly highlights the importance to study the wind and precipitation in details as they seems to act as controlling factors in shaping this phenomenon in the region. The sensitivity experiment is based on the evaluation of downscaling of National Centers for Environmental Prediction (NCEP) / Department of Energy (DOE) Atmospheric Model Intercomparison Project (AMIP-II) reanalysis-2 (hereafter referred as R-2) global analysis data using RSM over South Asian region. The structure of this chapter is as follows; Section 2.2 is divided in to two parts. Part 2.2.1 will describe the setup for convective scheme experiment while section 2.2.2 will give the detail description about the SSBC methods applied in this evaluation experiment. Section 2.3 will be based on results obtained from the both experiments focusing summer of 2005 and then 10 years summer climatological comparison between SSBC methods. Section 2.4 will give the summary and conclusions.

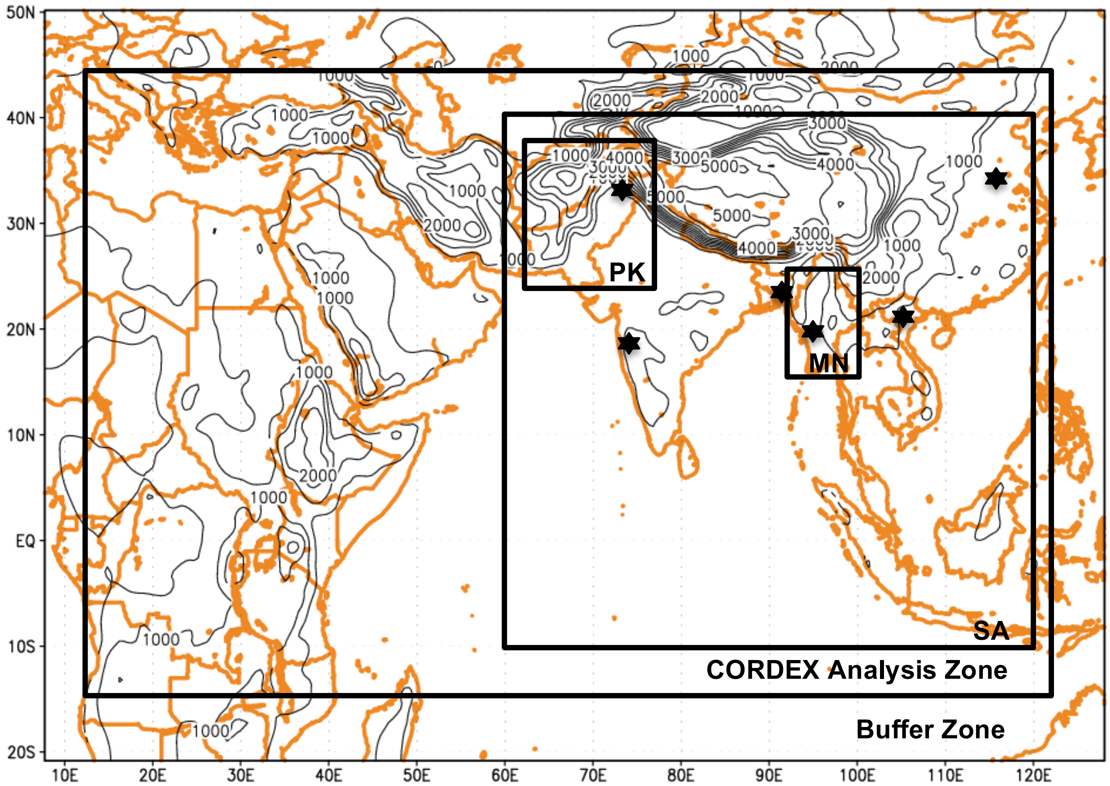

Fig2.1 Regional model domain and orography (m) of downscaling experiment for CORDEX-South Asia. Analysis zone with its multiple sub-domains is used in this study excluding the buffer zone (five grid columns from each side). Black Stars indicates the sites selected for extreme event study. Results for extreme events are shown in Fig.2.7.

2. 2 Experimental Setup

Figure 2.1 shows the downscaling experiment domain for CORDEX South Asia (hereafter referred as CORDEX-SA), which extends from 7^{O}E to 128^{O}E and 20^{O}S to 50^{O}N. The horizontal grid spacing is approximately 50km. Five grid columns from all sides are considered as buffer zone while the main analysis is performed within the analysis zone. The major CORDEX-SA domain is further divided into multiple sub-domains such as Myanmar (MN) which extended from 92^{O}E to 100^{O}E and 15^{O}N to 25^{O}N, Pakistan domain which extends from 63^{O}E to 77^{O}E and 25^{O}N to 37^{O}N and South Asia (SA) domain which extended from 60^{O}E to 120^{O}E and 10^{O}S to 40^{O}N. The grid points for west-east and north-south is 257 x 169 respectively. There are 28 sigma layers in vertical. R-2, 6 hourly dataset is used for initial and lateral boundary condition (Kanamitsu et al., 2002).

2.2.1 Convective scheme experiment

The relative strength of local forcing's (such as surface topography) and the large-scale circulation influence the regional simulations. The regional model skills are greatly affected by errors associated with large-scale conditions, which are provided as lateral boundary conditions for regional models (Singh et al., 2006).

Both the grid-resolvable forcing and sub-grid processes in the atmospheric models produce precipitation. Cumulus parameterization is the representation of sub grid-scale precipitation processes (Kang and Hong, 2008). There are number of CPS available for regional and global atmospheric models, but they are incapable of resolving the convective clouds. Therefore CPS has been considered as one of the most challenging and uncertain aspects in numerical atmospheric modeling. Each CPS has distinct design history and in some cases, they have completely different conceptual underpinnings (Mapes et al., 2004). The characteristics of the CPS are one of the most important factors in regional climate model that leads to diverse simulation results (Fu et al., 2005).

As mentioned earlier that different CPSs have different principles in representing the cumulus convection, which is due to their different the closure assumption. The selected schemes for this research study and their closure assumptions are described as follows;

Both the SAS and RAS schemes are based on the closure assumption of Arakawa and Schubert (1974) that describes, the convective clouds stabilize the environment as fast as the convective processes destabilize it. Grell (1993) further simplifies this original Arakawa-Schubert scheme with a single cumulus updraft/downdraft couplet within a single grid cell, the resulting scheme being termed the SAS scheme after further modifications at National Center for Environmental Prediction (NCEP) (Pan and Wu, 1995; Hong and Pan, 1998; Park and Hong, 2007). The main differences between the SAS and RAS schemes are two components: the clouds model and the treatment of downdrafts. The SAS scheme allows only one type of cloud, while the RAS scheme allows multiple clouds with different tops. The SAS considers saturated downdrafts on the basis of empirical formulation whereas the RAS does not. Due to these differences, models produce different vertical heating and moistening profiles and precipitation patterns. The trigger function for the SAS uses the parcel buoyancy method, whereas the RAS uses the relative humidity near the surface (Ham and Hong, 2013).

The CCM scheme (Zhang and McFarlane, 1995) is based on a plume ensemble approach in which it is assumed that an ensemble of convective-scale updrafts and their associated downdrafts may exist when the atmosphere is conditionally unstable in the lower troposphere. The updraft ensemble, composed of plumes rooted in the planetary boundary layer, can penetrate into the upper troposphere until they reach their neutral buoyancy levels. Convection occurs only in the presence of convective available potential energy (CAPE), which is subsequently eliminated due to convection at an exponential rate using a specified adjustment time scale. Zhang and McFarlane (1995) showed that the CCM scheme significantly improves the precipitation, surface evaporation, and surface wind stress in the tropical convective regimes, particularly in the western Pacific warm pool, compared with the previous version, i.e., CCM2. CCM scheme is further revised by Zhang and Mu (2005), but the original version is used in this study.

The KF2 scheme (Kain, 2004) is an updated version of the original KF scheme (Kain and Fritsch, 1990). In the KF2 scheme, the closure is based on the CAPE for an entraining parcel, which provides reasonable rainfall rates for a broad range of convective environments. In addition, the updraft algorithm has also been modified with a specified minimum entrainment rate and formulations to permit variability in the cloud radius and cloud-depth threshold for deep (precipitating) convection. The KF2 scheme has been widely used in meso-scale models (e.g., WRF model), successfully applied to meso-scale studies (e.g., Ridout et al., 2005), and has been incorporated into real-time forecasts using the WRF (e.g., Byun et al., 2011).

Most of the studies in the past (IPCC 1996) have shown that by using higher spatial resolution to represent local effects of surface topography, vegetation, and land-sea contrast regional climate models can produce reasonable simulations of precipitation, which are highly affected by regional features of the lower boundary conditions. At the same time, numerous studies have also suggested that the regional climate simulations could be very sensitive to the physical parameterizations schemes used. For example, Giorgi (1990) conducted a detailed analysis of summer time regional simulation over the western United States focusing on problem associated with unrealistically intense precipitation simulated over isolated grid points. These are sensitive to the physical parameterizations used in the model and reduce their skill in simulating precipitation over mountainous areas.

Four convective schemes, namely new Kain Fritsch (KF2) scheme from WRF (Kain, 2004) , Relaxed Arakawa Schubert (RAS) scheme (Moorthi and Suarez, 1992) which is the default convective scheme of RSM, Simplified Arakawa Schubert (SAS) scheme (Hong and Pan, 1998), and National Center for Atmospheric Research (NCAR) Community Climate Model version 3 (CCM) scheme (Zhang and McFarlane, 1995), are used in the first experiment to captured the week of drastic heavy precipitation event of Mumbai on 26July 2005. The two most conventional options for CPS studies in RSM are SAS and RAS. The SAS is used to provide the operational medium-range forecasts, while RAS is for seasonal forecasts at NCEP (Kanamitsu et al., 2002). The CCM is widely applied to climate studies (e.g., Zhang and Mu, 2005; Collier and Zhang, 2006) while KF2 scheme is used in meso-scale modeling (e.g., Wang and Seaman, 1997; Ridout et al., 2005).

Four experiments are conducted to equip the RSM with four convective schemes one by one as to obtain the results from 25 July till 28 July 2005 with spin of one day i.e. 24 July 2005. Previous studies have shown that spin up is not important in RSM if it forced by the analyzed data (Park and Hong, 2004). It can be associated to the facts that RSM employs the same physics package as it is used in the data assimilation for the R-2 data. Most importantly, the soil model of Mahrt and Pan (1984) with the same soil and vegetation types is utilized in the RSM used in this study and the global model in generating the R-2 data. Therefore, one-day spin is considered enough. Precipitation in RSM is produced by both large-scale condensation and the convective parameterization schemes. The large-scale precipitation algorithm tests for super saturation in the predicted specific humidity. Latent heat is released as the specific humidity, and the temperatures are adjusted to the saturation values. The scheme does not include a prognostic cloud; however, the evaporation of rain in unsaturated layers below the level of condensation is taken into account (Kang and Hong, 2008).

Tropical Rainfall Measuring Mission (TRMM) 3B42 daily precipitation data of version 7 is used with a spatial resolution of 0.25^{o} x 0.25^{o} for the validation of four convective schemes (For details please see http://mirador.gsfc.nasa.gov/cgi-bin/mirador). One week of experiment is considered enough to capture this event with 100 years return period to confirm the previous findings by Ham and Hong (2013) using four CPs for their sub-seasonal findings for tropical rainfall climatology of ISO. Much importance is given to the SSBC methods as they are applied for the first time in large domain of CORDEX-SA.

2.2.2 Scale Selective Bias Correction experiment

After selecting the CPs based upon its higher Spatial Correlation (hereafter referred as SCORR) with lower Root-Mean-Square-Error (RMSE), both SSBC methods of RSM namely SSBC_Def and SSBC_New are applied to CORDEX-SA domain. The model runs simultaneously for SSBC_Def and SSBC_New for 2005 to assess the performance of both correction methods in capturing the summer of 2005. The results are shown in Fig 2.3 while their description is given in section 2.3 based upon June-July-August (hereafter referred as JJA). The sensitivity experiment for SSBC is further analyzed for 10 years (1981-1990) with 1980 as spin-up year to perform more long-term analysis of both SSBC methods. TRMM monthly 3B43 version 7 with spatial resolution of 0.25^{o} x 0.25^{o} is used for the evaluation for JJA 2005 for both SSBC schemes (For details please see; http://mirador.gsfc.nasa.gov/cgi-bin/mirador). European Reanalysis (hereafter referred as ERA-interim) monthly data (http://data-portal.ecmwf.int/ data/d/interim_moda/) with spatial resolution of approximately 80km (T255 spectral) is used to evaluate the atmospheric variables such as 'zonal and meridional winds', 'relative humidity', 'air temperature' and 'geo-potential height'. 10 years surface precipitation analysis for JJA is validated using monthly precipitation data of Climate Prediction Center (CPC) Merged Analysis of Precipitation (CMAP) with spatial resolution of 2.5^{o} x 2.5^{o} (http://www.esrl.noaa.gov/psd/). The purpose of selecting this dataset is i) it used 5 kinds of satellite estimates such as GOES Precipitation Index (GPI; Arkin and Meisner., 1987), the outgoing longwave radiation (OLR)-based Precipitation Index (OPI; Xie and Arkin.,1997), Special Sensor

Microwave/Imager (hereafter Spencer., 1993) to prepare the monthly averages, ii) it covers both Ocean and Land part iii) it covers large time span from 1979 till present, which meet our selected time range of 1981-1990. The results of both experiments are discussed in section 2.4 below.

2.2.3 Extreme Events

Daily surface precipitation (mm day^{-1}) of Asian Precipitation – Highly- Resolved Observational Data Integration Towards Evaluation of the Water Resources (APHRODITE) version 1101 (Yatagai et al., 2012) hereafter referred as APHRO, for 10 years data is compared with R-2, SSBC_Def and SSBC_New using precipitation bins of ranges such as 0-10, 10-20, 20-30, 30-40, 40-50, 50-60, 60-70, 70-80, 80-90 and 90-100 respectively. (In order to visualize the extreme precipitation bin, we excluded the results of first 4 bins from the current analysis). Fig.7a and 7b shows the results of extreme event analysis. Black star signs in Fig 2.1 indicate the location of 6 selected sites in the SA domain for extreme event analysis. These sites are selected on the basis of their importance in the regions during SAM. Site 1 represents northern part of Pakistan, which receives heavy rainfall in SAM; site 2 represents Mumbai, India, which remain our focus in earlier half of this chapter. Another importance of this site is its close proximity to Western Ghats of India, (which receive heavy rainfall in SAM). Site 3 represents Chittagong, Bangladesh which closer to the Bay of Bengal (which experience tropical cyclones during SAM). Site 4 represents Myanmar region, which receive the maximum effects of SASM due to its topographic interactions with seasonal winds. Site 5 represents Hanoi, Vietnam, which is prone to flooding due to heavy rainfall in summer. Site 6 represents Nanjing, China neighboring Yangtze river to its north-west side, which is the longest river in Asia and third longest in the world (http://global.britannica.com, Retrieved on 10 November, 2014). Overall, the purpose of conducting this experiment is to analyze the tendency of R-2 in general and SSBC_Def and SSBC_New methods in specific, to capture the extreme precipitation events and to evaluate their performance with observation and driving global analysis.

2.3 Results and discussion

2.3.1 Convective scheme

Table 2.1 presents the results of four convective schemes for multiple domains of CORDEX-SA mentioned in Fig 2.1. Among the four convective schemes, the highest SCORR with lowest RMSE is shown by SAS convective scheme for almost all sub-domains along with the major CORDEX-SA analysis zone. Exceptions are found for PK domain where KF2 outperforms the other convective schemes with higher SCORR (0.24), while the lowest RMSE (4.58 mm day^{-1}) is shown by CCM scheme. If we look at Fig 2.3 (a) using TRMM observations, it can be seen that in relation to other South Asian countries, Pakistan receives less summers rainfall mostly concentrated in the northern parts while the rest of the country shows arid to semi-arid climate especially towards south western parts which include Baluchistan province.

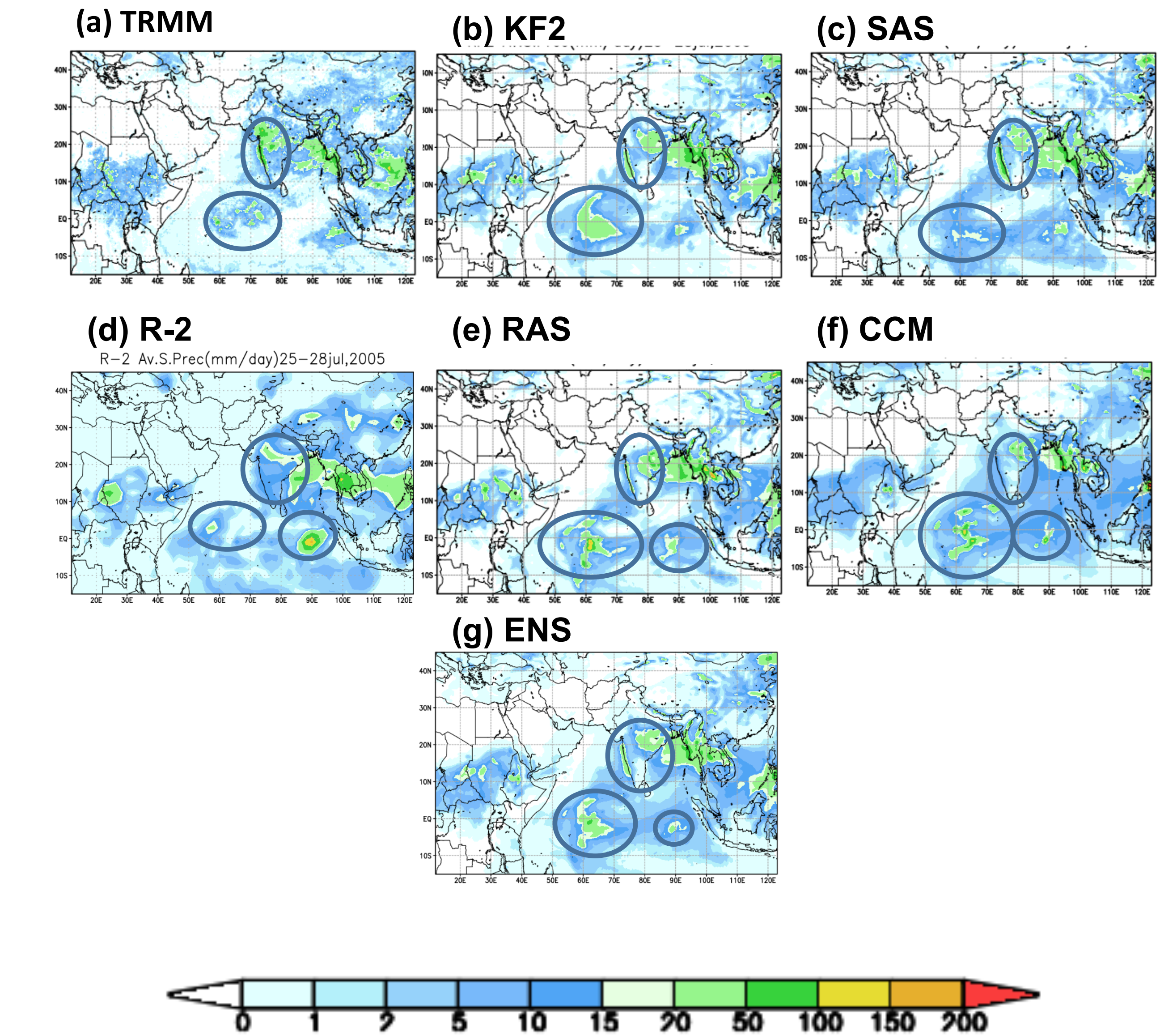

Fig 2.2 Comparison of (a) TRMM daily precipitation data (3B42_V7) in mm day^{-1} with surface precipitation of four convective schemes, such as (b) KF2, (c) SAS, (e) RAS and (f) CCM (d) Reanalysis-2 (R-2) and four CPS ensemble (f) ENS for four days average (25-28 July, 2005).

Table 2.1 Root-Mean-Square-Error (RMSE) in mm day^{-1} and Spatial Correlation (SCORR) for four convective schemes and their ensemble used for four days average precipitation (mm day^{-1}) from 25-28 July 2005 against TRMM 3B42_V7 Daily precipitation data.

Domain	Convective Scheme	RMSE	SCORR
CORDEX-SA			
	KF2	8.84	0.49
	RAS	10.23	0.37
	SAS	**7.95**	**0.54**
	CCM	9.89	0.32
	ENS	8.27	0.49
South Asia (SA)			
	KF2	11.91	0.44
	RAS	13.75	0.31
	SAS	**10.56**	**0.51**
	CCM	13.01	0.25
	ENS	11.52	0.43
North Pakistan (PK)			
	KF2	4.59	**0.24**
	RAS	4.80	-0.03
	SAS	4.67	0.20
	CCM	**4.58**	0.19
	ENS	4.60	0.23
Myanmar (MN)			
	KF2	27.62	0.46
	RAS	32.89	0.05
	SAS	**17.82**	**0.71**
	CCM	25.25	0.36
	ENS	22.91	0.48

The regions with no or little precipitation pose great limitations on CPs and it may suggest that for the case of PK, the cloud formation processes are different than other regions of South Asia. Another important finding of this analysis is identifying the inadequate performance of RSM's default RAS convective schemes in complex terrain areas of MN and PK. In case of PK, the correlation falls to negative value. Overall, the evaluation results of four CPs for South Asia suggested the SAS is superior than other convective schemes. Therefore, we equipped the model with SAS convective scheme and applied SAS convective scheme on both SSBC methods. The results of this finding are presented in section 2.3.2.

The results for APHRODITE showed similar results except for KF2 . In contrast to TRMM validation, the APHRODITE shows that KF2 has higher SCORR and less RMSE for northern Pakistan.

Table 2.2 same as table 2.1 but with APHRODITE comparison.

Domain	Convective Scheme	RMSE	SCORR
South Asia (SA)			
	KF2	11.24	0.44
	RAS	13.47	0.32
	SAS	**9.09**	**0.54**
	CCM	11.37	0.31
	ENS	10.27	0.44
North Pakistan (PK)			
	KF2	**1.71**	**0.51**
	RAS	2.03	-0.04
	SAS	1.93	0.48
	CCM	1.84	0.27
	ENS	1.71	0.50
Myanmar (MN)			
	KF2	31.54	0.27
	RAS	34.92	0.08
	SAS	**18.88**	**0.48**
	CCM	25.73	0.28
	ENS	25.43	0.29

The vertical profile of air temperature and relative humidity for all the convective schemes and their ensemble is studied to determine the physical processes causing the sensitivity. Three domains are selected; Equatorial Indian Ocean (50-75^{o}E, 10^{o}S-10^{o}N), India (70-90oE, 10N-25N), and Myanmar, Thailand and laos region (85-110^{o}E, 10^{o}N-25^{o}N). These regions are selected due to the precipitation bands observed over this region in four days average time scale.

For equatorial Indian Ocean, the temperature bias is similar between the entire convective scheme and their ensemble. At lower atmospheric level the biases have similar trend while at higher atmospheric levels (200hPa and 100hPa), SAS shows

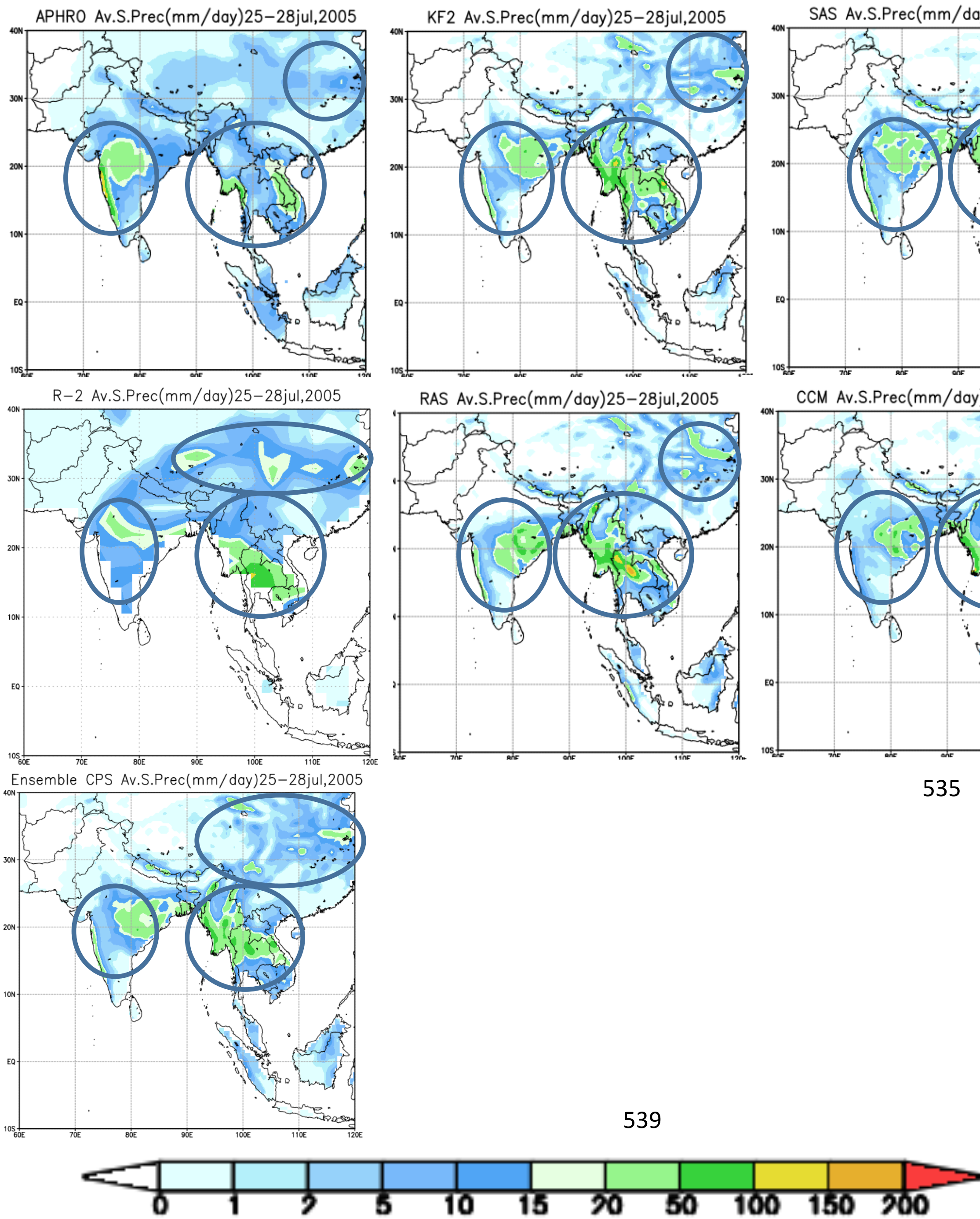

Figure 2.3 Same as figure 2.2 but with APHRODITE comparison.

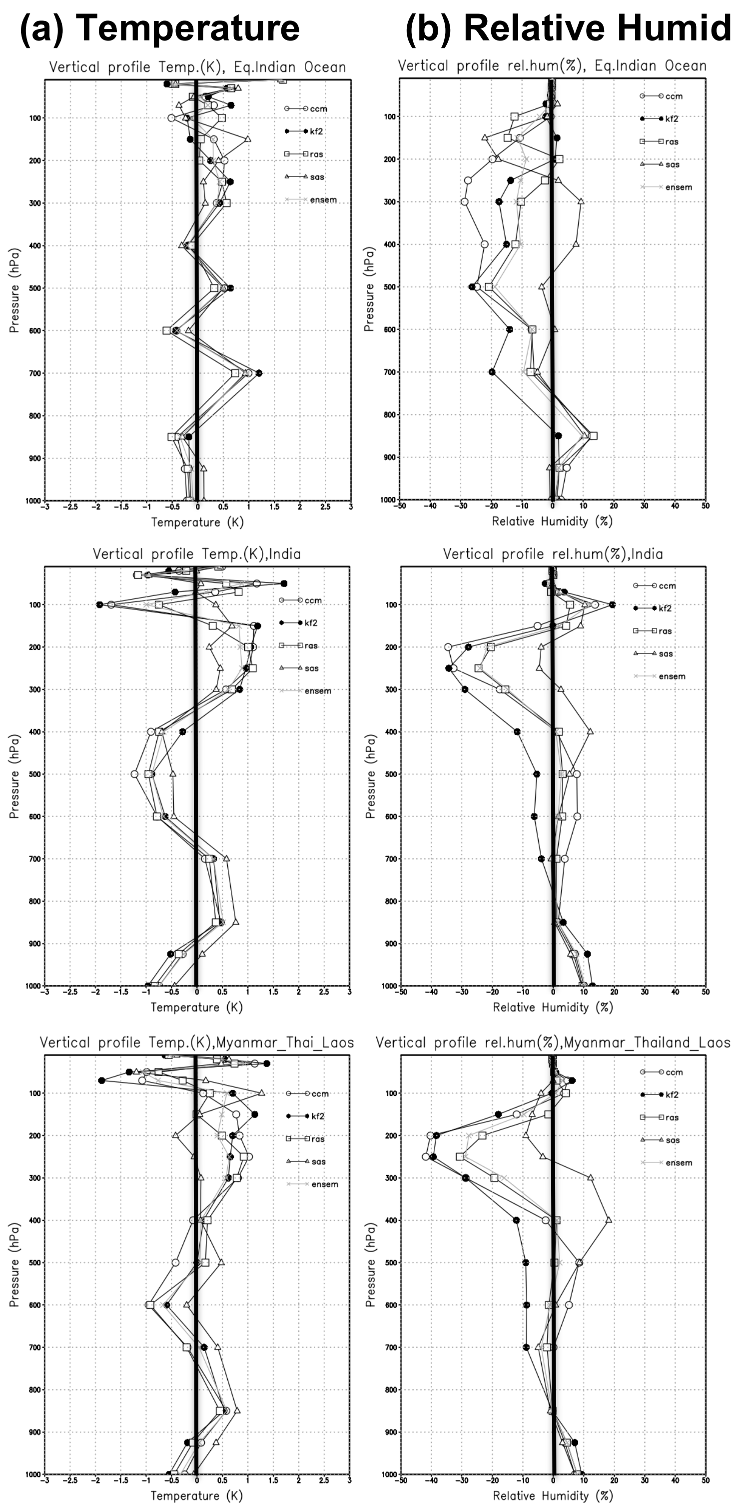

Figure 2.4 Vertical profile of CPS biases from Reanalysis-2 for (a) temperature (^oC)and (b) relative humidity (%)

distinct warming than other convective schemes. However, the relative humidity shows distinct bias differences among them. The difference between SAS and RAS is evident in the vertical profile experiment, which can be contributed to their different cloud type and downdraft mechanism. Due to this difference we can see the different vertical heating and moistening profile by these two schemes as well as their different precipitation patterns discussed earlier. In contrast to due studies conducted by Kang and Hong, 2008 the results for south Asian study shows more dryness of CPS over land than over ocean.

The physical ensemble approach have scores closer to KF2 schemes but not better than SAS which suggests that application of ensemble experiment not necessarily enhance the model skills as it is greatly influenced by the under or overestimations of participating members within ensemble.

The reason why SAS is better than other can be attributed to the fact that this scheme has been optimized for a longer time in the RSM . Similarly the second better performaning scheme is widely being tested and get updated time to time by mesoscale community usually by means of MM5 model. KF2 in particular is designed to resolve the mesoscale features which gave nice results in topographic region of northern Pakistan. Therefore, due to continuous up gradation and improvement these schemes have relatively better skill in capturing the precipitation events quite well. It is also being proved by the findings of Kang and Hong (2008) studies in East Asia.

The results of comparison between APHRODITE and convective schemes shows that three out of four convective schemes are able to capture the Mumbai precipitation event.

These include KF2, RAS and SAS respectively. CCM is unable to capture the Mumbai rainfall. The added value of downscaling can be seen when compare the boundary condition (Reanalysis-2) with four convective schemes. It is evident over China and eastern parts of India. Among four convective schemes, SAS shows closer precipitation to observation data over Myanmar and Thailand region. Comparison with TRMM dataset over equatorial Indian Ocean shows the SAS convective scheme closer to observation as compared to other convective schemes.

In conclusion, SAS captures the precipitation trends fairly well followed by KF2, RAS and than CCM respectively. Further high resolution is needed between Western Ghats, Vindhya ranges and Saputra ranges of India. Another region where four convective schemes do not resolve the spatial topography is between Myanmar and Vietnam region.

The physical ensemble experiment which consider all four convective schemes showed that the precipitation bias over the equatorial indian ocean does not minimize by considering the ensemble as it combines the over estimations of KF2, RAS and CCM schemes over the equatorial indian ocean thus making it less reliable in this region as compared to SAS convective scheme.

Similarly in comparison with APHRODITE precipitation dataset, the ensemble experiment overestimated the precipitation on parts of Myanmar and Thailand/Vietnam regions due to the over-estimations by KF2,RAS and CCM over these rgions. Although the precipitation amount is less than these aforementioned schemes but it is greater than SAS convective scheme.

It is therefore concluded that physical ensmebles are always not a good choice to get an aggregated picture of a phenomenon. Sometimes due to the large bias by one or more member can overall change the meaning/advantage of ensemble members approach. In this case for example, SAS convective scheme performance is relatively better than the other convective schemes and their ensemble experiment. On the other hand it is also found out that 50km resolution is not enough to resolve the P-shape precipitation band observed in the observation datasets. To resolve the precipitation between western and eastern Ghats of India more higher resolution is needed. Similarly precipitation between Myanmar and Vietnam is not resolved by RSM, which again attributes the limited resolution of model for the smaller hilly regions. It is the reason that we get uniform precipitation band over Myanmar, Vietnam and Thailand region in all four convective schemes as well as the driving reanalysis dataset.

2.3.2 Scale Selective Bias Correction method

The results for SSBC_def and SSBC_New for JJA, 2005 are presented in Table 2.2 and Figure 2.3. R-2 data set for surface precipitation is also included in the comparison to highlight the added value of downscaling over the coarse resolution global data.

Table 2.3 Comparison of RMSE and SCORR of Reanalysis-2, SSBC_Def and SSBC_New compared with TRMM_3B43V7 monthly surface precipitation data (mm day^{-1}) for June-July-August (JJA) and December-January-February (DJF), 2005.

Precipitation	Analysis	RMSE	SCORR
JJA			
	Reanalysis-2	3.61	0.66
	SSBC_Def	3.73	0.63
	SSBC_New	**3.17**	**0.74**

The result of JJA, 2005 for R-2, SSBC_Def and SSBC_New showed highest SCORR (0.74) with lowest RMSE (3.17 mm day^{-1}) for SSBC_New as compared to others. It can be attributed to i) more compatibility of SAS convective scheme with SSBC_New as compared to SSBC_Def , ii) vertically weighting damping coefficient (Chang et al., 2012) improvised the precipitation patterns and bring it more closer to observation. The results for atmospheric variables are shown in Table 2.3. For both wind levels (850hPa and 500hPa), the SSBC_New showed higher SCORR with lower RMSE as compared to default one which can be attributed to the freedom provided by vertically weighting damping coefficient and less freedom by full wind nudging in the SSBC_New method which improved the ageostropic wind components near lower atmospheric levels in tropical and sub-tropical regions compared to SSBC_def which is independent of height and applied nudging only to rotational component of wind and considered vorticity nudging which is more evident in extra-tropics (Chang et al., 2012). This behavior is also considered as an important factor in improving the precipitation, which is consistent with findings by the studies conducted for CORDEX-East Asia (Chang et al., 2012).

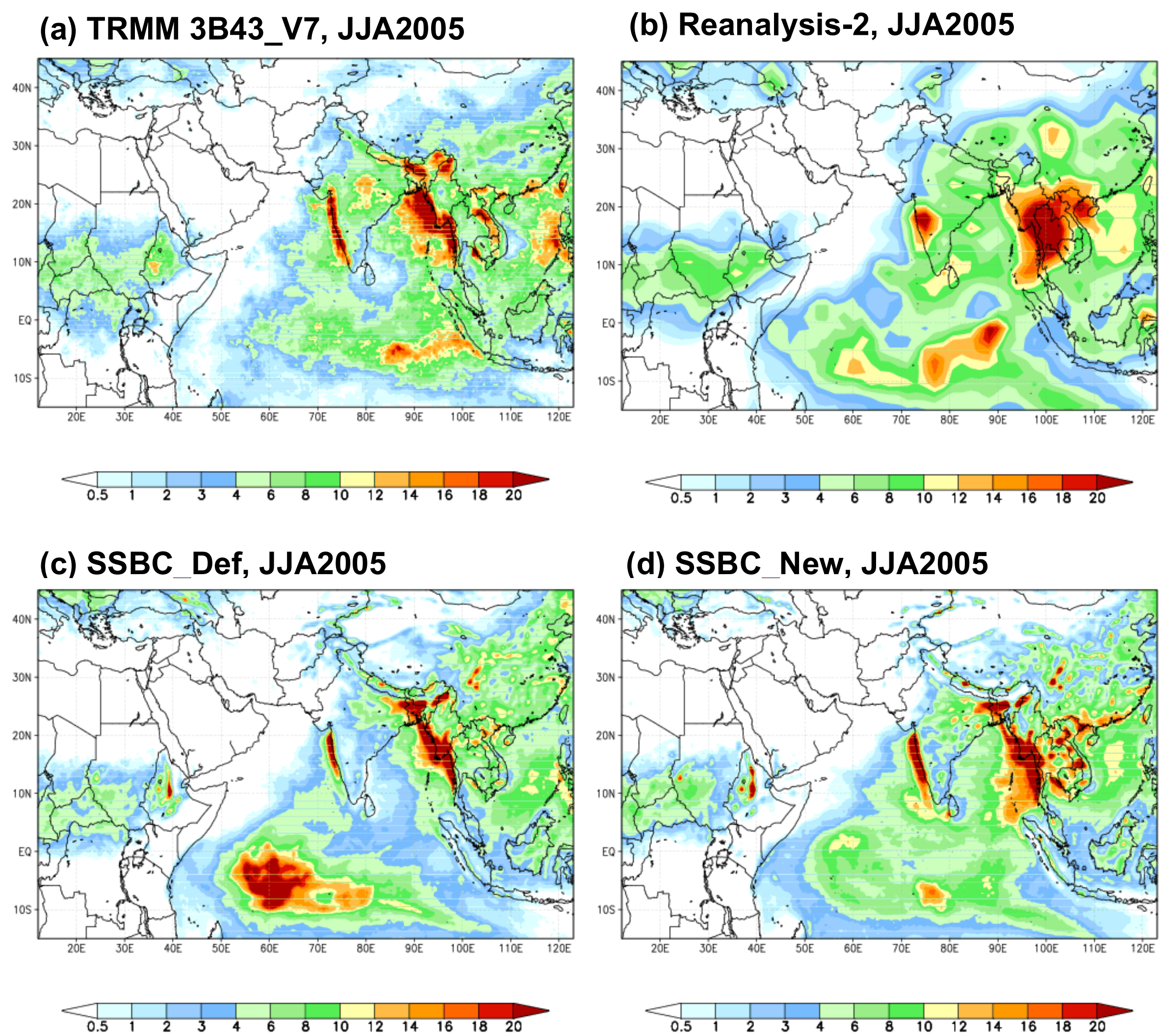

Fig 2.5 Comparison of SSBC_Def and SSBC_New surface precipitation (mm day^{-1}) for JJA, 2005 with TRMM satellite 3B43_V7 surface precipitation (mm day^{-1}) and Reanalysis-2 surface precipitation (mm day^{-1}).

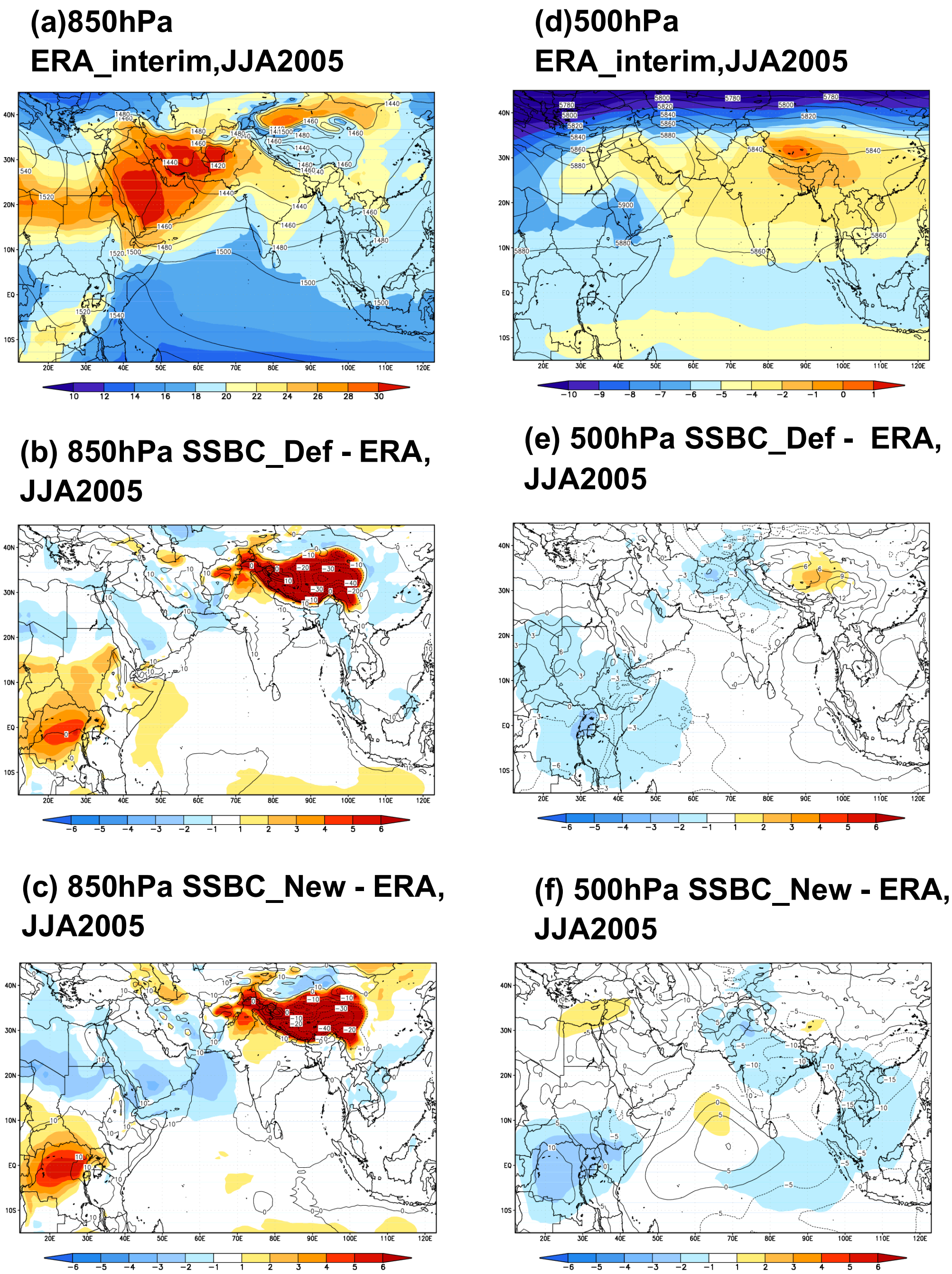

Fig 2.6 Temperature (shaded) and Geo-potential height (contour) difference between SSBC_D vs SSBC_N at 500hPA and 850hPa from ERA-interim Reanalysis data for JJA 2005.

For relative humidity (RH) at 850hPa, the SSBC_def showed better results over SSBC_New which can be indication that for RH at lower levels with damping coefficient of 0.04 hour nudging is well enough to bring it closer to global analysis but at 500hPa SSBC_new outperformed SSBC_Def which can be related to spectral nudging time of less then 2 hours should at least be applied to improve the results at higher atmospheric levels. It can also be related to monsoon mechanism, which bring moisture from the nearby ocean at lower atmospheric levels contributing to RH of the region. The improved precipitation can be associated with improved RH at lower levels as compared to middle or upper atmosphere. The results for air temperature at both levels 850 hPa and 500 hPa showed better results for SSBC_Def as compared to SSBC_New. Same results are obtained for geo-potential height. Both SSBC schemes showed cold bias over the India, Pakistan and central Africa (around Congo region) but the cold bias is more obvious in SSBC_New as compared to SSBC_Def. Under performance of SSBC_New for air temperature and geo-potential height at lower and middle atmospheric levels can be attributed to the full wind nudging which causes distortion of large scale variables.

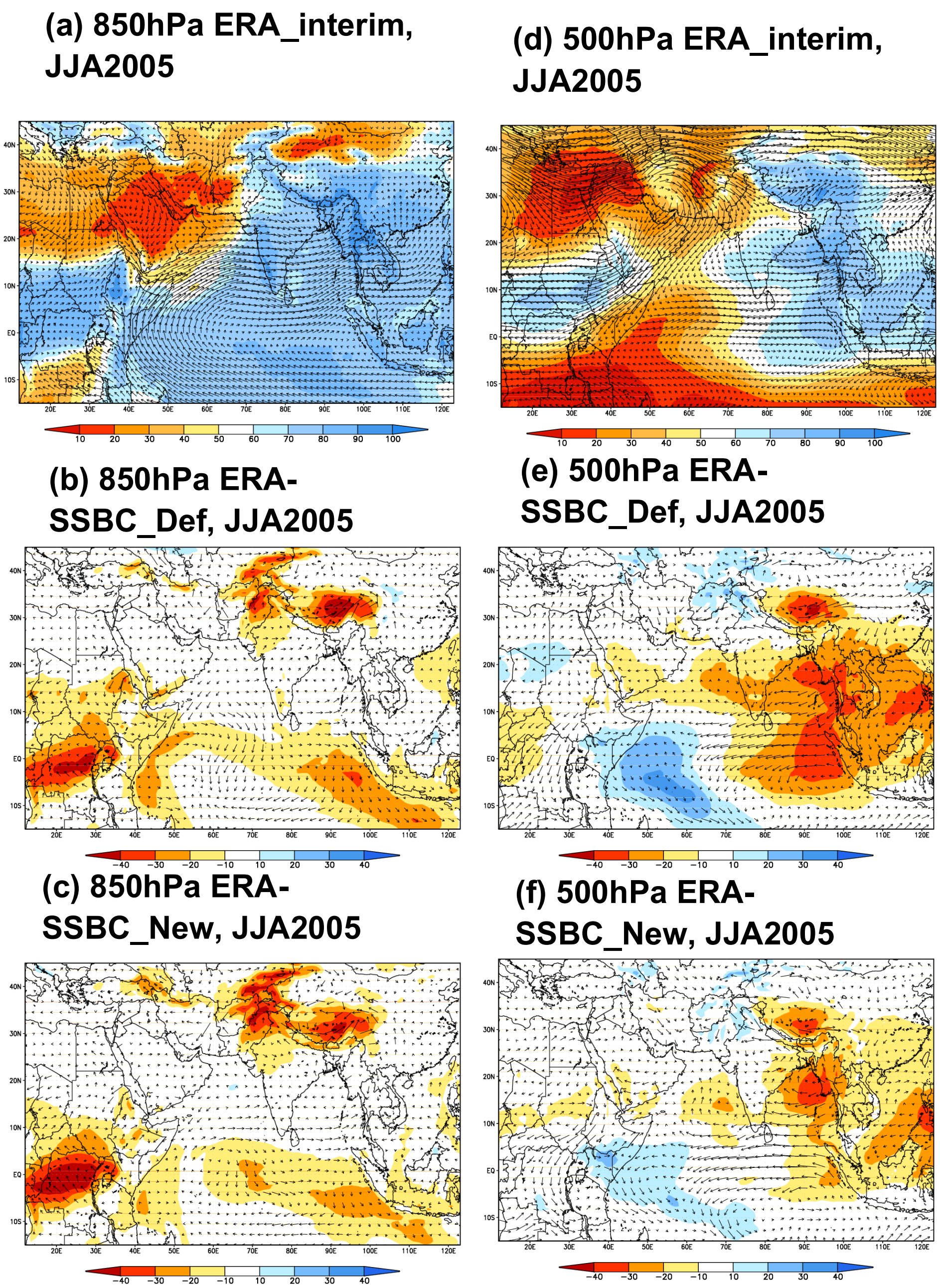

Fig 2.7 Difference between SSBC_Def and SSBC_New at 850hPa and 500hPa for wind vectors (m s^{-1}) indicated as arrows and Relative Humidity (%age) as shaded from ERA-interim Reanalysis dataset for JJA, 2005Temperature (shaded) and Geo-potential height (contour) difference between SSBC_D vs SSBC_N at 500hPA and 850hPa from ERA-interim Reanalysis data for JJA 2005.

Table 2.4 Comparison of RSME and SCORR of SSBC_Def and SSBC_New for variables such as Wind vector ($m\ s^{-1}$), Relative Humidity (%), Temperature (^{o}C) at 850hPa and 500hPa and Geo-potential height from ERA-interim (See figure 4 and 5 for more details).

	SSBC_Def		SSBC_New	
	RMSE	SCORR	RMSE	SCORR
Wind				
850hPa	1.47	0.94	**1.28**	**0.96**
500hPa	1.48	0.90	**1.17**	**0.92**
Relative Humidity				
850hPa	**13.09**	**0.89**	13.48	0.88
500hPa	15.69	0.73	**11.30**	**0.88**
Air Temperature				
850hPa	2.12	**0.88**	**2.11**	0.87
500hPa	**0.85**	**0.96**	0.97	0.92
Geopotential Height				
850hPa	**8.32**	**0.98**	8.44	**0.98**
500hPa	**3.40**	0.99	6.86	0.97

Figure 2.6 represents the 10 years precipitation climatology for JJA. The results followed the 2005 result findings highlighting the SSBC_New as outperformer by showing high SCORR (0.76) and low RSME (2.93 mm day^{-1}) as compared to SSBC_Def. The dry bias found in SSBC_def is greatly minimized by SSBC_new scheme in eastern equatorial Indian Ocean as well as in South China Sea. The wet bias over eastern China also showed significant reduction in SSBC_New. Similarly the wet bias over Ethiopia is reduced in SSBC_New as compared to SSBC_Def. Dry bias is seen in SSBC_New over western part of India which can be related to the cold bias observed in SSBC_New at 500 hPa for temperature as discussed above. Overall, the highest SCORR and lowest RMSE are observed for SSBC_New as compared to SSBC_Def confirming the superiority of new SSBC method over the default one.

Table 2.5 RMSE and SCORR for Surface precipitation of 10 years (1981-90) average for JJA from CMAP monthly data.

Precipitation	Analysis	RMSE	SCORR
JJA			
	SSBC_Def	3.02	0.72
	SSBC_New	**2.93**	**0.76**

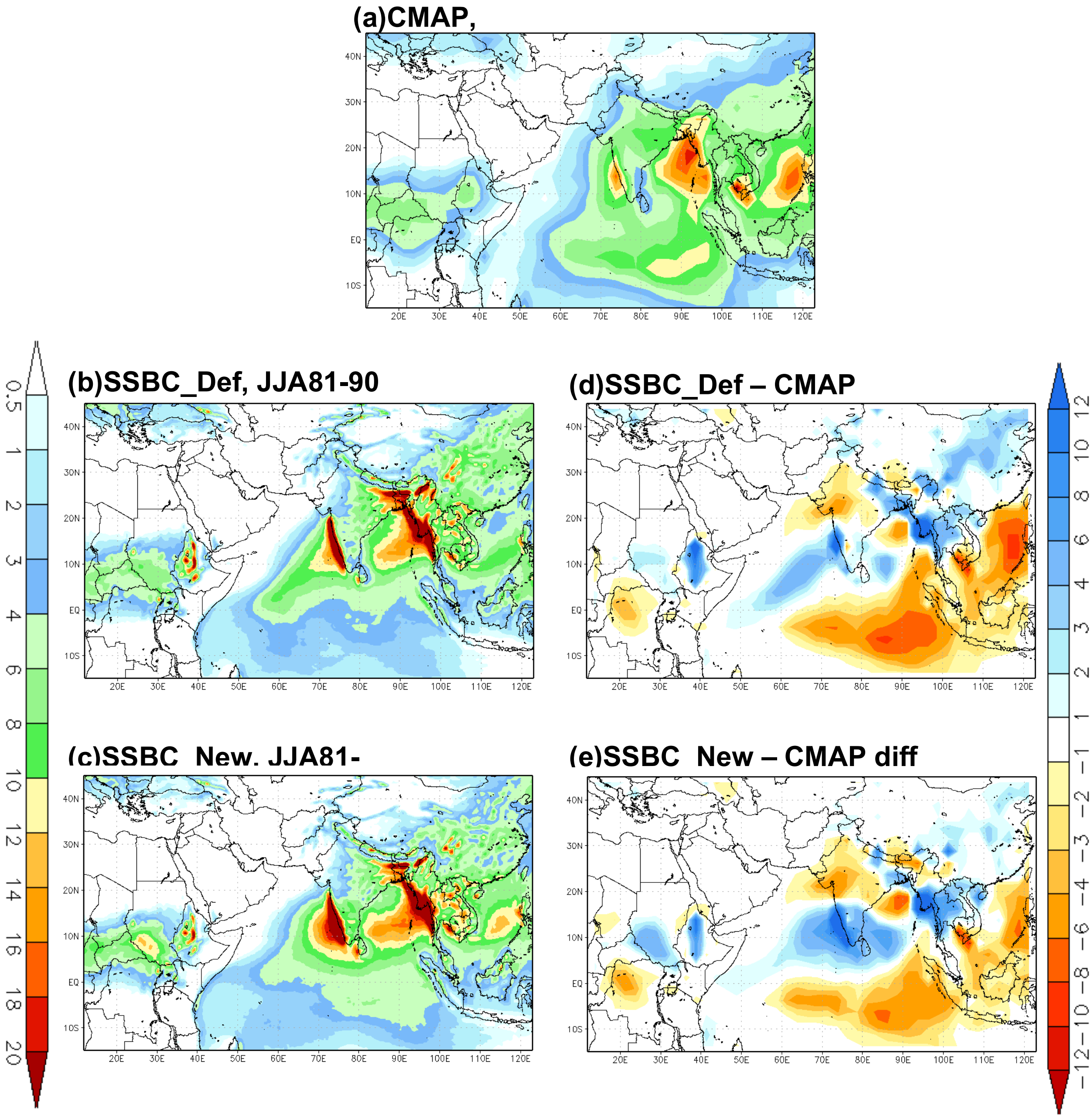

Fig 2.8 Surface Precipitation of (a) CMAP surface precipitation (mm day^{-1}) compared with (b) SSBC_Def and (c) SSBC_New and their difference (e) and (f) respectively, for 10 years average JJA (1981-90) from CMAP.

2.3.3 Extreme events outcomes

The results for 10-years extreme events analysis for daily surface precipitation for six selected sites will be discussed as follows; For Northern Pakistan, both SSBC methods showed over estimations, but SSBC_Def showed more overestimated behavior then SSBC_New specially for bins of extreme precipitation (70-80, 80-90 and 90-above). For Mumbai, India, SSBC_Def showed closer agreement with APHRO for almost all precipitation bins as compared to R-2 and SSBC_New. For Chittagong, Bangladesh overall SSBC_New shows more close association with APHRO then SSBC_Def except for bin 40-50 where SSBC_Def showed improved results. Similarly for Myanmar SSBC_Def showed closer relation to APHRO but as the bins move to higher level, the SSBC_New showed improved results then SSBC_Def. Similar trend is observed for Hanoi, Vietnam and Nanjing, China. The result of this analysis shows the dominance of SSBC_New in capturing higher frequency of extreme events then SSBC_Def which can capture the medium range precipitation bins but show limited performance at higher levels. R-2 shows closer proximity to APHRO in medium range bins while for higher bin it showed usually shows under-estimations or trend more similar to SSBC_Def. Overall, among three competitors, SSBC_New showed improved skills of capturing higher precipitation events quite well as compared to default scheme.

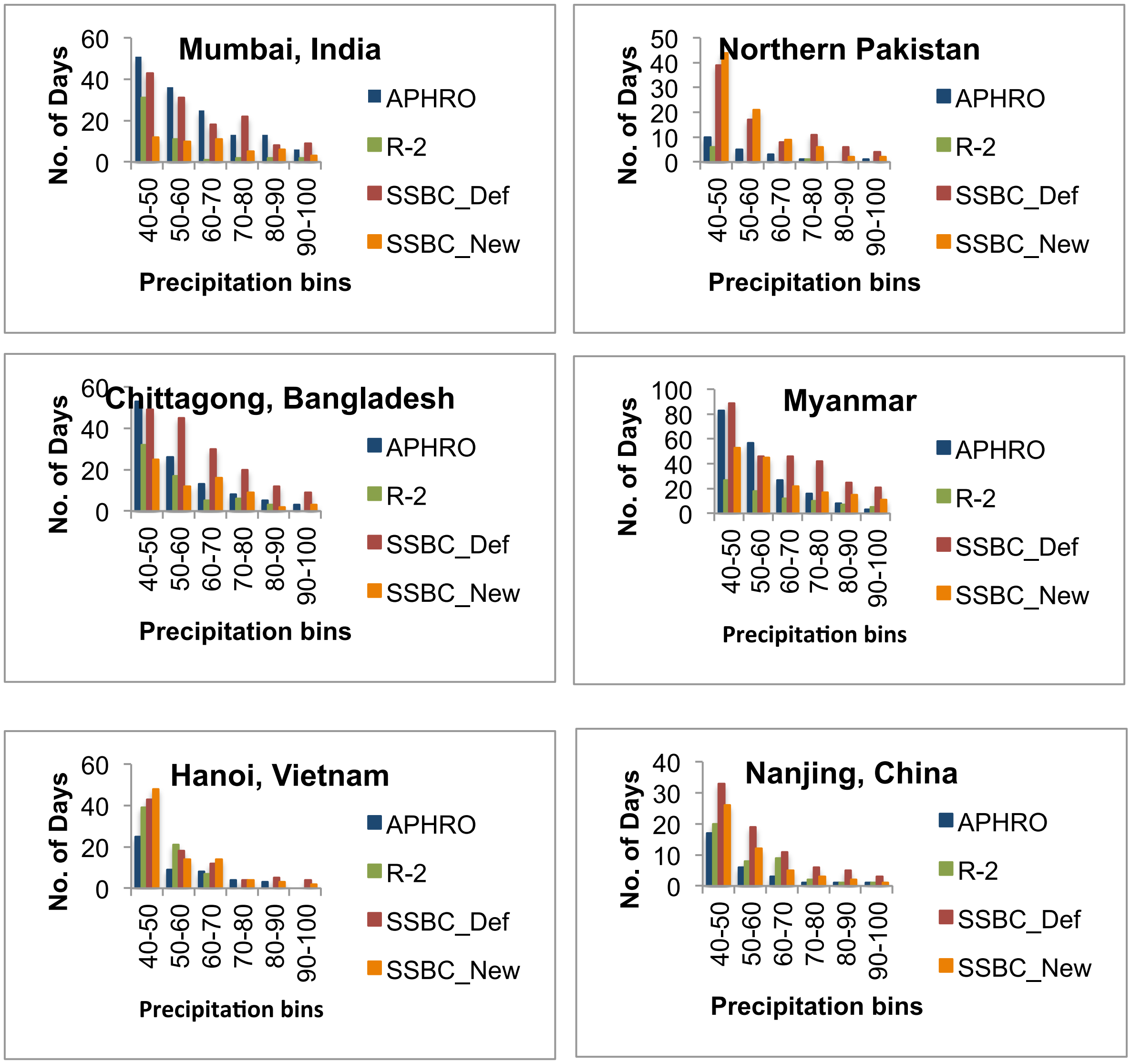

Fig 2.9 Number of Heavy Precipitation events in each bin captured by APHRODITE (APHRO), Reanalysis-2 (indicated as R-2), SSBC_Def and SSBC_New surface precipitation (mm day^{-1}) for time period 10 years. Location of the selected sites can be seen on fig2.1

2.4 Summary and concluding remarks

The sensitivity experiments examined the performance of four convective schemes using RSM to study the CORDEX-SA domain. Four convective parameterization schemes are selected for RSM and applied to the heavy rainfall event which happened in Maharashtra, Mumbai, India on 26 July 2005 which proven to be the great disaster for the metropolitan. Time period ranging from 25-28 July is selected. The result of four convective schemes in terms of lower RMSE and higher SCORR, highlighted SAS convective scheme as out performer in major as well a multiple sub-domains of CORDEX-SA except for KF2 which showed better performance in PK domain along with CCM scheme. It can be inferred from these results that SAS scheme perform well in plain and areas of rather simple topography while the KF2 and CCM is more suitable for regions with complex topography such as Northern Pakistan which can be explored in future studies. Among the SSBC methods, the SSBC_New showed great improvements then the default SSBC_Def scheme in terms of precipitation and wind at both lower and middle troposphere. It can be attributed to the application of vertically weighting damping coefficient and full wind nudging applied in new scheme, which gives more freedom at lower tropospheric levels especially in tropical and sub-tropical regions where wind components are more important than vorticity. The drawback of new process is the distorted large-scale fields for temperature and geo-potential height at 850 hPa and 500 hPa levels. Overall, the results are consistent with the findings of Chang et al., (2012) for CORDEX-EA domain. It can be inferred that this SSBC_New is applicable to CORDXE-SA as well. The use of SSBC_New scheme is dependent on the users purpose. In current research, the improved precipitation and wind pattern give satisfactory results, which fulfill the requirements of conducting preliminary sensitivity experiments, which act as a milestone for long-term reliable future study.

CHAPTER 3

Twentieth Century Analysis of Temperature and Precipitation Climatology

3.1 Introduction

This chapter is described the detailed description of 20C analysis. The analysis will be based upon the temperature and precipitation climatology comparison to see the performance of RSM in capturing the general climate trend over the region.

3.2 Experimental Design

The twentieth century simulations are conducted using RSM for CORDEX-SA domain with horizontal resolution of approximately 50 km. The model domain is shown in figure 2.1 of chapter 2 following the protocol of CORDEX-SA. The boundary condition for 20C run (1980-2005) is provided by HadGEM2-AO coupled model (hereafter referred as HadGEM) of National Institute of Meteorological Research of Korea Meteorological Administration (Baek et al., 2013). The horizontal resolution of HadGEM is composed by an atmospheric component with resolution1.875x1.25 while the vertical resolution is 38 vertical levels with 38km of top altitude and an ocean part is 1^{o} horizontal and 40 vertical levels (Lee, J.W. et al., 2013). The convective parameterization scheme applied for this study is SAS convection scheme (Hong and Pan, 1998). The land surface model is by National Centers for Environmental Prediction (NCEP)-Oregon State University-US Air Force-National Weather Service office of Hydrological Development (NOAH). SSBC_new method is applied to avoid distortion of large-scale features (Hong and Chang, 2012) and its satisfactory performance in sensitivity experiments.

The validation of model results is done for variables such as near surface temperature (^{o}C) and surface precipitation (mm day-1). Near surface temperature is validated using Climate Research Unit (CRU) TS 3.21 with resolution of 0.5 x 0.5 degree (http: //badc.nerc.ac.uk/view/badc.nerc.ac.uk). For surface precipitation, large set of precipitation observation datasets is utilized to validate the results. It is done because of the fact that precipitation observations in south asia show great variability in time and space so the use of ensemble observations will help us to understand the RSM results in a better way. The observation datasets for surface precipitation over land and ocean includes Global Precipitation Climatology Product (GPCP) with spatial resolution of 2.5 x 2.5 obtained from NOAA/OAR/ESRL PSD, Boulder, Colorado, USA, from their website at http://www.esrl.noaa.gov/psd/, Tropical Rainfall Measuring Mission (TRMM) Multi-Satellite Precipitation Analysis, 3B43_V7 monthly data with resolution of 0.25^o x0.25^o for time period of 1998-2005 (TMPA; Huffman et al. 2007). Climate Prediction Center (CPC) merged analysis of precipitation (CMAP) with spatial resolution of 2.5^o x 2.5^o. CMAP Precipitation data is obtained from the NOAA/OAR/ESRL PSD, Boulder, Colorado, USA, from their website at http://www.esrl.noaa.gov/psd/. Land only precipitation datasets include Global Precipitation Climatology Center (GPCC) data with spatial resolution of 0.5^o x 0.5^o (http://www.esrl.noaa.gov/psd/data/gridded/data.gpcc). Daily precipitation analysis focusing extreme events are validated by APHRODITE daily precipitation with spatial resolution of 0.5^o x 0.5^o for Middle Asia V1101 (Yatagai et al., 2012). The model-simulated variables are usually compared with observations to ensure their applicability for future projections (Wang et al., 2004). Therefore, great emphasis should be give to 20C analysis for reliable future projections.

3.3 Results and Conclusion

Section 3.2 is further sub-divided to 3.2.1 and 3.2.2 describing the near surface temperature and surface precipitation climatology's of 20C analysis. Section 3.3 will be based upon conclusions.

3.3.1 Near Surface Temperature Climatology

The near surface temperature of RSM is compared with CRU observation data and driving global model HadGEM.. The analysis is conducted for summer (JJA) and winter (DJF) climatology for 26 years. The results are shown in figure 3.1

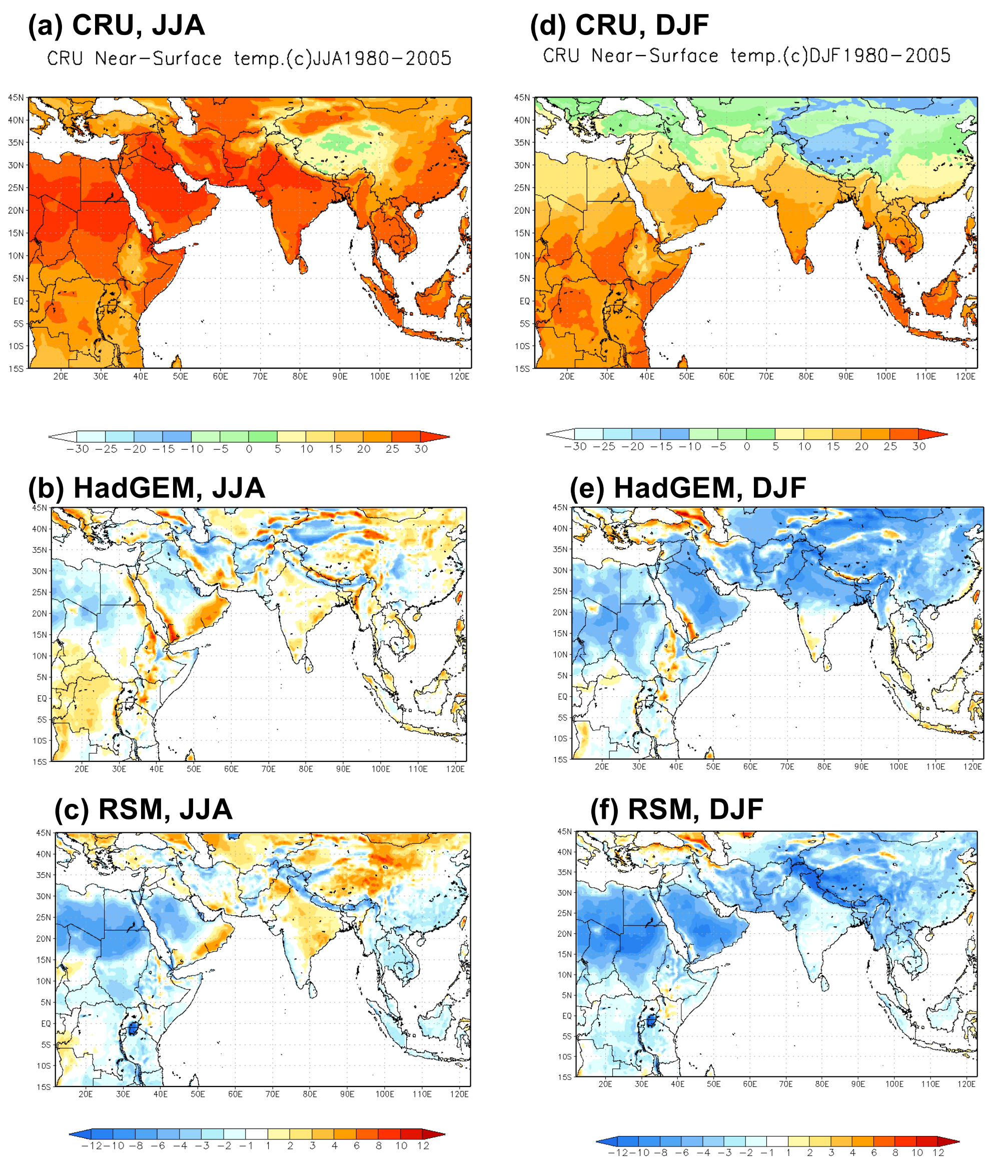

Figure 3.1 Seasonally averaged Near Surface temperature (°C) for time period 1980-2005 from (a and d) CRU, (b and e) from HadGEM and (c and f) from RSM for JJA and DJF respectively.

For JJA HadGEM showed slightly warm bias over eastern Ghats of India, northern China, United Arab Emirate (hereafter refereed as UAE) and central Africa while the cold bias is observed over north west of Pakistan and extreme western China and west Africa. For RSM, the warm bias is observed over India and north-central China while the cold is enhanced over UAE and Northern Africa. The South East Asia over all showed slight cold bias in summer. In winter, the cold bias is dominated in both HadGEM and RSM simulations. Few place in HadGEM showed slightly warm bias but overall cold bias is obvious in both models.

Table 3.1 Near surface temperature Spatial Correlation and Root-Mean-Square-Error of HadGEM and RSM for JJA and DJF against CRU observation.

Near Surface Temperature (°C)	SCORR	RMSE
JJA		
HadGEM	0.92	2.48
RSM	0.90	2.95
DJF		
HadGEM	0.97	4.24
RSM	0.97	4.43

The results of statistical analysis for JJA showed higher spatial correlation of 0.92 with lowest RSME of 2.48 ^{o}C, while RSM should lower SCORR of 0.89 with RSME of 2.94 ^{o}C. The winter simulations are HadGEM SCORR almost close to RSM but in case of RSME the HadGEM showed less error 4.24 then RSM 4.43.

3.3.2 Surface Precipitation Climatology

The surface precipitation comparison is done based upon three criteria, which include comparison of precipitation datasets with high-resolution dataset but shorter timespan, land plus ocean for longtime span and land only datasets. The results of precipitation climatology under these three criteria are discussed below;

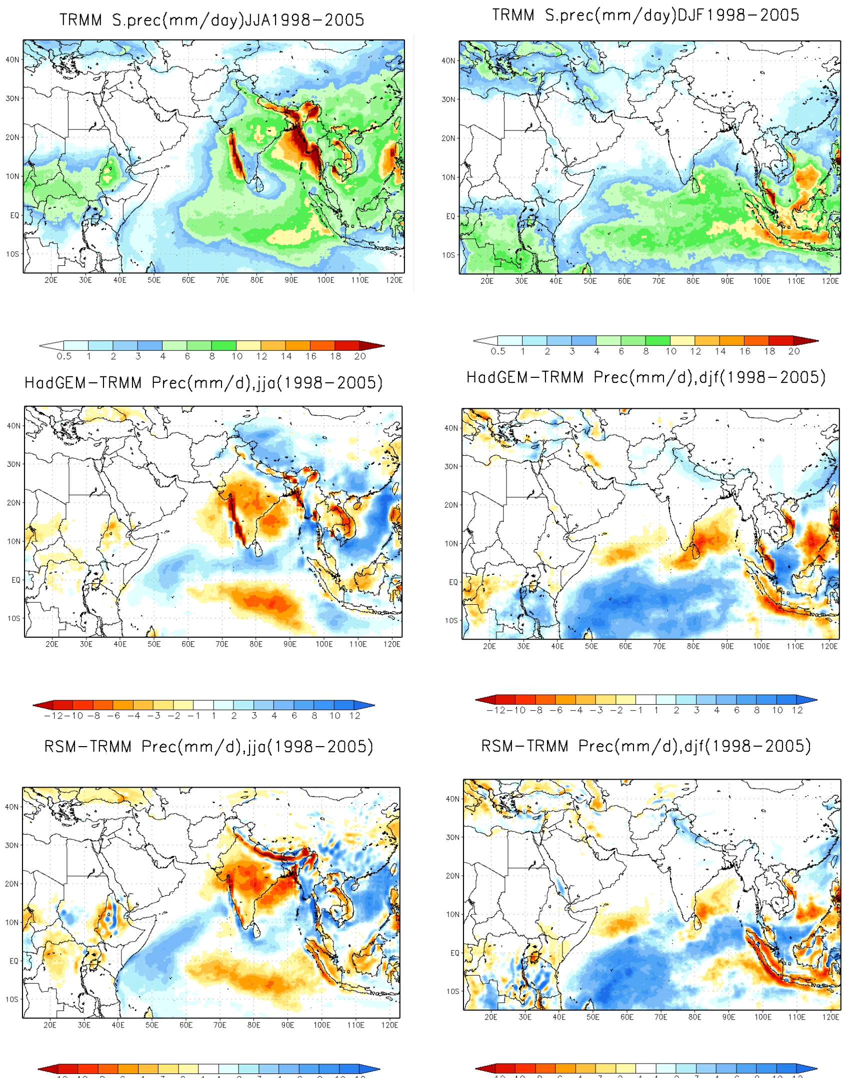

Figure 3.2 Surface precipitation comparison of TRMM 3B43_V7 precipitation (mm day^{-1}) with HadGEM and RSM simulations (1998-2005).

For High-resolution case, TRMM 3B43_V7 dataset is utilized. Although the time period for this dataset is from 1998 till 2005 but because of its high resolution it is used to see the precipitation over land and ocean. The comparison of HadGEM results with RSM should that for JJA the trend of wet and dry wet biases is similar to previous discussion. Wet bias over the Tibetan plateau in HadGEM reduced in RSM simulations. Over the Ocean part, RSM performed better by reducing the bias observed in HadGEM run. for winter, most precipitation bias are observed over ocean in terms of wet bias. The wet bias and dry bias close to Srilanka and Malaysia and south China seas are minimized in RSM simulations as compared to HadGEM. In terms of SCORR, HadGEM showed high correlation with less RMSE in JJA while for DJF, RSM performed better.

The surface precipitation comparison for land plus ocean data set is done using GPCP precipitation. The reason of selecting this dataset is to observe the models performances over ocean as well as we are interested to see the trends of climate change future projection scenarios over ocean as well. The comparison of HadGEM with observation showed the almost same trend over India, Vietnam, Indonesia and Malaysia showing dry bias although with less intensity as compared to land only results. The wet bias is consistent with the results obtained in the above section. Over the ocean, HadGEM showed wet bias over the Arabian seas, closer to Srilanka, Malaysia, over South China Sea while the dry bias is observed over gulf of Thailand and Bay of Bengal. RSM simulation showed minimized bias over Tibetian Plateu while it showed increase in dry bias over India. Over the ocean, the dry bias is minimized in RSM simulations over the Indian Ocean and South China Sea. For winter simulations, HadGEM showed pronounced wet bias over most of parts of Indian Ocean alonf with Gulf of

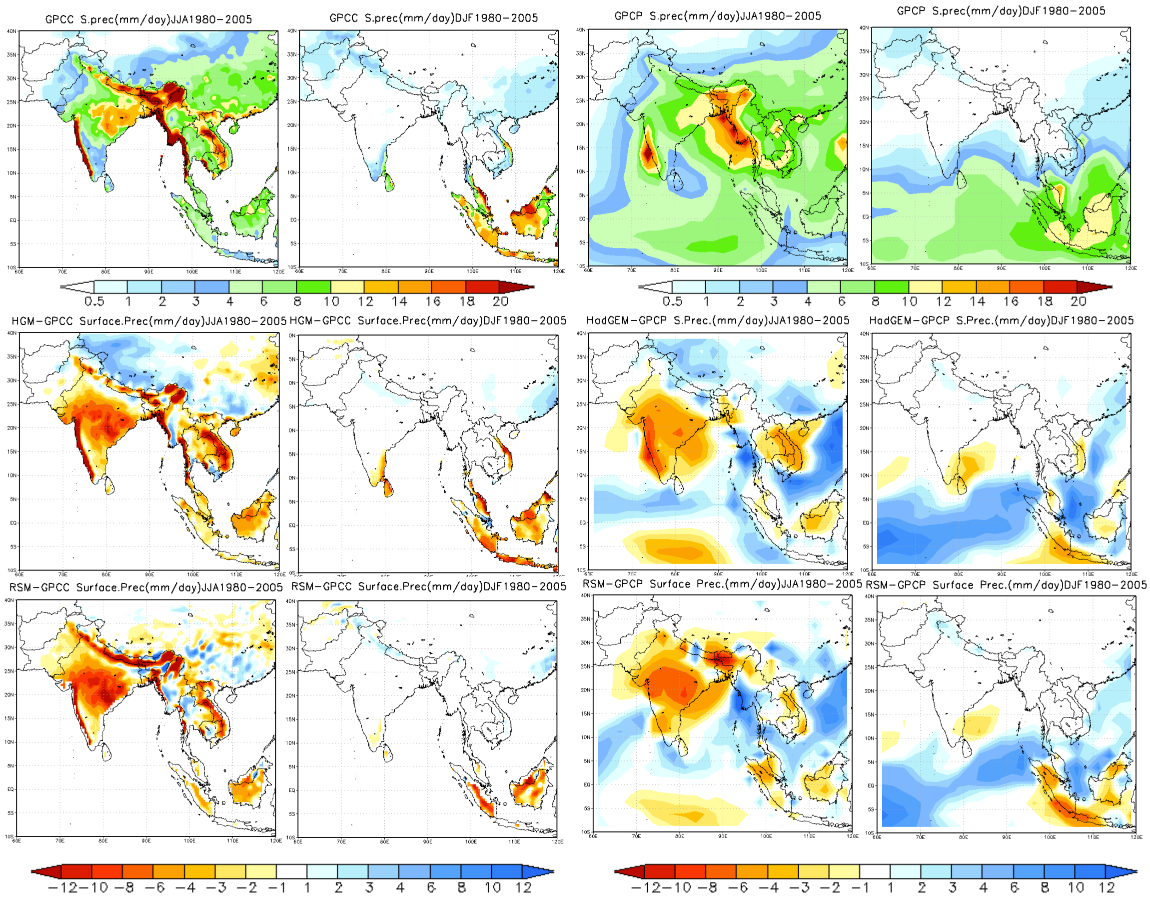

Figure3.4 Comparison of GPCC (Land only) and GPCP (Land+Ocean) precipitation with HadGEM and RSM for JJA and DJF (1980-2005).

Thailand and some parts of south china sea while the RSM simulations tends to decrease those biases. For GPCP, the performance of RSM in JJA is better with 0.72 SCORR and 3.40 RMSE while for HadGEM it is 0.69 and 3.51. For DJF, HadGEM showed better performance then RSM in term of better correlation 0.82 and but for RMSE it showed higher error 3.26 then RSM 2.83.

There are number of number of precipitation datasets which observed precipitation over land only based upon the utilization of station data and its interpolation over the uniform grid surfaces in order to make the dataset uniform. The number of station varies from region to region which will effect the quality of observation datasets. In this context GPCC dataset is used to validate the results of 20C simulations over land. The comparison of surface precipitation for 26 year dataset is done by comparing JJA AND DJF of HadGEM and RSM with GPCC. The results of JJA showed that HadGEM represents wet bias over the Tibetian Plateu and southern China while for India, Vietnam, Indonesia and Malaysia it showed dry bias. RSM minimizes the wet bias produced by driving Global Model over the Tibetian. While for dry bias, the trend is similar the HadGEM. For DJF, the dry bias is seen in HadGEM simulations except for eastern China which showed slight warm bias. The biases depicted in parent model are nicely minimized in RSM. The statistical analysis for JJA in reference to GPCC showed that RSM scores higher in terms of spatial correlation 0.68 as compared to HadGEM 0.67 while in DJF HadGEM showed highest correlation of 0.92 and lowest RMSE of 1.43 as compared to RSM which showed 0.86 for spatial correlation and 1.67 for RMSE error respectively.

3.3.3 Intra-seasonal variability

The comparison of Intra-seasonal variability between CRU, HadGEM and RSM is hown in figure 3.5. Both HadGEM and RSM shows great capability in caputuring the variations quite well. RSM performance is more obvious in May till September the HadGEM.

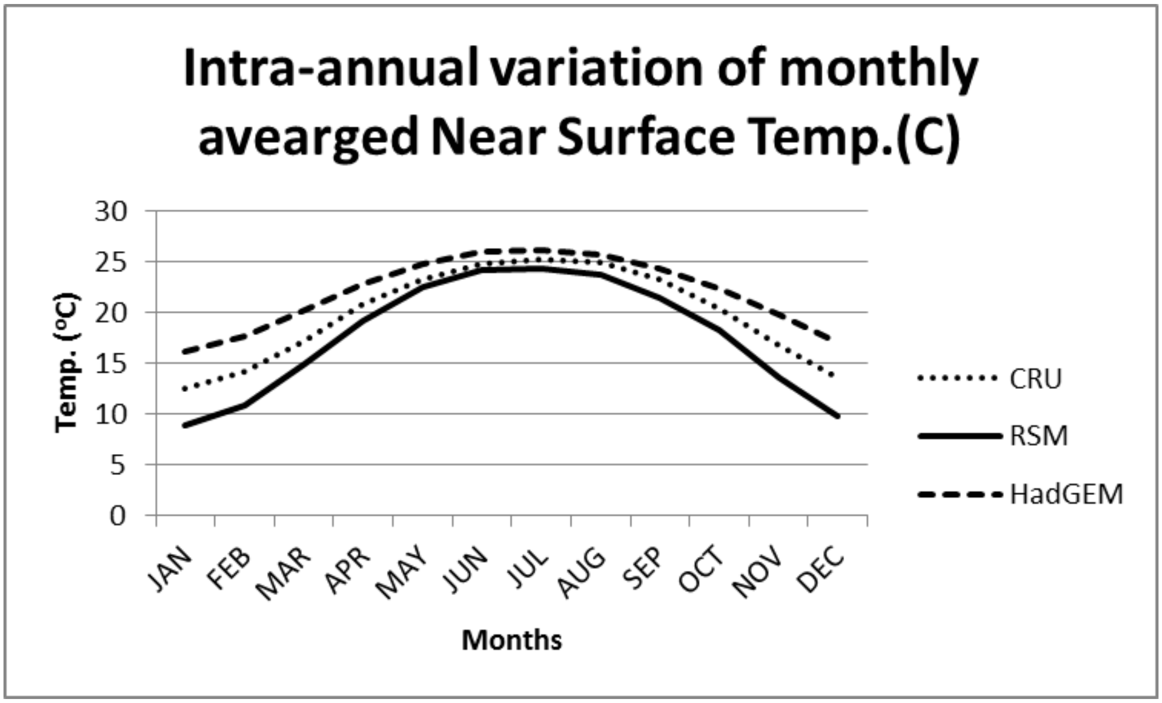

Figure 3.5 Intra-seasonal variation of near surface temperature (^oC) for CRU observation(black dotted line), RSM (black solid line) and HadGEM(black long dashed line) respectively.

Figure 3.6 shows intra-seasonal variation of TRMM against HadGEM and RSM. The intra-seasonal comparison showed closer correlation of RSM then HadGEM from January till May. From June till October both HadGEM and RSM showed closer relation with observation, while for November abd December again RSM seems closer to TRMM observation the HadGEM.

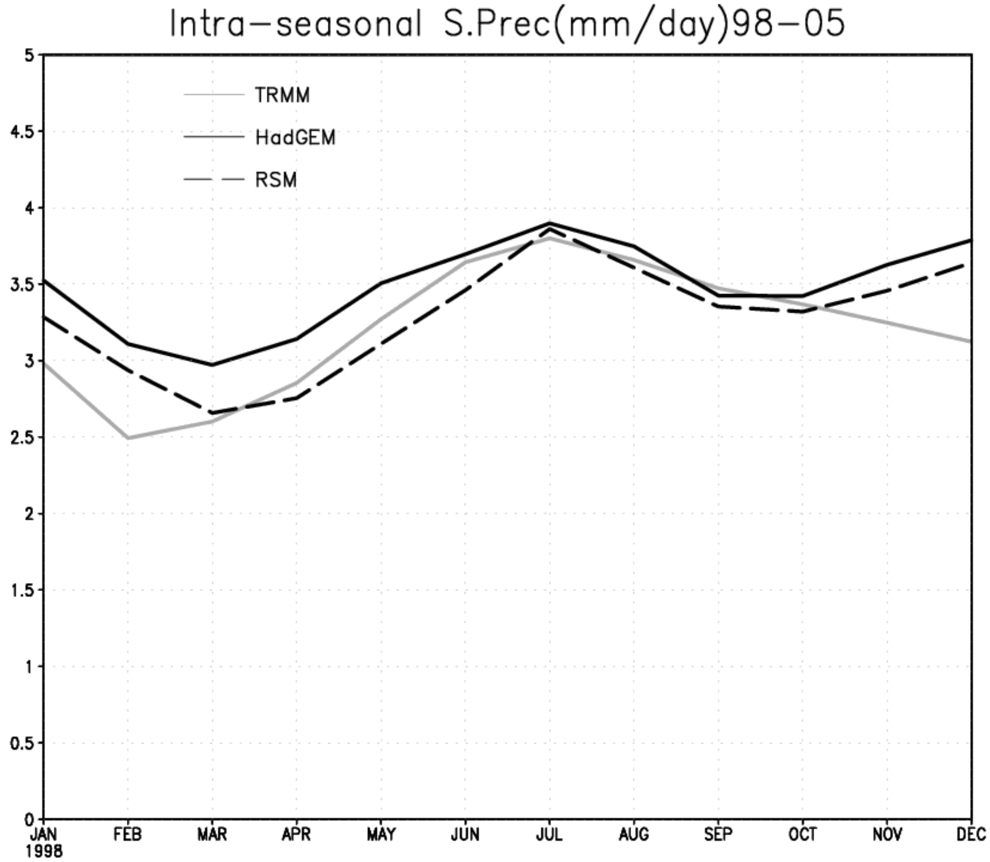

Figure 3.6 Intra-seasonal surface precipitation (mm/day) comparison of TRMM against HadGEM and RSM.

Table 3.3 Spatial correlations and Root-Mean-Square-Error of TRMM data against HadGEM and RSM.

Precipitation	Analysis	RMSE	SCORR
JJA			
	HadGEM2	2.48	0.82
	RSM	2.82	0.80
DJF			
	HadGEM2	2.89	0.77
	RSM	2.82	0.78

Figure 3.7 shows the comparison of GPCC and GPCP intra-seasonal variation The intra-seasonal comparison for land only precipitation (GPCC) showed closer correlation of HadGEM to GPCC as compared to RSM. While for land and Ocean data sets (GPCP) comparisons, RSM showed nicely trend as compared to HadGEM. In both these cases, HadGEM and RSM nicely captured the peaks of monsoon season in South Asia.

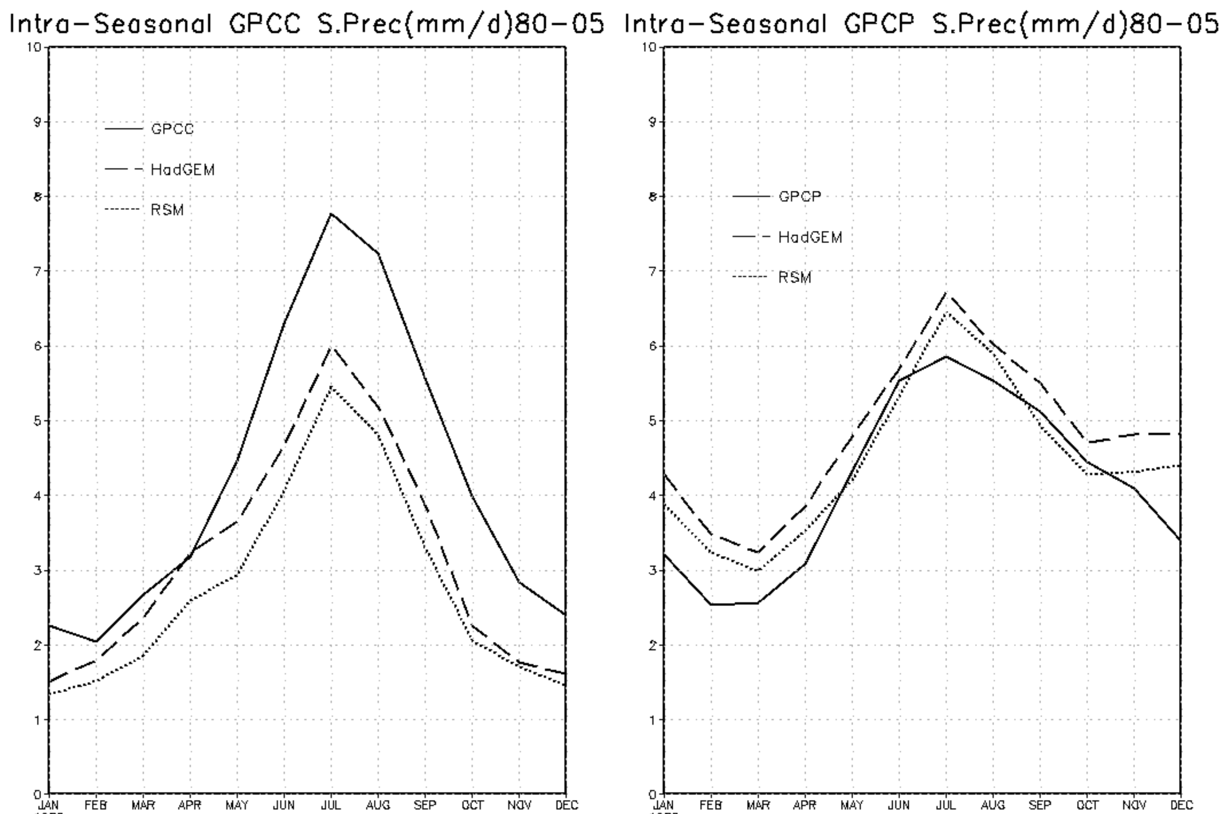

Figure 3.7 Intra-seasonal precipitation comparisons between GPCC and GPCP with HadGEM and RSM simulation

Table 3.4 Spatial correlations and Root-Mean-Square-Error of GPCC and GPCP surface precipitation (mm/day)

	GPCC		GPCP	
	SCORR	**RMSE**	**SCORR**	**RMSE**
JJA				
HadGEM	0.67	4.96	0.69	3.51
RSM	0.68	5.13	0.72	3.40
DJF				
HadGEM	0.92	1.43	0.82	3.26
RSM	0.86	1.67	0.79	2.83

3.3.4 Intra-annual variability

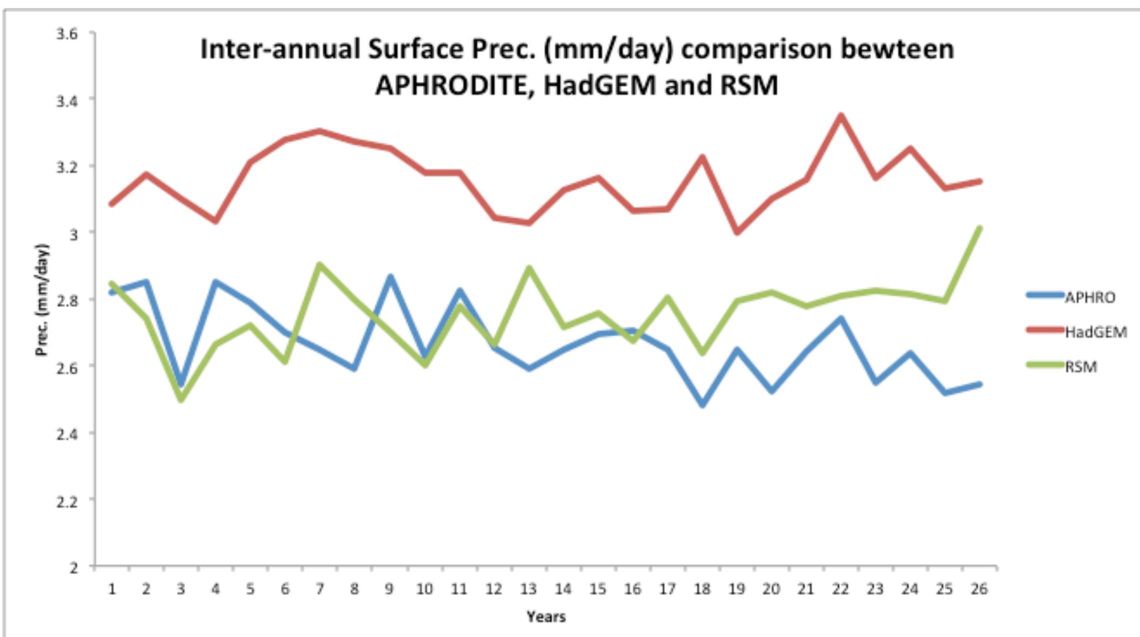

Figure 3.8 Intra-annual precipitation comparisons between APHRODITE, HadGEM and RSM results for 1980-2005 for South Asia Domain (SA).

Figure 3.8 represents the inter-annual variability of surface precipitation (mm/day) starting from 1980 till 2005 for south Asian domain indicated as SA in figure 2.1. Annual precipitation averages of APHRODITE, HadGEM and RSM are compared. It is clearly evident from this comparison that RSM shows more closer trend to APHRODITE as compared to HadGEM in capturing the inter annual pattern. Although, multiple reasons can be attributed to this analysis results, one among them will be the high resolution of RSM as compared to HadGEM. South Asian terrain is complex with mountains on its north , east and west which offer great challenge to coarser GCM to resolve its details.

Figure 3.9 shows the added value of RSM in comparison to HadGEM in capturing the precipitation classified into different bins. The results are validated with APHRODITE daily precipitation data. It can be seen that for lower bins (40 to 70) the precipitation results vary for each region mostly, the HadGEM has better reults in smaller bin ranges but figure 3.9 (b) shows quite opposite results for HadGEM where most of the higher precipitation bins are caputured by RSM as compared to HadGEM which showed limited performance.

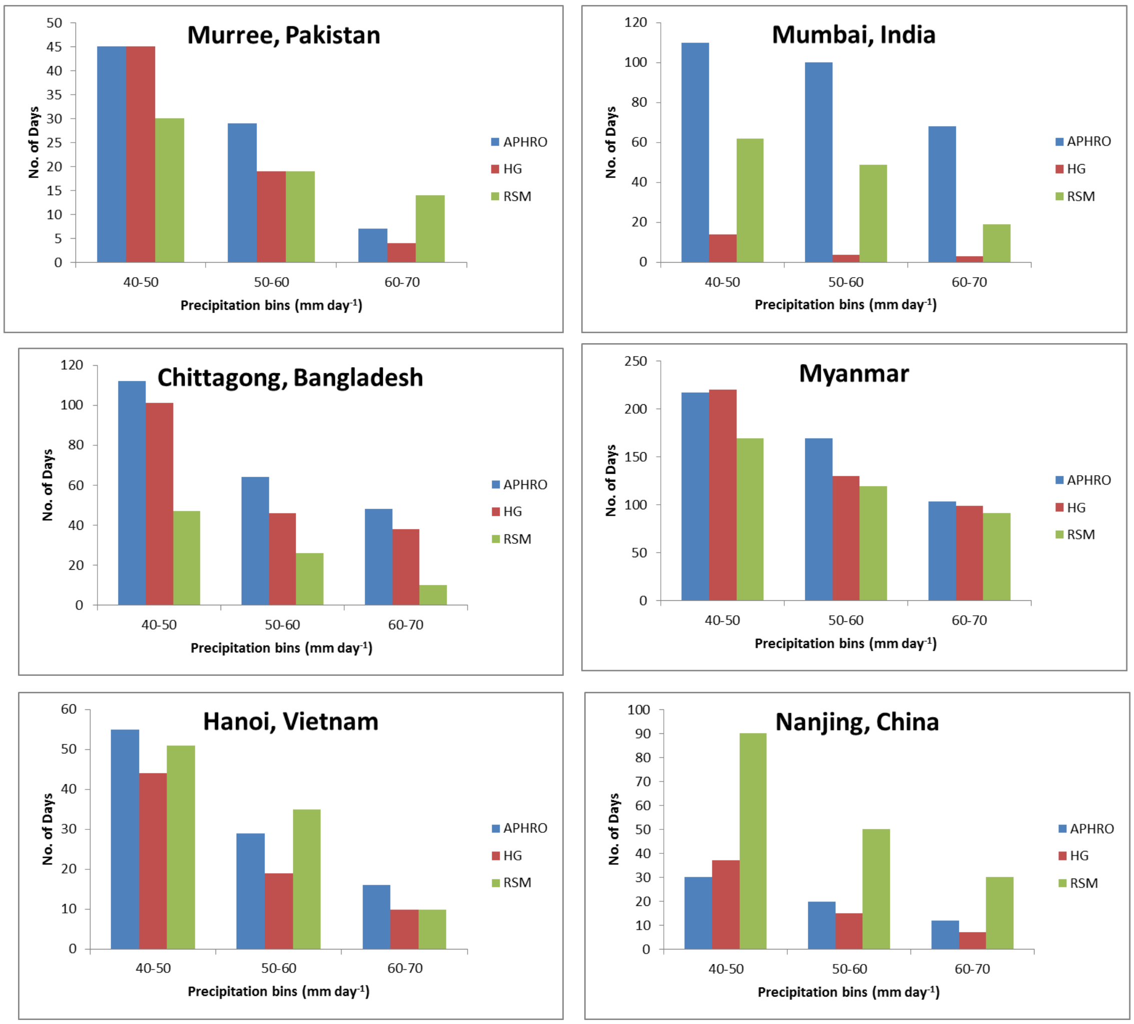

Figure 3.9 (a) Precipitation bins 40 to 70 with for APHRODITE, HadGEM (HG) and RSM for 1980-2005 daily data.

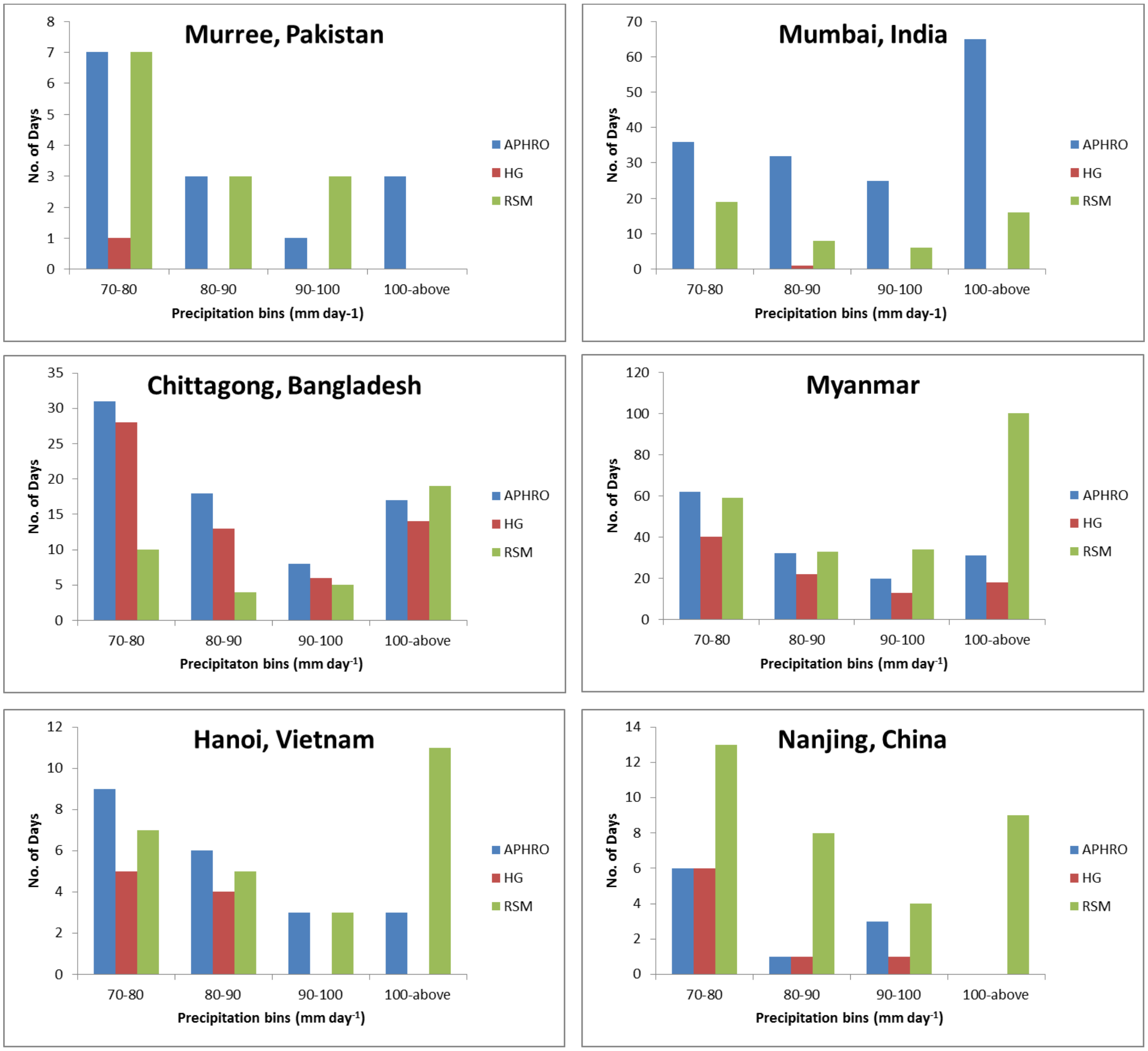

Figure 3.9 (b) same as figure 3.9 (a) but for bins 70 and above.

Figure 3.10 and 3.11 shows the 99 percentile results for RSM in terms of surface precipitation and surface air temperature. The precipitation results shows wet bias over the China region while the dry bias is evident in Indian region while for 99 percentile temperature, the results are quite reasonably captured by RSM

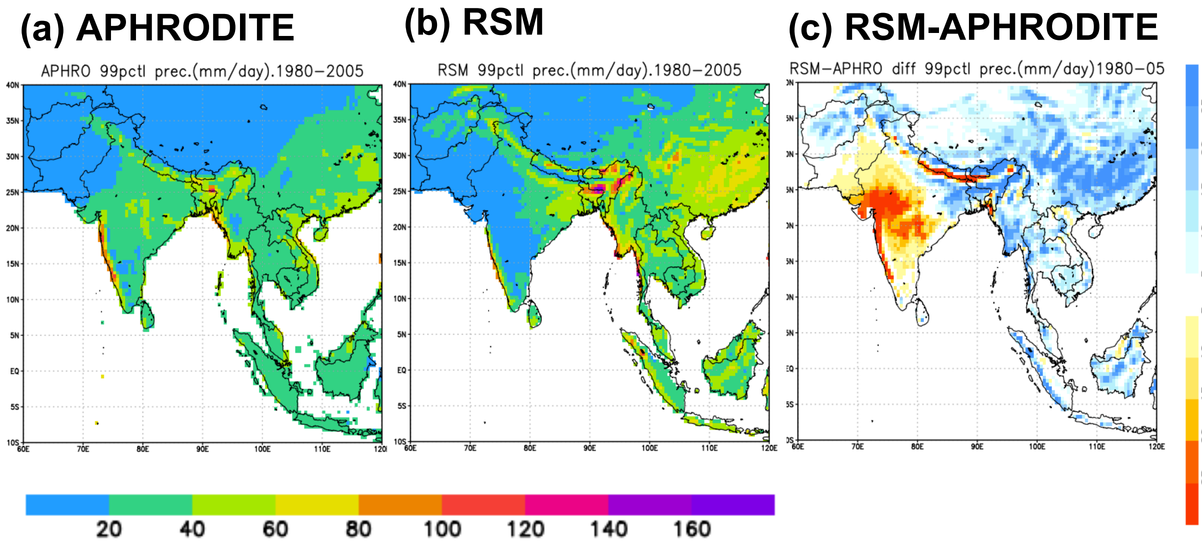

Figure 3.10 99 percentile surface precipitation (mm/day) from 1980-2005.

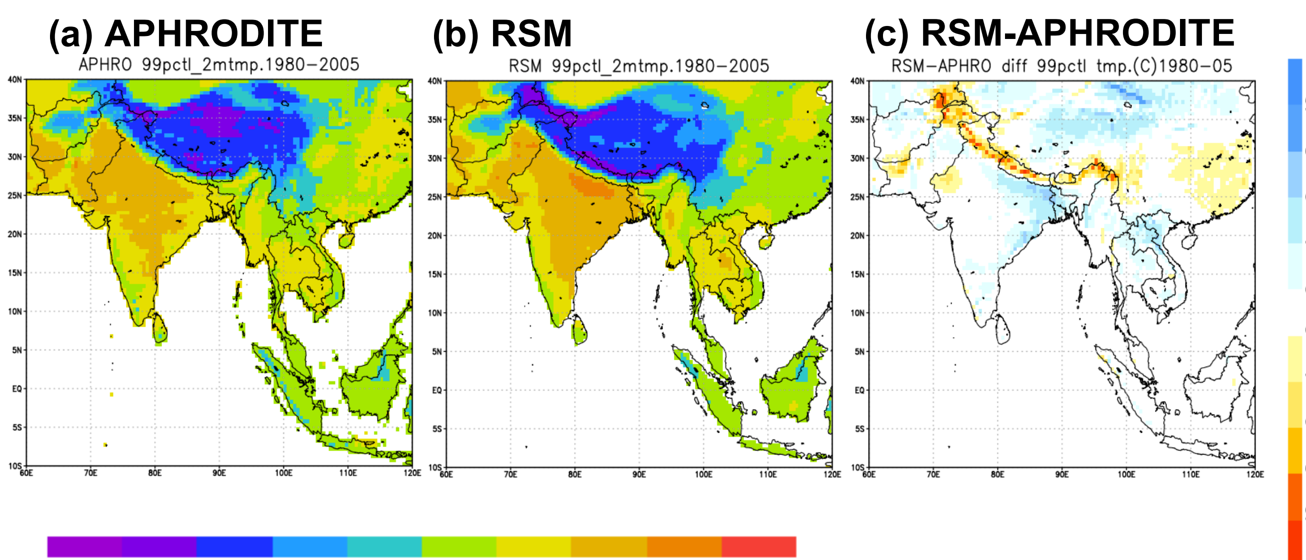

Figure 3.11 Same as figure 3.9 but for surface air temperature.

CHAPTER 4

Assessment of Future climate Projections of South Asia using Representative Concentration Pathways Scenarios

4.1 Experimental Setup

In this chapter, the future South Asia is analyzed with focus on temperature and precipitation change. In order to see the changes in aforementioned variables, the results are compared with RSM 20C century analysis. RSM is forced by HadGEM selecting two Representative Concentration Pathways (hereafter referred as RCP) 4.5 and 8.5 for Intergovernmental Panel on climate change fifth assessment report. The time period ranges from 2020 till 2100 (hereafter referred as 21C). The resolution for future study is 50 km same as for twentieth century analysis.

4.2 Results and Conclusions

4.2.1 Future projections of Temperature change

Figure 4.1 shows the inter-annual variation of 2m temperature from 20C analysis for RSM to 21C projections. Both RCP 4.5 and RCP8.5 showed the increase in temperature in future. Although, the change in temperature varies among both RCP scenarios. RCP8.5 showed steeper slope then RCP4.5 which shows rather smoother rise in future. This trend clearly indicates that global warming is evident in the region.

Figure 4.2 represents spatial distribution of change in 2m temperature for JJA and DJF in future RCP scenarios from current climate. Overall both RCP scenarios represents that temperature will rise in the future in both near future and far future. The rate of change is different among two scenarios. In Rcp4.5 near future, temperature will rise by 1 to 2 ^{o}C for JJA over land and ocean. While for winters, the increase is bit higher than JJA as it repents that temperature in DJF will be above 3^{o}C over the Himalayans Mountains, Afghanistan and parts of Pakistan.

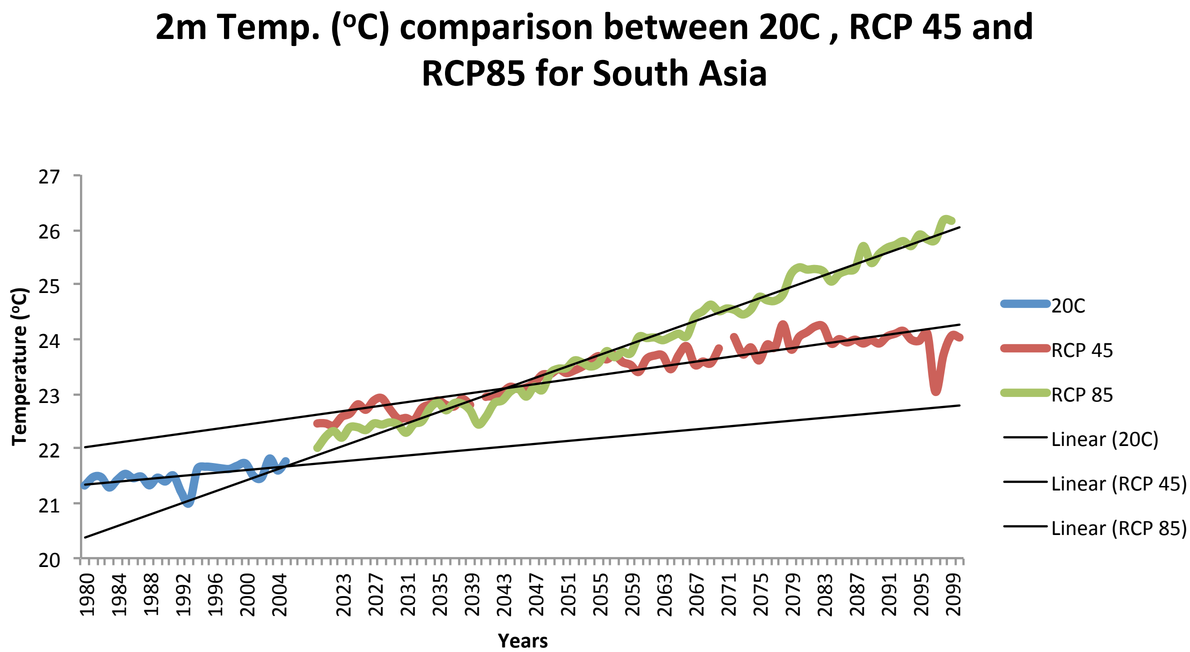

Figure 4.1 Time series of annual 2m temperature (° C) for RSM 20C (blue), RCP4.5 (red) and RCP8.5 (green) for South Asia domain. R2 represents the coefficient of determination representing the variation of 2m temperatures on y-axis to its relation with years on X-axis.

In far future RCP4.5 scenario, the increase in temperature at wide spatial extent is observed over all Afghanistan, Tajikistan, Tibetan plateau and western Pakistan for JJA. For DJF, the temperature increase and its spatial extend is much larger then near future. It shows the spread from China, Vietnam, Thailand, Malaysia and Indonesia while for Afghanistan, Tajikistan and part of Northern china shows temperature increase greater than 5 ° C.

Similar trend are observed for RCP8.5 for near future and far future but with more intensity. Especially for DJF of both time scales the temperature increase is representing an alarming picture of the future in temperature intensive behavior.

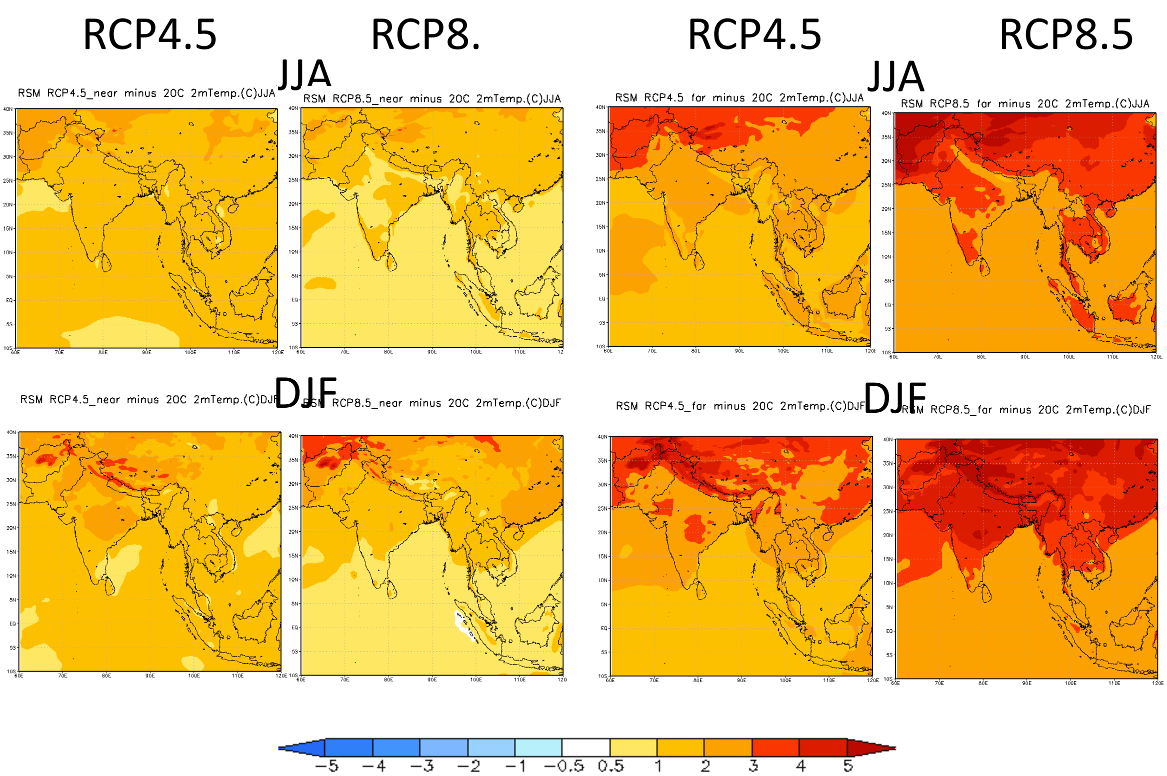

Figure 4.2 Difference of seasonally average 2 m temperature (^{o} C) from RSM 20C simulations for JJA and DJF for two RCP scenarios in near future(2020-2050) and far future(2051-2100).

4.2.1 Future Projections of Surface precipitation (mm/day)

Change of surface precipitation for future scenarios of RCP4.5 and RCP8.5 are presented in figure 4.3. Initially a decreasing trend of surface precipitation in observed for both RCP 4.5 and RCP8.5 scenarios in near future as compared to present climate but moving towards far future represents an increasing trend. RCP4.5 scenario shows decreasing trend then 20C results in near future but for far future it shows the annual precipitation increase. RCP8.5 shows slight decline then 20c surface precipitation but this decline is sharply replaced by the steeper increase in middle and far future then reference 20C data..

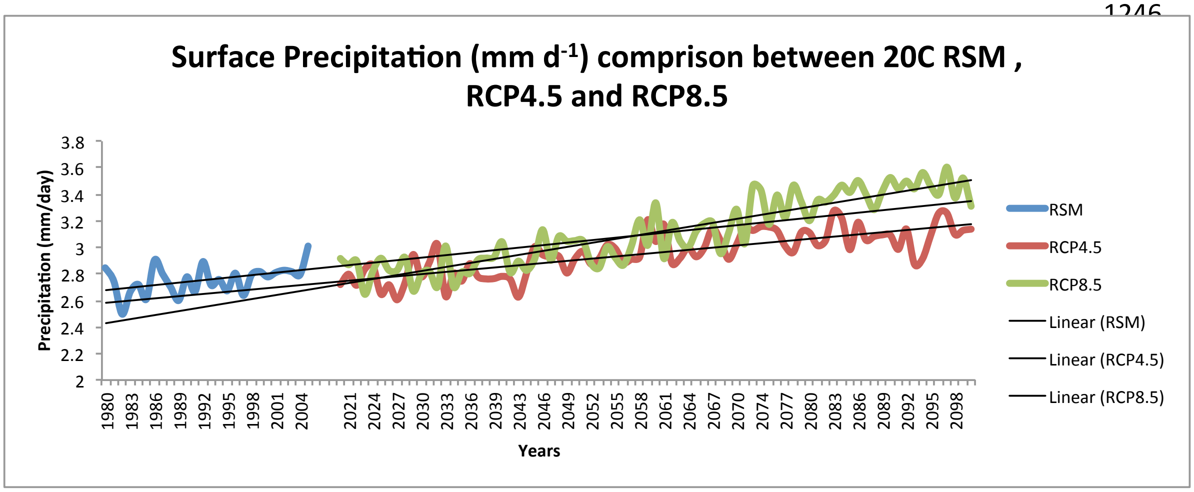

Figure 4.3 same as figure 6.1 but for surface precipitation (mm/day).

Figure 4.3 represents the intra-seasonal variability of surface precipitation for APHRODITE (APHRO), 20C and 21C RSM simulation (RCP4.5 and RCP8.5). The results of this analysis show that RSM 20C simulations are following the APHRODITE's intra-seasonal trend. While the future results for intra-seasonal precipitation shows that both RCP4.5 and 8.5 intra-seasonal variations will be more 20C RSM simulations and the peak season July precipitation will be larger in future as compared to the present.

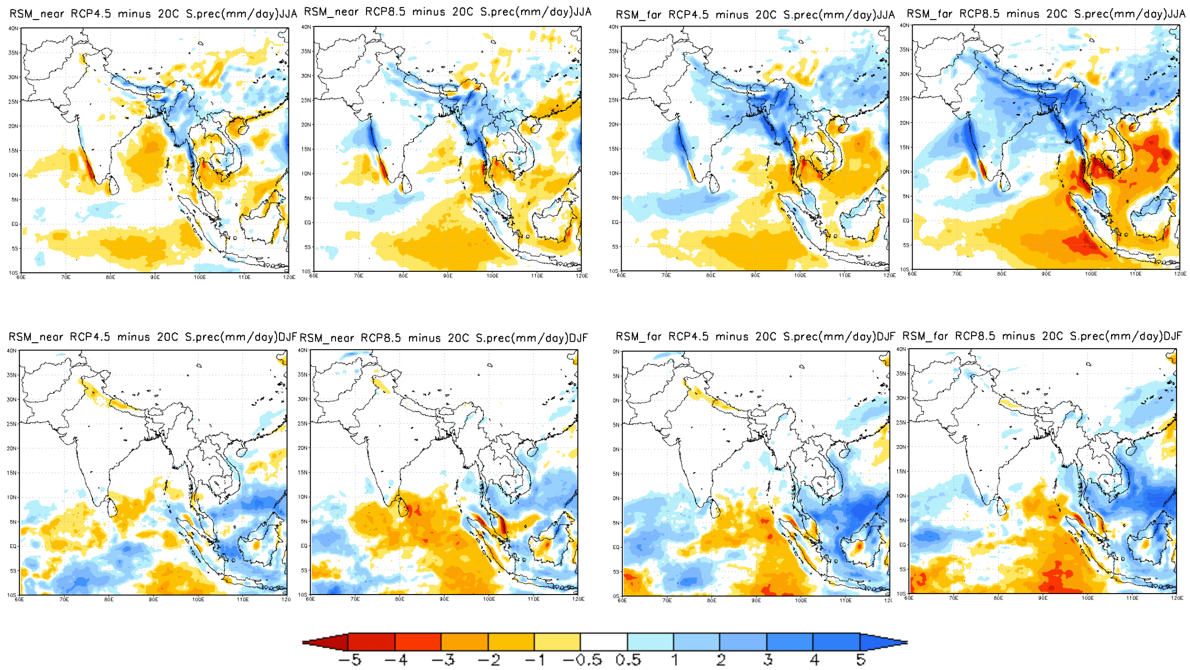

Figure 4.4 same as figure 4.2 but for surface precipitation (mm/day).

Figure 4.4 represents the changes in seasonal precipitation for future climate then present is discussed with reference to changes in near future (2020-2050) and far future (2051-2100) respectively. Both RCP scenarios show that in near future, there will be a decrease in precipitation over the Indian Ocean in summers. while for land part, rcp4.5 shows decreasing precipitation trend over the western Ghats of India and some parts of China and Pakistan while it shows an increasing precipitation trend over the foothills of Himalayas over Bangladesh and Myanmar and southern china. for djf alternating bands of decreasing with east west alignment shows an increasing trends are observed over the Indian ocean and South China Sea . For RCP8.5, for JJA mostly increasing precipitation trend is observed over the land parts focusing south Asian monsoon regions surrounded by mountains. while over the ocean a distinct decreasing trend is observed near Malaysia and south china seas and parts of south western India near westerns Ghats. for DJF, the alignment of precipitation bands is rather north south with alternating increasing and decreasing bands respectively.

For far future, RCP4.5 in JJA shows remarkable increasing precipitation over monsoon hit regions of south Asia while it showed a significant deficient of precipitation over south east Asia. for DJF, The bands shifted from east –west to north –south alignment with increasing and decreasing alternation precipitation patterns with increased width. For RCP8.5, the more significant increase is observed with more spatial spread the rcp4.5. Over all, JJA showed that almost all parts of south Asia will experience the increased precipitation in future. While Southeast Asia will face more decreased precipitations in the summer. Significant decrease is also observed over the eastern Indian Ocean and South China Sea. For DJF far future, RCP8.5, the precipitation bands shows similar pattern to rcp4.5 but with increase intensity in drier region alternated by wet bands. The wet bands show more increasing trend on the eastern half then over the western part of the Indian Ocean.

The results of 99 percentile presents that both 99 percentile precipitation and surface air temperature will increase in future while the comparison of mean and extreme projections for future shows more significant increase in extreme 99 percentile than mean value.

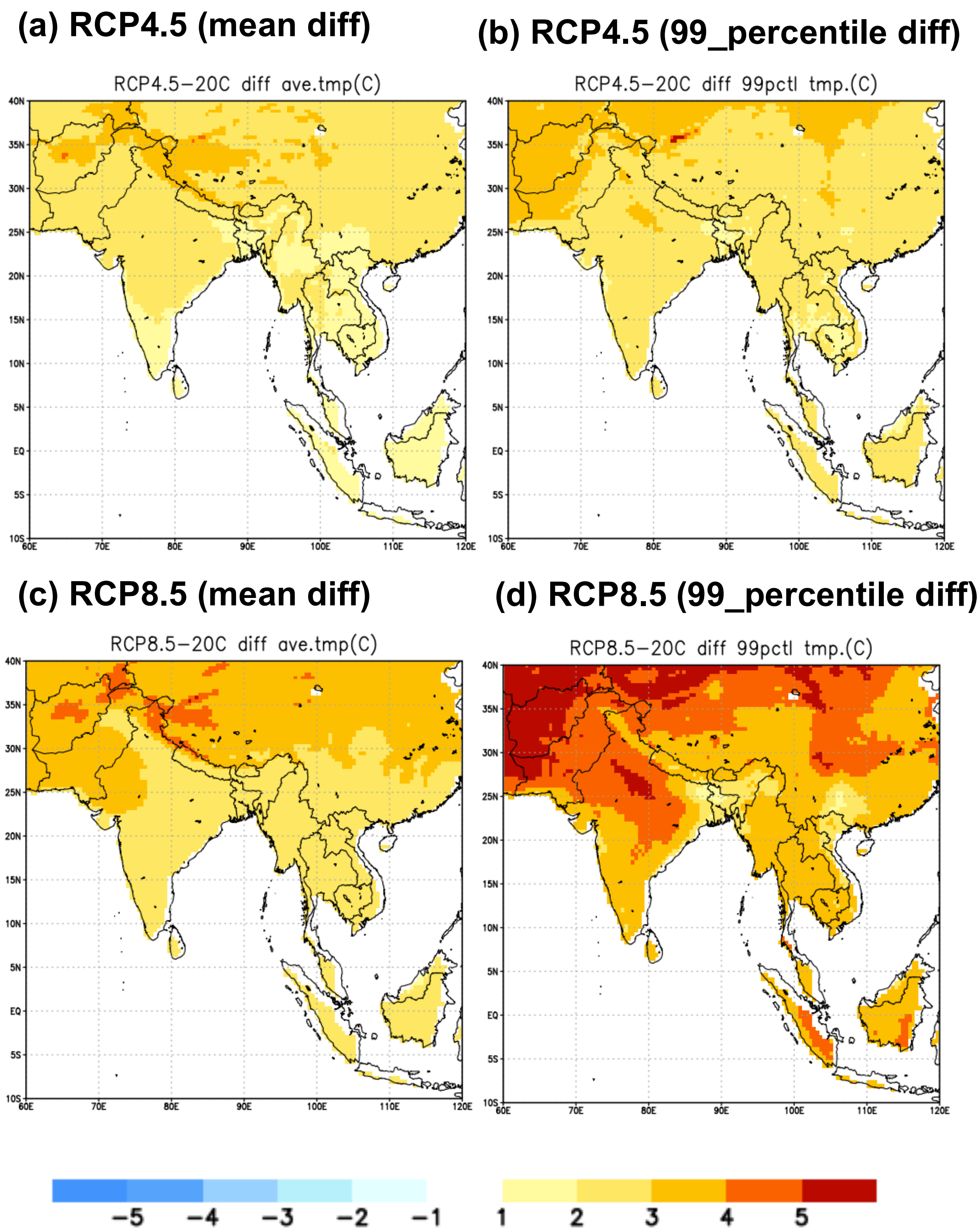

Figure 4.5 Comparison of Mean and 99 percentile of surface air temperature (^{o}C) fro RCP4.5 and RCP8.5 scenario for time period 2020-2100.

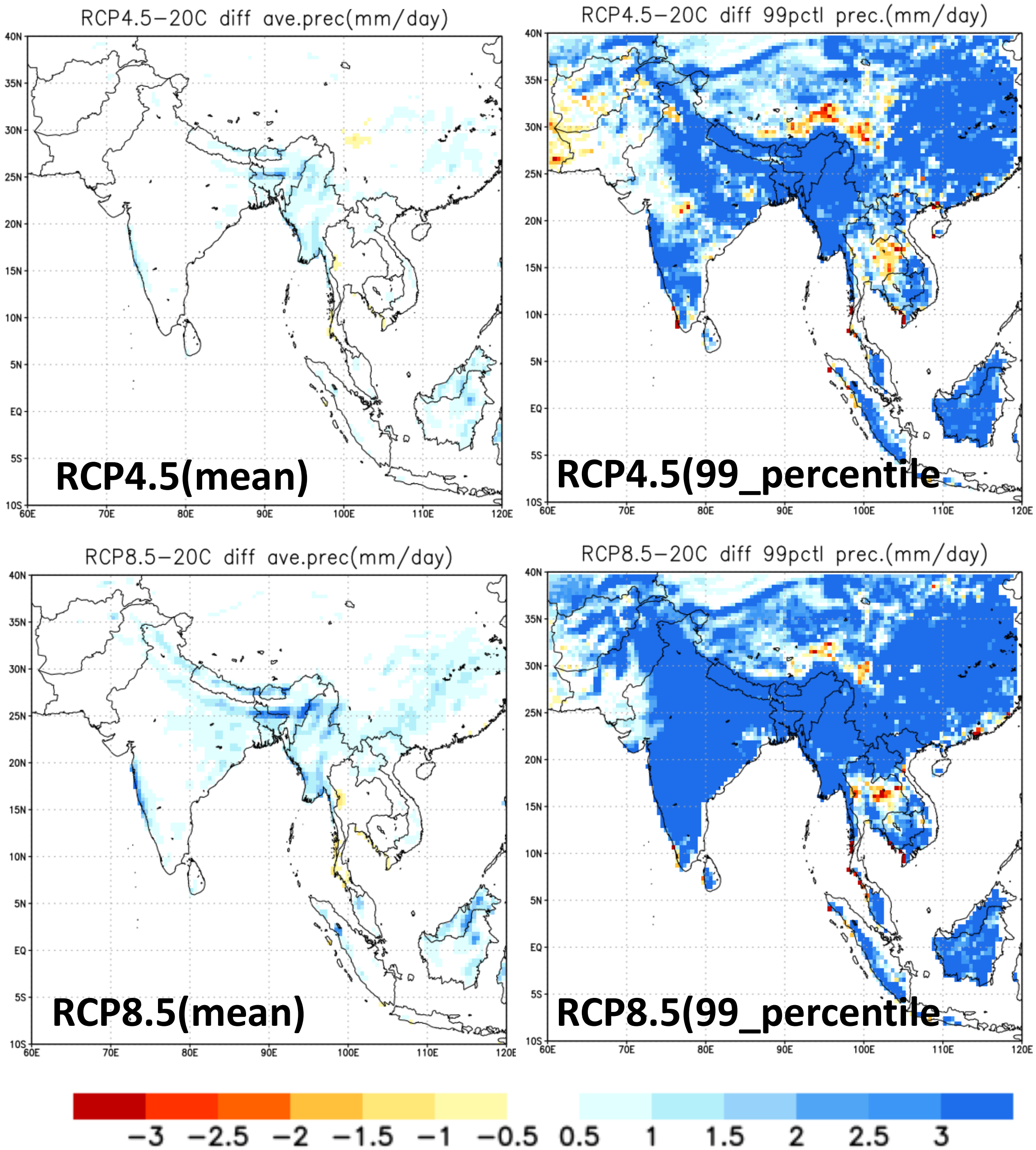

Figure 4.6 Same as figure 4.6 but for surface precipitation (mm/day).

Table 4.1 Mean versus 99 percentile of surface precipitation for 2020-2100.

Mean and 99 percentileprecipitation change (%age)				
	RCP4.5		RCP8.5	
	Mean	99percentile	Mean	99percentile
South Asia	6.8	8.7	11.4	13.3
Northern Pakistan	2.9	8.2	16.0	20.7
Myanmar	12.0	10.8	14.9	15.0

Table 4.2 Same as table 4.1 but for surface air temperature.

Mean and 99 percentile temperature change (°C)				
	RCP4.5		RCP8.5	
	Mean	99percentile	Mean	99percentile
South Asia	2.4	2.6	3.0	4.0
Northern Pakistan	2.7	3.0	3.4	4.8
Myanmar	2.0	2.4	2.5	3.4

4.3 Conclusion

This chapter describes the potential future climate change in South Asia with reference to basic variables such as Near Surface temperature and surface precipitation using two RCP scenarios 4.5 and 8.5 respectively. The 21C RSM simulation trends are obtained by subtracting the 21C above mentioned variables from 20C RSM simulations. An increasing temperature trend is obtained for both RCP4. 5 and RCP8.5 scenarios. The later one showed steeper increaser then the former one. Among the seasonal trend, more increase temperature trend is seen for DJF as compared to JJA. For precipitation, the near future showed a decreasing trend while the far future shows an increasing trend in the region. The impact of increased surface precipitation more obvious nears the mountainous regions of South Asia. Overall, we can see the global warming signals in the region.

CHAPTER 5

Hydro-temperature Intensities for South Asia and Extreme Indices

5.1 Introduction

This chapter will describe the two important variables which are responsible for creating a balance of hydrological cycle. These variables are temperature and precipitation. These two variables are also sensitive to Global Green House Gases rise (GHG). Therefore special attention is given to determine these variables using several indices to overall capture there trend in the 20C and how will they be in future. The first half will be based upon hydro climate intensity index while the second half is dedicated to hydro-temperature extremes indices.

5.2 Hydro-climate Intensity (HY-INT)

Among the extreme indices, more consideration is usually given to precipitation indices. It may be due to the fact that among the natural disasters, the damages caused by precipitation intensity, duration and frequency are more harmful as compared to other disasters.

Giorgi et al (2011) have introduced a new hydro climate intensity (hereafter refereed as HY-INT) index, which quantitatively combines precipitation intensity (hereafter referred as INT) and dry spell length (hereafter referred as DSL) to provide overall metrics of hydro climate intensity.

HY-INT can be calculated by computing the mean annual intensity (intensity during wet days) and the mean annual Dry Spell Length (DSL) where wet days are defined as the number of days when precipitation amount is greater than 1mm and dry days as those when precipitation amount is less than 1mm. HY-INT for any year and location can be obtained using the equation 5.1.

$$\text{HY-NT} = \text{INT X DSL} \qquad \text{(eq 5.1)}$$

Equation 5.1 the increase of HY-INT will indicate the increase in INT or DSL or both. So this equation according to Giorgi et al (2011) will measure the changer in hydrological cycle related to intensity and frequency of events. It is worth mentioning here that HY-INT is not the index of precipitation or drought extreme but an index of hydro climatic intensity.

5.2.1 Experimental design

HY-INT index is calculated using CORDEX-South Asia RSM simulations for 20C and its trend for future projections including RCP4.5 and RCP 8.5. 26 year mean of HY-NT for 20C is used as base period to calculate the future trends. The time period selected for future trend is divided into near future (2020-2039), mid future (2050-2069) and far future (2080-2099) respectively for both future scenarios. The results of this analysis is are presented in figure 5.1, 5.2 and 5.3 for HY-INT, INT and DSL respectively.

5.2.2 Results and discussion

The Results for HY-INT in figure 5.1 for near future simulations for HY-INT for RCP4.5 shows a slight HY-INT increase around the Thar Desert area. In RCP8.5, the general increasing trend is larger for HY-INT but its extreme values shows little spread in Thar area as compared to RCP4.5.

For mid future, RCP4.5 shows patchy increase in term of extreme values in Thar desert, south of central Punjab, Pakistan and western parts of China. For RCP8.5, HY-INT

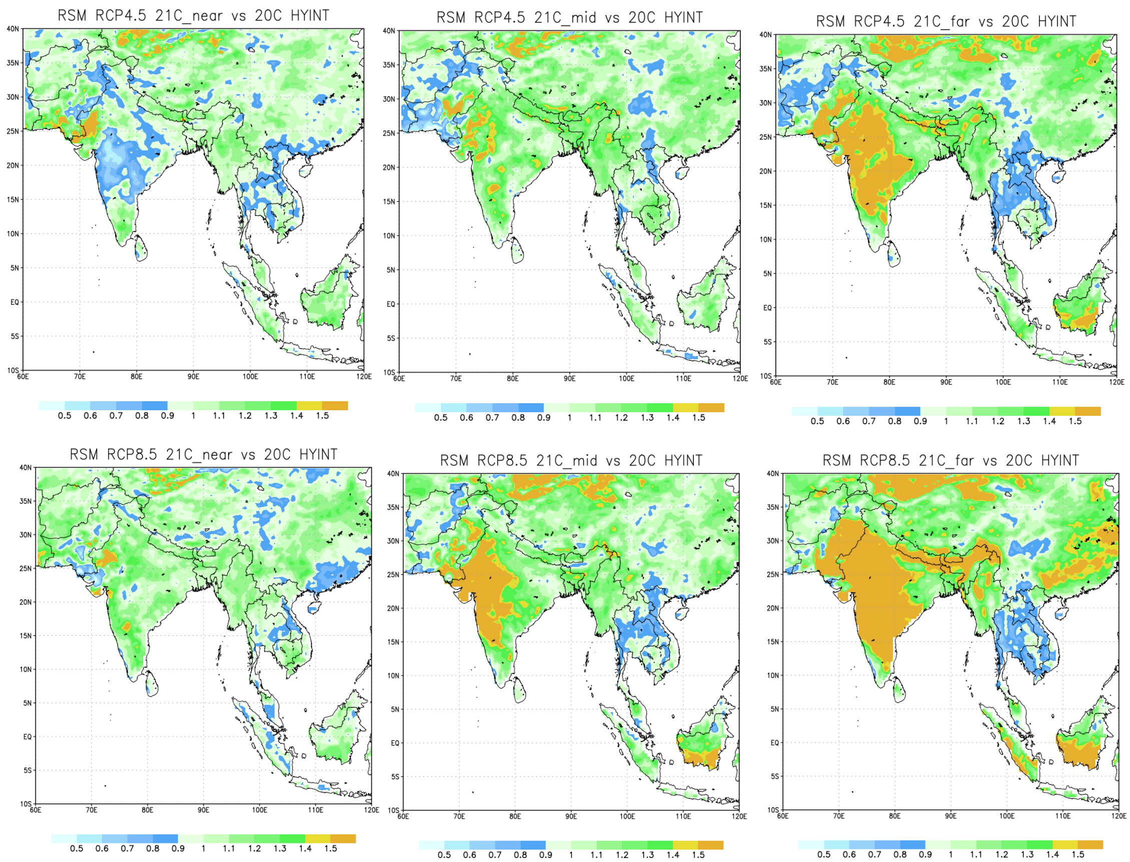

Figure 5.1 RSM future climate projections of HY-INT for near future (2020-2039, left), mid future (2050-2069, middle) and far future (2080-2099, right) for RCP4.5 (upper row) and RCP8.5 (bottom row) respectively.

showed great spread covering the thar desrt along with south west parts of India. Over China, the spread of HY-INT is larger then RCVP4.5 strecting from west to northern center of China. Another observable trend is seen over south of Indonesia which is not observed in near future simulations and mid future e simulations of RCP4.5.

For far future, RCP4.5 shows HY-INT increasing trend over South west of India and south-east of Pakistan covering the Thar desert area. While for China the trend is increasing in northern areas but not so obvious. Over Indonesia, increasing HY-INT values are obtained in far future simulations of RCP4.5.

HY-INT shows a wide spread increase over large part of India and Pakistan. The trend over China also showed large coverage as compared to RCP4.5 simulations. The spread of HY-INT is first time observed prominently over Bangladesh and Nepal and Malaysia. Over Indonesia, the spread of HY-INT became wider than before. Another obvious change is observed over South-eastern China which shows HY-INT increase for the first time in all future projections.

The results for INT simulations are presented in figure 5.2 for both RCP4.5 and 8.5 simulations.

For RCP4.5, INT shows overall increasing trend over south Asia with more obvious increase over other desert area and north western China. while for central India and Northern Pakistan , the INT values shows less increasing trend as compared to other areas.

For RCP8.5, near future the increasing trend of INT covers almost all parts of South and South East Asia. The obvious increases are observed in Thar areas along with with

northern China, same as RCP4.5 but the less INT values in RCP4.5 over central; India are replaced by increased values of INT in RCP8.5. However, two less value patches are seen on extreme north and south of China unlike RCP4.5.

For mid future simulations, RCP4.5 shows increasing trend over India, China and South east Asia while over Southern tips of Pakistan and parts of Afghanistan, INT shows less values as compared to others. Obvious increases are seen over Northwest of China and Thar area.

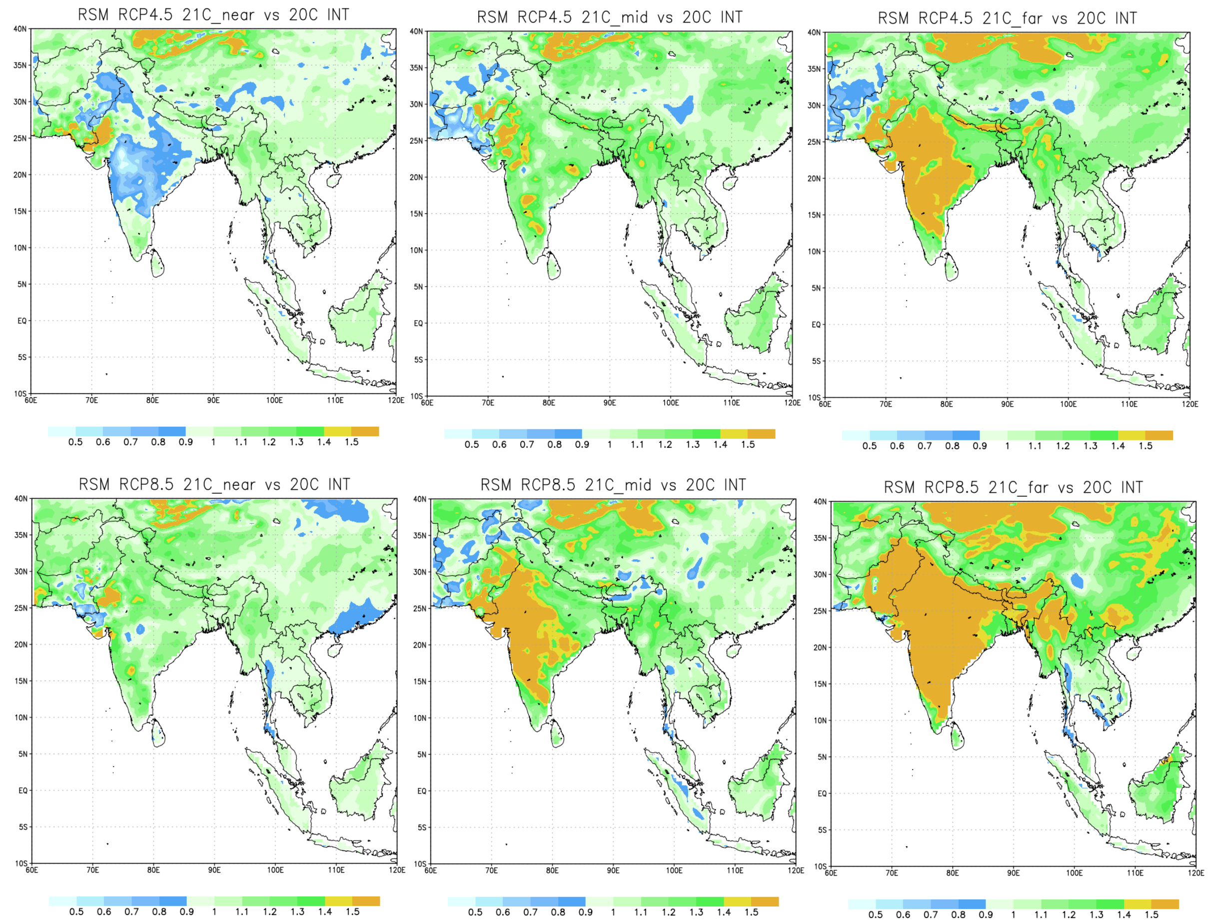

Figure 5.2 Same as figure 5.1 but for INT.

For RCP8.5, mid future shows two increasing trend patches, one over the India-Pakistan region and other over north western China. A slight decreased value is seen over Afghanistan alternating with increasing values.

Far future simulations of RCP4.5 shows prominent INT increase over Central and western parts of India along with Larger belt covering the northern China spreading in east west direction. The INT decrease is seen over South of Afghanistan and some patchy trends over south centre of China. The south east asia over all shows medium values for INT.

For RCP8.5 future INT trend, a much wider increase is seen over almost entire India and Pakistan region long with Bangladesh and northern Myanmar. Another obvious increasing INT area is northern –western China with patchy increases over east and south of China. South East Asia shows medium to low level increase in INT. Over Thailand the values are much less than other south East Asian countrie

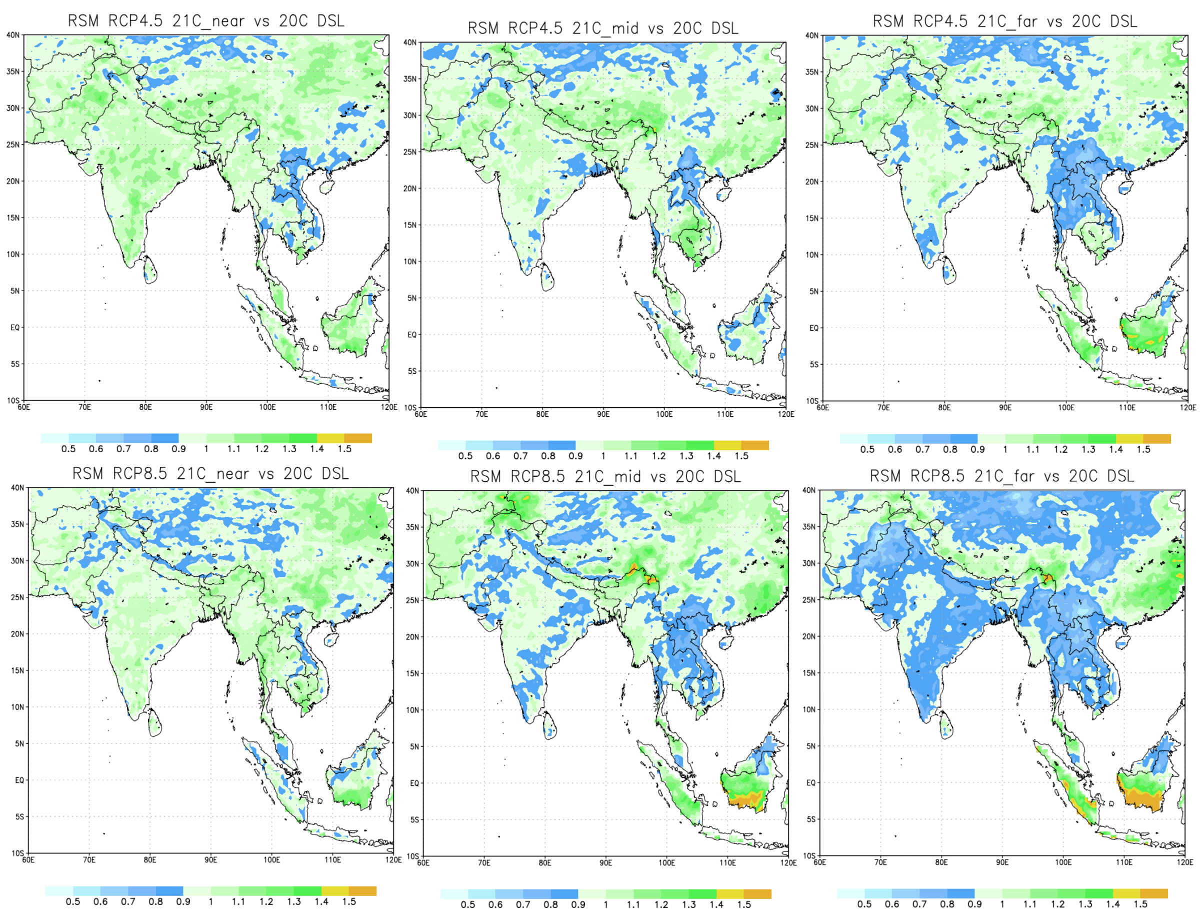

Figure 5.3 Same as figure 5.1 but for DSL.

The DSL simulations for future projections are presented in figure 5.3.

For RCP4.5, near future a medium increase is seen over Afghanistan, Pakistan and India along with Northern eastern and Central China. Over south East Asia the trends ranges from medium values over Indonesia, Malaysia and parts Thailand. While low DSL values are seen over Laos and Vietnam. The low values are also seen in a scatter pattern over north western China and South east ends of China.

For RCP8.5 near future, the DSL values further decrease in intensity over Pakistan and western China Malaysian And Indonesia while for Laos and Vietnam it shows shift from low values to medium values.

For RCP4.5 mid future, DSL values shows decreasing trend spreading from western China to northern China. The DSL values also shows decreasing trend over Laos and Vietnam along with parts of Indonesia and Malaysia. The decreased values are also seen over east of India and over Thar Desert.

For RCP8.5, mid future, the changes observed in RCP4.5 mid future are further move towards decrease in DSL values. Among the [prominent decreasing trends, the Laos, Vietnam eastern parts of India and Pakistan and western China shows decreasing DSL trend in mid future. While a slight increasing trend in seen over south west of Indonesia. The northern part of Pakistan and South East of China shows DSL increase to a medium range.

For far future RCP4.5 simulations, the most prominent decrease is seen over Laos, Vietnam, Thailand and north western China with patterns of decrease in southern tip of India. The increased DSL is seen over Southern western parts of Indonesia and

Malaysia, while over Pakistan, Afghanistan north eastern and parts of Central China the DSL trend remain in a medium range.

For RCP8.5 for future simulations, the large DSL decrease is seen over almost all parts of Pakistan, eastern and central parts of India, north and west of China, northern Myanmar, Laos, Vietnam, Thailand and eastern Malaysia. The me4dium increase of DSL is seen in eastern China while a extreme DSL values are seen over southern parts of Indonesia.

In summary, the analysis of INT identified Pakistan, India, and northwestern China as the more susceptible areas prone to precipitation intensity rise in future. A sudden appearance of another susceptible area in northeastern China is also observed in terms increased INT in RCP8.5 simulations. It is also worth mentioning here that INT shows an increasing trend over Thar desert for all future simulations irrespective of which scenario is being used.

The dry spell length will most probably increase in southern Indonesia while the medium level of increased DSL will occur in southeastern China. For other regions the DSL will decrease in future.

The results of HY-INT index for future identified the hydro-climatic sensitive regions, which includes almost all parts of Pakistan, India, northwestern and south eastern-China and Indonesia. These above mentioned regions are identified as the most the affected regions by global warming in future. Both the increase INT and DSL trends observed separately showed a combined HY-INT increase in South and South-East Asia.

This analysis also advocates the fact that in future, this shift will bring positive change to few regions while for other regions the change will be negative or makes no change at all.

5.3 Climate Extreme Indices

5.3.1 Introduction

Climate extremes are usually associated with precipitation and temperature increase and/or decrease then its normal climatological pattern. Past few decades have shown many extreme events in terms of heavy precipitation, heat waves, dry spells, cold spells etc. Unfortunately, the frequency of these climate extremes is rising at tremendous rate at present. Therefore study of these events is really crucial. One such effort is made by World Meteorological Organization (WMO) Expert Team on Climate Change Detection and Indices (ETCCDI) who defined climate extremes indices, which are computed for a number of global climate models participating in the Coupled Model Intercomparison Project Phase 3 (CMIP3) and Phase 5 (CMIP5), and reanalysis (Please see more details at http://www.cccma.ec.gc.ca/data/climdex/). While for observation data, Donat et al., (2013) made an effort to generate the gridded land based dataset of indices of temperature and precipitation named as HadEX2 using ETCCDI indices definitions.

In the current study, 3 climate indices of ETCCDI are selected for the study of extreme events. More emphasis is given to temperature extreme events as the precipitation indices are already discussed in more details in the earlier half of this chapter. The list of these indices is shown in table 5.1.

Table 5.1 represents the details of extreme indices defined by ETCCDI used in current study.

Symbol	Index Name	Index Definition	Units
RX1day	Max 1 day precipitation	Let PRij be the daily precipitation amount on day i in period j. The maximum 1 day value for period j are: RX1dayj = max (PRij)	mm
SU	Summer days	Let TX be the daily maximum temperature on day i in period j. Count the number of days where TXij > 25 C	days
TR	Tropical nights	Let TN be the daily minimum temperature on day i in period j. Count the number of days where TNij > 20 C	days

There was no standard internationally recognized definition of extreme events developed until late 1990's which poses great difficulty of studying extreme event (Choi et al., 2009). Even today some extreme events like extended heat waves and cold spells do not have any universally accepted definition (Trewin, 2009).

Therefore, to overcome this issue multiple international workshops were held mostly under the supervision of ETCCDI that is World Meteorological Organization (WMO)'s Commission for Climatology under World Climate Research Program's Project on Climate Variability and Predictability (CLI-VAR) and the joint WMO-Intergovernmental Oceanographic Commission for Oceanography and Marine Meteorology (Choi et al., 2009).

From the beginning of 21st Century, many extreme indices definitions are agreed upon and monitored on regional and global scale. Therefore for this study the definitions proposed by ETCCDI are being used to define extreme temperature and precipitation events.

5.3.2 Experimental setup

Following the definition of selected indices, RSM 20C rsimulations are used to calculate the extreme indices for time period of 1980-2005. All these indices are based upon daily precipitation and near surface temperature datasets. The validation of these extreme indices is done by ETCCDI dataset available on their archive mentioned above. Two types of reanalysis datasets ETCCDI indices are used which include NCEP/DOE indices and ERA-Interim indices for the same time period as RSM. While for obserbation data HadEX2 dataset is being used which is obtained from their archive at http://www.climdex.org/gewocs.html. All the selected idices for RSM simulations are first calculated fro each year and then 26 years annual average is created. After 20C validation, the future projections of the selected indices are being examined in the later half of this chapter.

5.3.3 Precipitation Extreme Index

(a) Maximum 1 Day Rainfall

The selected index to study precipitation extreme is Maximum1 day precipitation (hereafter referred as Rx1day), which estimates the maximum amount of precipitation, accumulated in one day.

5. 3.4 Temperature Indices

As mentioned earlier, two indices are selected to determine the extreme temperature trend in south Asia. These include;

(a) Summer Days

Summer days are defined as the number of days when the Tmaximum exceeds 25^{o}C. The summer days are calculated for each year for RSM simulation and then 26 years average it being taken.

(b) Tropical Nights

Tropical nights are defined as the number of days when Tminimum exceeds 20^{o}C (Sillman et al., 2013). These indices hold really important place for south Asia as the climate of this region is tropical at the south to arid and semi arid and then become temperate at higher latitudes.

5.3.5 Results and Discussion

Figure 5.4 shows the results of 20C for Rx1day comparison of RSM simulations with HadEX2, NCEP2 and ERA-INTERIM respectively. As it can be seen in figure 5.4 that HadEX2 shows index values over certain areas (for example India, Eastern Chin, parts of Indonesia and Malaysia) while for others, the map shows blank regions (for example Pakistan, north west of China, Afghanistan, Myanmar etc).

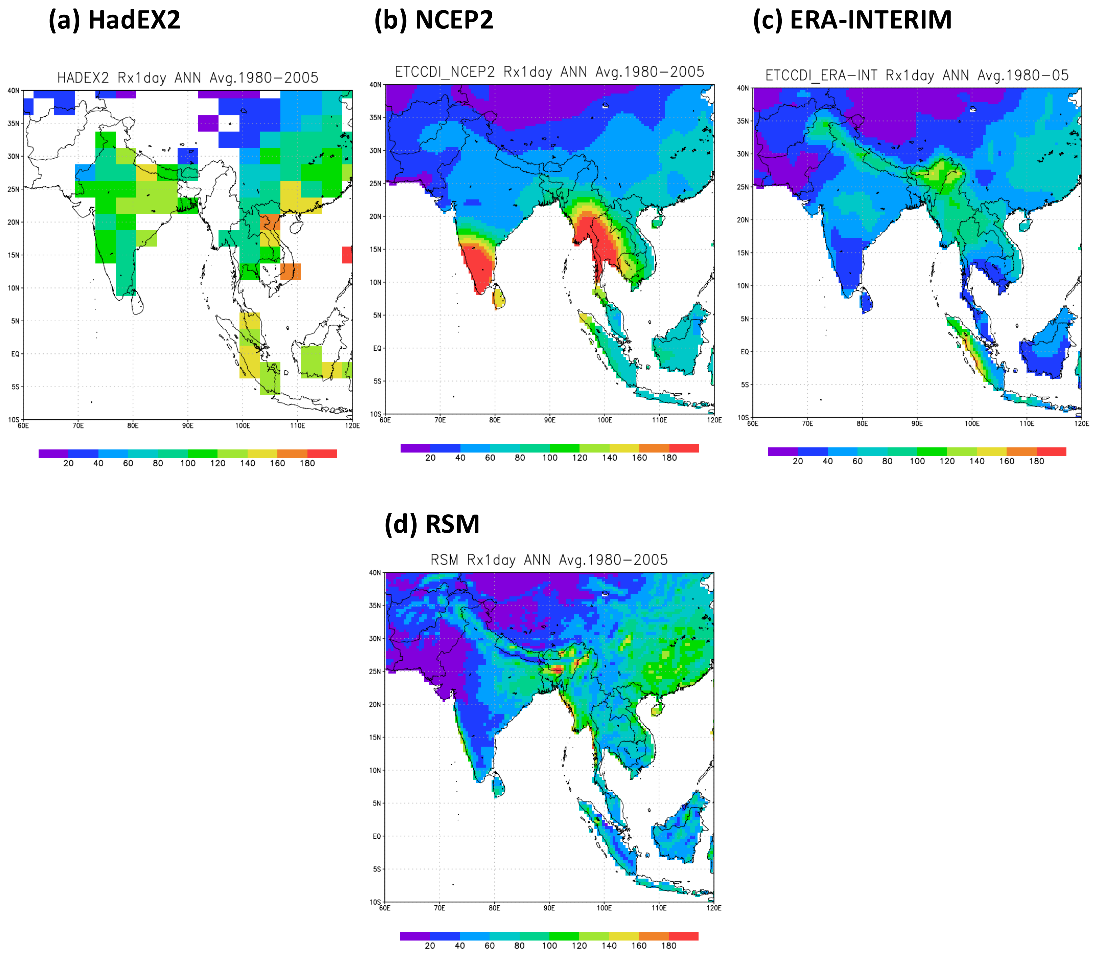

Figure 5.4 represents the Max 1 day precipitation amount (mm) for time period 1980-2005 for (a) HadEX2, (b) NCEP2, (c) ERA-INTERIM and (d) RSM respectively.

The comparison of RSM derived Rx1day index with HadEX2 shows almost similar trend over North and South of eastern China, north eastern India and part of Bangladesh while a decreased Rx1day values for RSM are observed over almost all parts of India, Malaysia and Indonesia.

NCEP2 because of its coarse resolution shows more wide area coverage as compared to RSM index. It shows similar index values for north china as HadEX2 but underestimated on south eastern china, north and central India, Indonesia and Malaysia. Some over estimations are also observed over south of India and Thailand regions.

ERA-INTERIM almost shows similar trends as RSM but with some underestimations over southeastern China same as NCEP2. On the other hand, it captures the higher index values similar to HadEX2 over western Malaysian island and hoot hills of Himalayas.

Overall, RSM simulations shows satisfactory performance in capturing the extreme index compare to observation based index i.e. HadEX2 and its results shows more closer resemblance to EAR-INTERIM as compared to NCEP2 which can be attributed to resolution difference between them.

Figure 5.5 shows the results of summer days index for HadEX2, NCEP2, ERA-INTERIM and RSM respectively for time period of 1980-2005. It can be seen that as compared to Rx1day index, the coverage of HadEX2 for Summer days index is more evenly distributed.

Th ecomaprsion of RSM summer day index woth HadEX2 shows very agreement strecting from east o westet and south ward comparison. while for northern parts, HadEX2 shows less number of summer days in comparison with NCEP2, ERA-INTERIM AND RSM indices. It can be attributed to the limited observation networks in the topographically complex regions while the reanalysis does not face such limitations so does the RSM.

Overall, RSM shows satisfactory performance in capturing the extreme temperature trend over the domain.

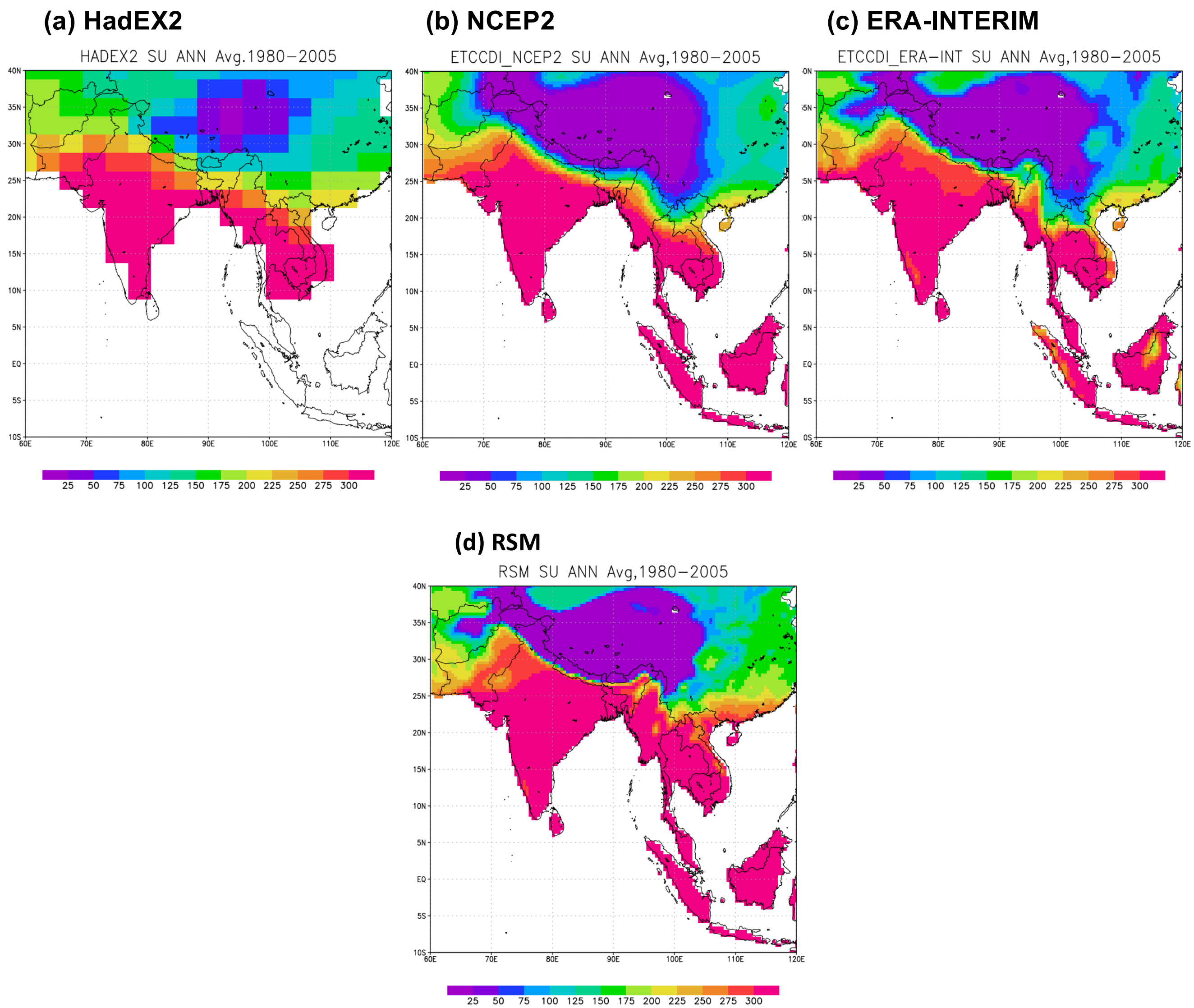

Figure 5.5 Same as figure 5.4 but for summer days

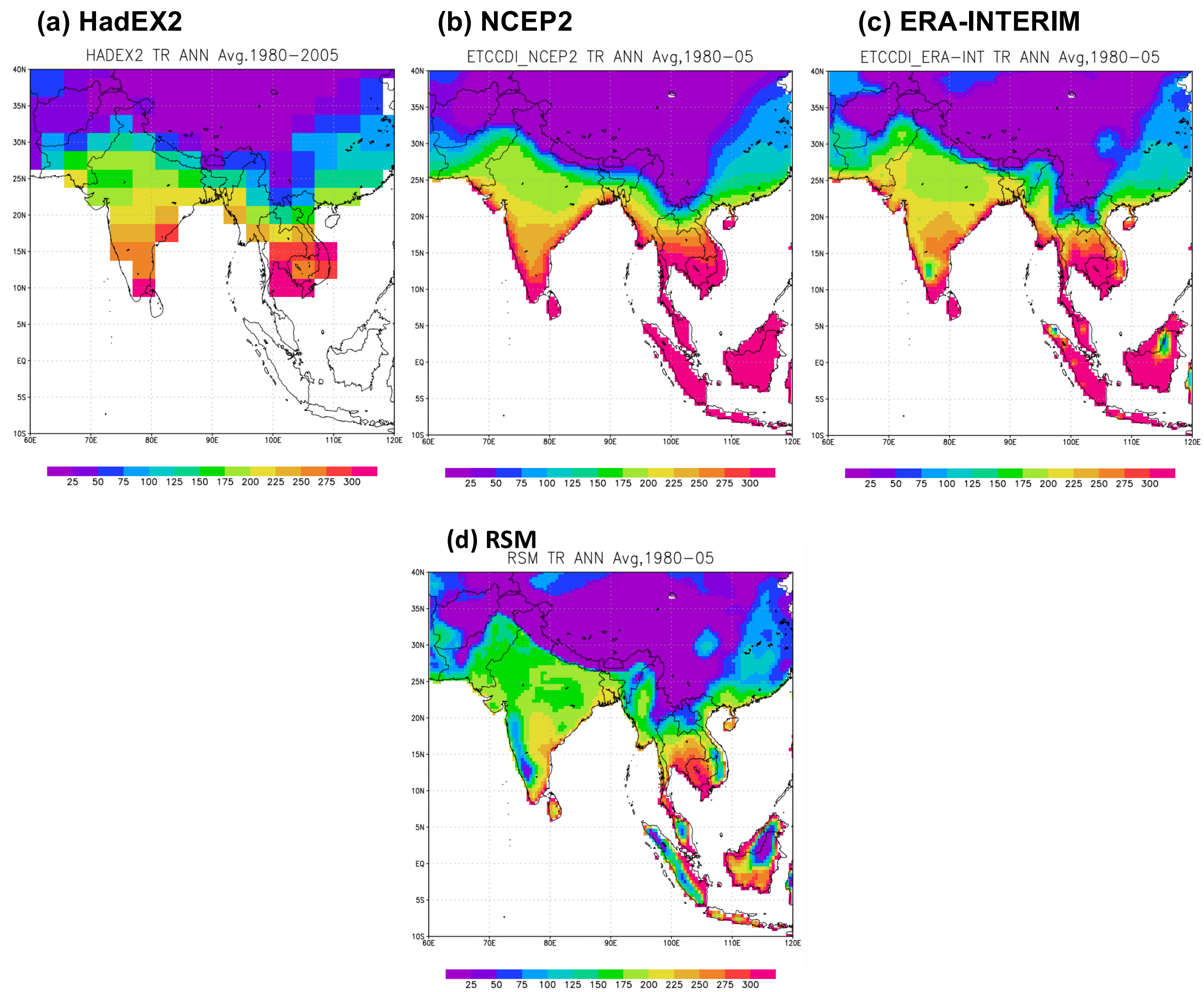

Figure 5.6 Same as figure 5.4 but for Tropical nights

Figure 5.6 presents the tropical night comparison of RSM simulations with HadEX2, NCEP2 and ERA-INTERIM respectively. In contrast to summer days index, the tropical night index comparison shows closer trend between aforementioned datasets in the northern parts of domain as compared to southern half. For southern half, the results of NCEP2 simulations are more comparable to HadEX2 as compared to ERA-INTERM and RSM indices. Few regions in ERA-INTERIM shows under-estimations as compared to HadEX2 that are further under estimated in RSM index. It might be because of the fine resolution of these datasets as compared to the former ones.

Overall, RSM captured the general trend on tropical nights in the region, which will help us to study the future simulations results with more reliability.

5.4 Future Projection

The results of future projections for precipitation and temperature extremes are estimated for RSM 21C relative to the reference period of 1980-2005.

Figure 5.7 shows the future projections trend for Maximum one day rainfall for RCP4.5 and RCP8.5 scenarios. The trend for near future the Rx1day shows more wide spatial distribution in terms of increasing and decreasing one-day max rainfall. An increasing trend is shown near foot hills of Himalayas, southern tip of India, Myanmar while a decreasing trend is observed over central and western part of India and south China and parts of Vietnam. RCP8.5 simulations for near future shows more increasing trend of 1day maximum rainfall then RCP4.5. The noticeable feature of rcp8.5 simulations is that the decreasing trend seen in RCP4.5 near index is replaced and showed increasing trend over central and western India and parts of eastern China. For mid future, over all an increasing trend is seen over most parts of India, Bangladesh, and south China and south east Asia. While for Pakistan and western china there is no obvious change is observed. The increasing index trend are further enhanced in RCP8.5 mid future simulations. An other observable in change is seen over Pakistan in RCP8.5

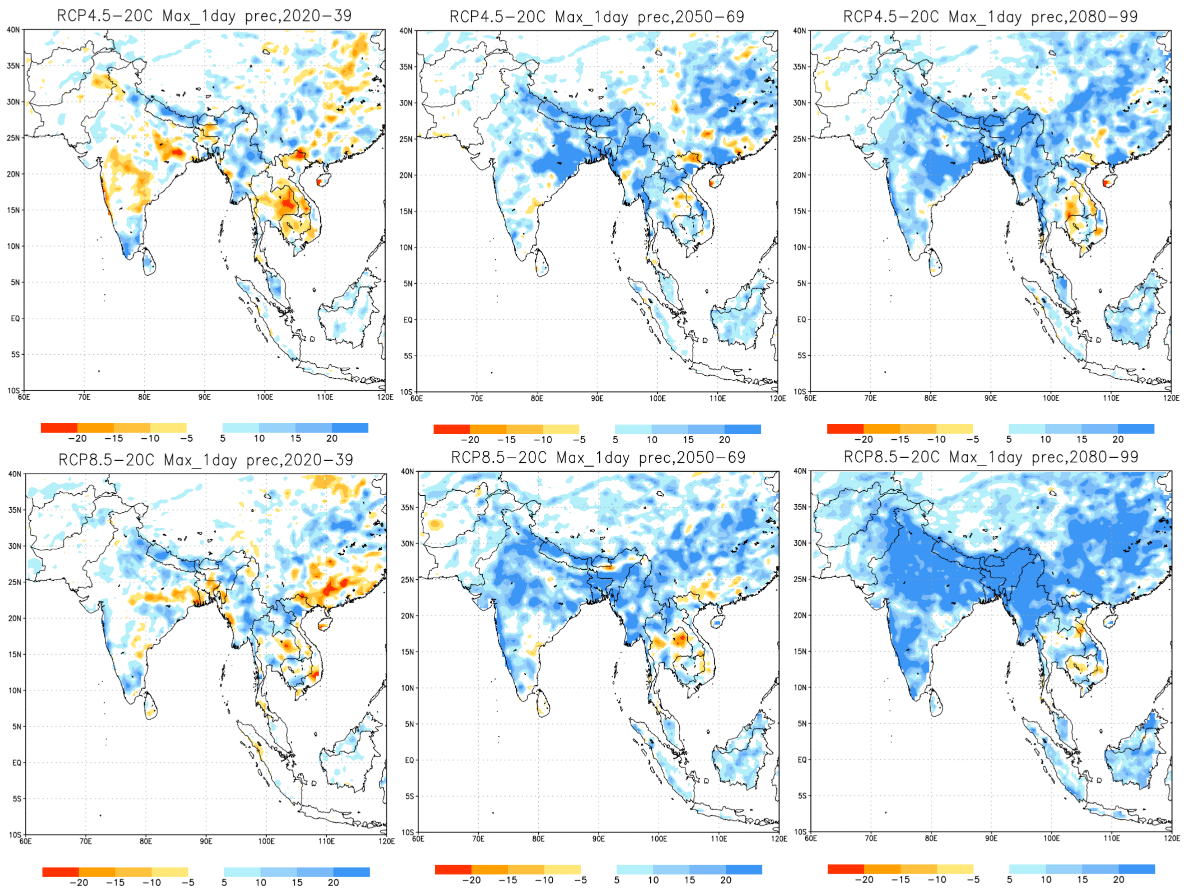

Figure 5.7 shows the spatial distribution of Maximum One day rainfall for future projections for RCP4.5 near (a), mid(b) and far (c) future. Figure (d), (e) and (f) shows RCP8.5 results for near, mid and far future respectively.

Simulations in terms of increasing Rx1day trend as compared to RCP4.5 mid future. The far future trend for RCP4.5 for far future are similar to mid future but with increased intensity. Few decreasing trends are also seen over eastern part of Thailand and Vietnam. For far future RCP8.5 simulations, the index shows further intensified behavior with more enhanced increase over North eastern Pakistan, over almost all India, Bangladesh, Nepal, Myanmar and south central parts of China while a decreasing trend is minimized over Thailand and Vietnam in RCP8.5 far future simulations.

Overall, it for bothRCP4.5 and 8.5 scenarios heterogeneity of Rx1day indices seen in near future while from mid and specifically in far future an increasing one day maximum rainfall will be considered in future.

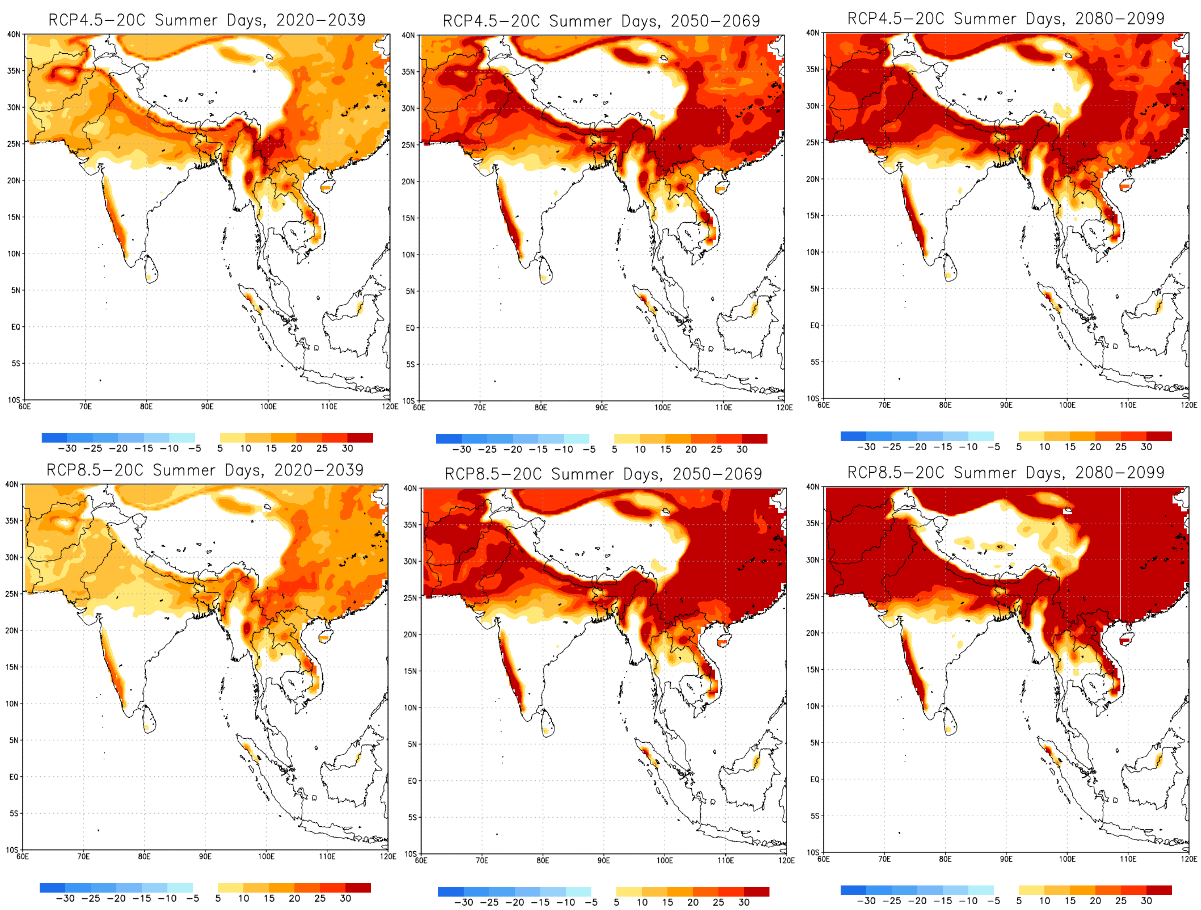

Figure 5.8 Same as figure 5.7 but for summer days

Figure 5.8 shows the spatial distribution of summer days in RCP4.5 and RCP8.5 in near, mid and far future projections. The future projection index for summer days in near future shows an increasing trend in near future covering the almost all parts f Pakistan, north and western Ghats of India, eastern and northern China. The number of increased summer days lies in the range of 10-25 days. For RCP8.5 near future the increase of summer days is rather less as compared to RCP4.5 near future with little exception in south of china. For mid future, RCP4.5 shows further increase and the number of summer days confined to the same regions as near future but it increased from 25 days and over. The RCP8.5 mid future shows similar trend to RCP4.5. The far future showed further increase in far future in both RCP4.5 and RCP8.5. Overall, the summer days will increase keep on increasing from near to far future for both scenarios.

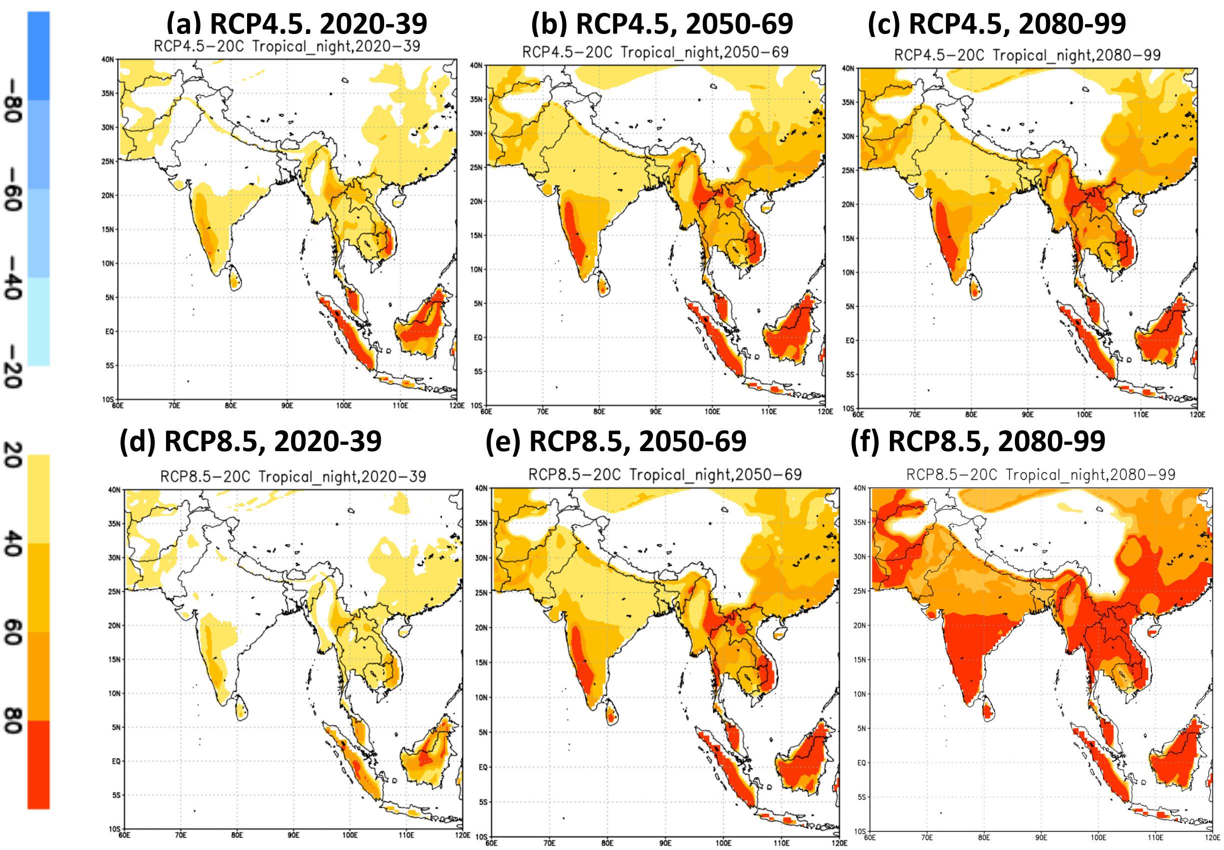

Figure 5.9 Same as figure 5.7 but for Tropical Nights

Figure 5.9 shows the future projection trend for Tropical nights. The near future RCP4.5 simulations show an increasing trend over south east of Pakistan, India South East Asia and South China while for main land areas of China shows no change in tropical nights. RCP8.5 shows increase but the change in tropical nights is less as compared to

RCP4.5. For mid future, the tropical nights increases moving towards north. More increase is seen near Western Ghats, Malaysia and Indonesia and northern Myanmar as compared to other regions. The trends are almost similar for RCP8.5 mid future with bit number of days in northeastern China. For far future, RCP4.5 shows further expanding of tropical nights while the number of tropical nights exceeded over 80 days in far future RCP8.5 simulations.

Overall, the tropical nights will increase in future. The trend of their spread starts from tropical regions to sub-tropical and arid and semi arid regions. While for Tibetan plateau there will be no change in tropical nights in future simulations.

CHAPTER 6

Concluding Remarks and Recommendations

6.1 Conclusions

Following conclusions are drawn from the current study;

High-resolution dataset set for South Asia is prepared in this research study following the protocol of CORDEX experiment. The selection of better parameterization scheme and new Scale Selective Bias Correction method played an important role in capturing the precipitation trends over South Asia. SAS convective scheme has over all better results than other CPS and their physical ensemble.

Dynamic Downscaled RSM showed more efficiency in capturing the details of topographically complex regions than the coarser global A-O coupled model (HadGEM2).

Very diverse research topic is covered in this study. It is based upon the fact that when we talk about climate change, the most important indicators of this change are felt in terms of temperature and precipitation changing behavior. In this research, very intense work is being done to study each single aspect to understand their behavior. For example, the 20C validation study for South Asia showed very diverse spatial spread of temperature and precipitation biases when validated against observation. But when the temporal analysis (intra-seasonal and inter-annual) analysis is applied than we get the clearer picture of RSM performance relative to driving parent model. Validation of model results for 20C presented great challenges. It can be attributed to the number of factors. For example, uncertainty among observation datasets, their temporal and spatial coverage in South Asia. The coarse resolution of dataset if both land and ocean parts are included (e.g. CMAP and GPCP). Inclusion of land and ocean in validation process of RSM showed great variation. For example, if both land and ocean are considered during the validation process than the RSM performance becomes better than driving model HadGEM. It is due to the fact that RSM shows really nice results over the ocean as compared to HadGEM.

The added value of high-resolution simulations becomes more obvious in studying the extreme events. Both sensitivity experiments in chapter 2 and 20C analysis results in chapter 3 showed the capability of RSM in capturing extreme events focusing higher precipitation and temperature bins. Extreme events are discussed in variety of ways. In addition to the bins approach, the innovative extreme indices defined by Expert Team on Climate Change Detection and Indices (ETCCDI) is also analyzed in this study. RSM shows great capability in capturing the ETCCDI defined indices. High resolution of RSM at times supersedes the coarser resolution NCEP2 and ERA-INTERIM extreme indices, for example the maximum one-day precipitation index over eastern China. 99 percentile of temperature and precipitation extremes further confirms the capability of RSM in capturing extreme events.

The results of future projections for temperature showed increasing trend in RCP4.5 and RCP8.5 simulations of RSM. Among the seasonal comparison, DJF showed more rise in temperature than JJA for both scenarios.

Future projections of surface precipitation for both RCP scenarios showed varied behavior in terms of its spatial spread. The general trend is decreasing in the near future (2020-2050) for both RCP scenarios, which is replaced by an increasing trend in far future simulations (2051-2100). Among the RCP scenarios, the trend is steeper in RCP8.5 simulations than RCP4.5.

Overall, it is evident from future projection study that global warming is evident over South Asia. The results of HY-INT for future projection also support this statement. The extreme indices shows a rising one maximum rainfall along with increase summer days and nights which seems to reduce the diurnal temperature variation in future which need further analysis.

Added value for long tail phenomenon is seen in 99 percentile future projections which shows that, although both mean and 99 percentile values of temperature and precipitation will increase in future but there will more increase in extreme 99 percentile events than climatological mean. It is really important finding of this research, which forecast the disasters situations of South Asia and thus conveys a very useful message to the local authorities to be prepared for such situations in future.

Finally, the generation of high-resolution data for South Asia including the 20C and 21C simulations will be of great use for the CORDEX-South Asia project. The availability of multi-model simulations for this region generated under the CORDEX project will help us to understand the prevailing climate and its future in more detail.

6.2 Recommendations

Few recommendations for future research are mentioned as follows;

Higher resolution is needed in complex mountain regions of Himalayan and Karakorum ranges to understand these regions well.

The observation data shows variations in terms of spatial and temporal resolutions. Also the number of station locations varies from year to year which sometime poses difficulty in validation of model results. It is therefore recommended to use an ensemble of observation.

The resolution of reanalysis datasets is mostly coarser then regional model, which poses difficulty in validation procedure. It is therefore recommended to use as high-resolution dataset if possible.

It is found out from this study that higher resolution is required to study the hilly areas precipitation of, for example Aravalli and vindhya ranges of India and the region between Myanmar and Laos.

Last but not least, there are number of other factors, which are responsible for impacting the region. The most important among them is fragile infrastructure, lack of management of resources, increasing population and poverty. These socio-economic factors cannot be ignored when extreme events are studied. This research shows that South Asia is going to experience a changing climate and more particularly extreme events in future. Therefore, if the above socio-economic factors are ignored than its most likely that the impact of extreme events will become double or even more than presently estimated.

Reference

Byun, U.-Y., Hong, S.-Y., Shin, H., Lee, J.-W., Song, J.-I., Hahm, S.-J., Kim, J.-K., Kim, H.-W., and Kim, J.-S., 2011. WRF-based Short-Range Fore- cast System of the Korea Air Force: Verification of prediction skill in 2009 summer. Atmosphere, 21(2), 197-208. (in Korean with English abstract).

Chao, W. C. and Deng, L., 1998. Tropical intraseasonal oscillation, super cloud clusters, and cumulus convection schemes. Part II: 3D aquaplanet simulation. J. Atmos. Sci., 54, pp. 2429-2440.

Donat, M. G., Alexander, L. V., Yang, H., Durre, I., Vose, R., Dunn, R. J. H., Willett, K. M., Aguilar, E., Brunet, M., Caesar, J., Hewitson, B., Jack, C., Klein Tank, A. M. G., Kruger, A. C., Marengo, J., Peterson, T. C., Renom, M., Rojas, C. O., Rusticucci, M., Salinger, J., Elrayah, A. S., Sekele, S. S., Srivastava, A. K., Trewin, B., Villarroel, C., Vincent, L. A., Zhai, P., Zhang, X., and Kitching, S., 2013. Updated analyses of temperature and precipitation extreme indices since the beginning of the twentieth century: The HadEX2 dataset, J. Geophys. Res. Atmos., 118, doi:10.1002/jgrd.50150.

Dube, A., Ashrit, R., Ashish, A., Sharma, K., Iyengar, G.R., Rajagopal, E.N. and Basu, S., 2014. Forecasting the heavy rainfall during Himalayan flooding—June 2013, Weather and Climate Extremes, 4. pp. 22–34

Field, C.B., Barros, V., Stocker, T.F., Qin, D., Dokken, D.J., Ebi, K.L., Mastrandrea, M.D., Mach, K.J., Plattner, G.-K., Allen, S.K., Tignor, M., and Midgley, P.M. 2012. Managing the Risks of Extreme Events and Disasters to Advance Climate Change Adaptation. A Special Report of Working Groups I and II of the Intergovernmental Panel on Climate Change. Cambridge University Press, Cambridge, UK, and New York, NY, USA, pp. 582.

Frich, P., Alexander, L. V., Della-Marta, P., Gleason, B., Haylock, M., Klein Tank, A. M. G. and Peterson, T., 2002. Observed coherent changes in climatic extremes during 2nd half of the 20th century, Clim. Res., 19, pp. 193 – 212.

G. P. Singh, Jai-Ho Oh, Jin-Young Kim and Ok-Yeon Kim, 2006. Sensitivity of Summer Monsoon Precipitation over East Asia to Convective Parameterization Schemes in RegCM3. SOLA, 2006, Vol. 2, 029–032, doi:10.2151/sola.2006–008 29.

Gadgil, S. and Sajani, S., 1998. Monsoon precipitation in the AMIP runs. Clim. Dyn, 14, pp. 659- 689.

Giorgi, F., and Bi, X., 2005. Regional changes in surface climate interannual variability for the 21st century from ensembles of global model simulations, Geophys. Res. Lett., 32, L13701, doi:10.1029/ 2005GL023002.

Giorgi, F., Bi, X. and Pal, J. S., 2004. Mean, interannual variability and trends in a regional climate change experiment over Europe. Part II: Future climate scenarios (2071–2100), Clim. Dyn., 23, pp.839–858.

Groisman, P.Y., Karl, T.R., Easterling, D.R., Knight, R.W., Jamason, P.F., Hennessy, K.J., Suppiah, R., Page, C.M., Wibig, J., Fortuniak, K., Razuvaev, V.N., Douglas, A., Førland, E. and Zhai, P., 1999. Changes in the probability of extreme precipitation: important indicators of climate change. Climatic Change., 42, pp.243–283.

Gwangyong Choi, Dean Collins, Guoyu Ren, Blair Trewin, Marina Baldi, Yoshikazu Fukuda, Muhammad Afzaal, Theeraluk Pianmana, Purevjav Gomboluudev, Pham Thi Thanh Huong, Norlisam Lias, Won-Tae Kwon, Kyung-On Boo, Yu-Mi Cha and Yaqing Zhou., (2009) .Changes in means and extreme events of temperature and precipitation in the Asia-Pacific Network region, 1955–2007. Int. J. Climatol. 29: 1906–1925.

Ham, S. and Hong, S.-Y., 2013. Sensitivity of Simulated Intraseasonal Oscillation to Four Convective Parameterization Schemes in a Coupled Climate Model. Asia-Pacific J. Atmos. Sci., 49(4), 483-496.

Hong, S.-Y. and Chang, E.C., 2012. Spectral Nudging Sensitivity Experiments in a Regional Climate Model. Asia-Pacific J. Atmos. Sci., 48(4), pp. 345-355. doi:10.1007/s13143-012- 0033-3.

Hong, S.-Y. and Pan, H.L., 1998. Convective trigger function for mass flux cumulus parameterization scheme. Mon. Wea. Rev., 126, pp. 2599- 2620.

Juang, H.-M.H., and Kanamitsu, M., 1994. The NMC nested regional spectral model. Mon. Wea. Rev., 122, pp. 3-26.

Kain, J. S., and Fritsch, J. M., 1990. A one-dimensional entraining/detraining plume model and its application in convective parameterization. J. Atmos. Sci., 33, pp.1890-1910.

Kanamaru, H. and Kanamitsu. M., 2007. Scale-Selective Bias Correction in a Downscaling of Global Analysis Using a Regional Model. Mon. Wea. Rev., 135, pp. 334-350.

Kanamitsu, M., Ebisuzaki, W., Woollen, J., Yang, S.-K., Hnilo, J. J., Fiorino, M., and Potter, G. L., 2002. NCEP–DOE AMIP-II Reanalysis (R-2). Bull. Amer. Meteor. Soc., 83, pp.1631 - 1643. doi: http://dx.doi.org/10.1175/BAMS-83-11-1631.

Kanamitsu, M., Yoshimura, K., Yhang, Y.B. and Hong, S.-Y., 2010. Errors of Interannual Variability and Trend in Dynamical Downscaling of Reanalysis. J. geophys. res.,115, D17115, doi:10.1029/2009JD013511.

Kang, H.-S. and Hong, S.-Y., 2008. Sensitivity of the simulated East Asian summer monsoon climatology to four convective parameterizaton schemes. J. Geophys. Res. 113, D15119, doi: 10.1029/2007JD009692.

Klein Tank, A. M. G., Peterson, T.C., Quadir, D.A., Dorji, S., Zou, X., Tang, H., Santhosh, K., Joshi, U.R., Jaswal, A.K., Kolli, R.K., Sikder, A.B., Deshpande, N.R., Revadekar, J.V., Yeleuova, K., Vandasheva, S., Faleyeva, M., Gomboluudev, P., Budhathoki, K.P., Hussain, A., Afzaal, M., Chandrapala, L., Anvar, H., Amanmurad, D., Asanova, V.S., Jones, P.D., New, M.G. and Spektorman,T., 2006. Changes in daily temperature and precipitation extremes in central and south Asia, J. Geophys. Res., 111, D16105, doi:10.1029/2005JD006316.

Lau, K.-M., and Kim, K.-M., 2006, Observational relationships between aerosol and Asian monsoonrainfall, and circulation, Geophys. Res . Lett., 33, L21810,doi:10.1029/2006GL027546.

Lee, M.-I., Kang, I.-S. and Mapes, B. E., 2003. Impacts of cumulus convection parameterization on aqua-planet AGCM simulations of tropical intraseasonal variability.

J. Meteor. Soc. Japan, 81, pp. 963-992.

Luis, M.D., Raventós, M., González-Hidalgo, J., Sánchez, J.R. and Cortina, J., 2000. Spatial analysis of rainfall trends in the region of Valencia (east Spain). Int. J. Climatol. 20 (12), pp.1451–1469.

Manton, M.J., Della-Marta, P.M., Haylock, M.R., Hennessy, K.J., Nicholls, N., Chambers, L.E., Collins, D.A., Daw, G., Finet, A., Gunawan, D., Inape, K., Isobe, H., Kestin, T.S., Lefale, P., Leyu, C.H., Lwin, T., Maitrepierre, L., Ouprasitwong, N., Page, C.M., Pahalad, J., Plummer, N., Salinger, M.J., Suppiah, R., Tran, V.L., Trewin, B., Tibig, I. and Yee, D., 2001. Trends in extreme daily rainfall and temperature in southeast asia and the south pacific: 1961–1998, International journal of climatology *int. j. climatol*. (in press) doi: 10.1002/joc.610.

Moorthi, S. and Suarez, M. J., 1992. Relaxed Arakawa-Schubert: a parameterization of moist convection for general circulation models. Mon. Wea. Rev., 120, pp. 978-1002.

Nikulin, G., Kjellström, E., Hansson, U., Strandberg, G. and Ullerstig, A., 2009. Evaluation and Future Projections of Temperature, Precipitation and Wind Extremes over Europe in an Ensemble of Regional Climate Simulations, Rossby Centre, Swedish Meteorological and Hydrological Institute, Sweden. Full description is available at : http://www.smhi.se/polopoly_fs/1.12877!/extremes.pdf

Park, S., Hong, S.-Y. and Byun, Y.-H., 2010. Precipitation in boreal summer simulated by an oscillation for dynamic seasonal prediction. J. Climate, 23, pp. 2801-2816.

Qu, M., Wan, J. and Hao, X., 2014. Weather and Climate Extremes Analysis of diurnal air temperature range change in the continental United States.4. pp. 86–95.

Ridout, J. A., Jin, Y., and Liou, C.-S., 2005. A cloud-base quasi-balance constraint for parameterized convection: Application to the Kain-Fritsch cumulus scheme, Mon. Weather Rev., 133, 3315–3334.

Roth, M., Buishand, T.A., Jongbloed, G., Klein Tank, A.M.G., Van Zanten, J.H., 2014. Projections of precipitation extremes based on a regional, non-stationary peaks-over-threshold approach: A case study for the Netherlands and north-western Germany. Weather and Climate Extremes, 4. pp.1–10

Sabin, T. P., Krishnan, R., Ghattas, J., Denvil, S., Dufresne, J.-L., Hourdin, F. and Pascal, T., 2013. High resolution simulation of the South Asian monsoon using a variable resolution global climate model. Clim Dyn.41. pp. 173-194. DOI: 10.1007/s00382-012-1658-8.

Schar, C., Vidale, P. L., Luthi, D., Frei, C., Haberli, C., Liniger, M. A. and Appenzeller, C., 2004. The role of increasing temperature variability in European summer heatwaves, Nature, 427. pp. 332–336.

Sillmann, J., V. V. Kharin, X. Zhang, F. W. Zwiers, and D. Bronaugh (2013), Climate extremes indices in the CMIP5 multimodel ensemble: Part 1. Model evaluation in the present climate, J. Geophys. Res. Atmos., 118, 1716–1733, doi:10.1002/jgrd.50203).

Sivakumar, M.V., and Stefanski, R., 2011. Climate Change in South Asia. In Lal, R., Sivakumar,M.V., Faiz, M.A., Mustafizur Rahman, A.H.M., Islam, K.R (Eds.), Climate Change and Food Security in South Asia (pp. 13-30). Springer. ISBN: 978-90-481-

9515-2.

Taxak, A.K., Murumkar, A.R. and Arya, D.S., 2014. Weather and Climate Extremes Long term spatial and temporal rainfall trends and homogeneity analysis in Wainganga basin, Central India, 4, pp. 50–61.

Trewin BC. 2009. A new index for monitoring changes in heatwaves and extended cold spells. Ninth International Conference on Southern Hemisphere Meteorology and Oceanography, Melbourne, 9–13 February 2009.

Wan Ahmad Ardie, Khai Shen Sow, Fredolin T Tangang, Abdul Ghapor Hussin, Mastura Mahmud and Liew Juneng, 2012· The performance of different cumulus parameterization schemes in simulating the 2006/2007 southern peninsular Malaysia heavy rainfall episodes. Journal of Earth System Science. Volume 121, Issue 2, pp 317-327

Wang, Y., Leung L.R., McGregor J.L., Lee D.-K., Wang, W.-C., Ding, Y. and Kimura, F., 2004. Regional climate modeling: progress, challenges, and prospects. J. Meteor Soc Japan, 82.pp.1599–1628.

World Bank. 2013. Turn Down the Heat: Climate Extremes, Regional Impacts, and the Case for Resilience. A report for the World Bank by the Potsdam Institute for Climate Impact Research and Climate Analytics. Washington, DC.

Yao, C., Yang, S., Qian, W., Lin, Z. and Wen, M., 2008. Regional summer precipitation events in Asia and their changes in the past decades, J. Geophys. Res., 113, D17107. doi:10.1029/2007JD009603.

Yatagai, A., Kamiguchi, K., Arakawa, O., Hamada, A., Yasutomi, N. and Kitoh, A., 2012. APHRODITE: Constructing a Long-term Daily Gridded Precipitation Dataset for Asia based on a Dense Network of Rain Gauges, Bulletin of American Meteorological Society. doi:10.1175/BAMS-D-11-00122.1.

Zhang, G. J. and McFarlane, N. A., 1995. Sensitivity of climate simulations to the parameterization of cumulus convection in the Canadian climate centre general circulation model. Atmos.-Ocean, 33. pp. 407-446.

Zhongfeng, Xu. and Yang, Z.L., 2012. An Improved Dynamical Downscaling Method with GCM Bias Corrections and Its Validation with 30 Years of Climate Simulations. J. Climate, 25. pp. 6271–6286. doi: http://dx.doi.org/10.1175/JCLI-D-12-00005.1.